Universidad Autónoma de Madrid

Departamento de Bioquímica

Aurora A shines on early T cell activation

Tesis doctoral

Noelia Blas Rus

Madrid, 2016

Departamento de Bioquímica

Facultad de Medicina

Universidad Autónoma de Madrid

Aurora A shines on early T cell activation

Memoria presentada por la licenciada en Bioquímica:

Noelia Blas Rus

para optar al título de Doctor por la Universidad Autónoma de Madrid

Director de la Tesis: Francisco Sánchez-Madrid, Doctor en Ciencias Biológicas y Catedrático de Inmunología de la Universidad Autónoma de Madrid.

Este trabajo se realizó en el Servicio de Inmunología del Hospital Universitario de la Princesa.

Madrid, 2016

Francisco Sánchez-Madrid, Doctor en Ciencias Biológicas y Catedrático de Inmunología de la Universidad Autónoma de Madrid,

CERTIFICA:

Que Noelia Blas Rus, licenciada en Bioquímica por la Universidad Autónoma de Madrid, ha realizado bajo mi dirección el trabajo de investigación correspondiente a su Tesis Doctoral con el título:

Aurora A shines on early T cell activation

Revisado este trabajo, el que suscribe considera el trabajo realizado satisfactorio y autoriza su presentación para ser evaluado por el tribunal correspondiente.

Y para que así conste y a los efectos oportunos, firma el presente certificado en Madrid a 20 de Octubre de 2016.

Fdo. Prof. Francisco Sánchez-Madrid

A mis padres y a mi hermana

A mi abuela

A Alberto

Agradecimientos

Después de cinco años y medio en el Hospital de la Princesa, son muchas las personas a las que tengo que agradecer tanto su ayuda como su compañía durante todo este tiempo. Espero haberme acordado de todos, pero pido perdón a aquellos que no aparezcan en estas líneas y que deberían hacerlo.

En primer lugar quiero agradecer a Paco por haberme dado la oportunidad de realizar esta tesis doctoral en su laboratorio. Además, quiero darle las gracias por su apoyo, su confianza en mí y sus ánimos desde el momento en el que llegué.

En segundo lugar a Eugenio, sin el que no habría sido posible terminar este trabajo, tanto por su apoyo científico como personal. Hemos pasado miles de horas compartiendo espacio en el laboratorio y aunque no ha sido nada fácil vivir con él por su extraño concepto del orden, siempre nos hemos apoyado el uno en el otro (a nuestra manera) para seguir hacia delante.

A mis *frikis* (siempre con cariño) entre los que cabe destacar a Rafa, Javi, Álvaro y, saliéndose de lo *friki*, a Norman, uno de mis primeros compañeros y quien me convenció de lo malo que era hacerse un tatuaje. Y, por supuesto, a Rocío que es la que me ayuda a lidiar con ellos. Aunque muchas veces nosotras no tenemos ni idea de qué están hablando, es muy divertido escucharles cuando discuten sobre Superman, el Señor de los anillos y esas cosas. Gracias de verdad por estar siempre ahí, incluso a las 9 de la noche, cuando el experimento del día ha sido un completo desastre y solamente necesitas a alguien a quien contarle lo terrible que son las células, el confocal, el fuji o cualquier otro cacharro. Gracias por la hora de la comida y por la hora del café, donde intentamos arreglar el mundo sin llegar a nada y gracias por esas tardes y esos fines de semana jugando al Saboteur o a lo que sea.

A mi equipo cactus, formado por Eva y Bea (y Rocío de nuevo) y a Aitana que aunque comparte párrafo con ellas, nada tiene que ver en lo que a besos y a abrazos se refiere. Sin vosotras esto no habría sido lo mismo y aunque en los últimos meses ya no estabais por aquí, sigo acordándome de vosotras y echándoos de menos. Siempre recordaré el momento en el que Eva me enseñó a diseñar primers para secuenciar Lck, la obsesión de Bea por guardar todo lo que pilla por medio y los buenos días de Aitana a los que más de una vez he respondido con un “bufido”. Sé que aunque ya no compartamos laboratorio, seguís ahí para lo que necesite. Y no solo vosotras, también Alberto, Víctor y Álvaro a quien me habéis dado la oportunidad de conocer y poder incluir en mi grupito de amigos.

A todos los Pacos, especialmente a Ángeles Ursa por habernos aguantado tan bien a Eugenio y a mí y por ofrecernos siempre su ayuda a nivel profesional y personal. Por soportar

nuestras quejas, nuestros alborotos y nuestros “descuidos” con las cabinas. Dentro de los Pacos 1 tengo que mencionar también a Mj, por haberme enseñado las primeras técnicas en el laboratorio y porque gracias a ella sé hacer geles, y mi tesis sin geles no habría sido posible. A Noa por esas horas en las que ha estado peleándose con el TIRF para que pudiéramos conseguir vídeos tan bonitos. A María Navarro por resolver todas mis dudas científicas y darme ideas para avanzar. A Raquel y a Cande por la compañía, por echarme una mano cuando lo he necesitado y por las risas en más de una ocasión. De los Pacos 2 a Lola, por todas las veces que nos hemos reído de miles de historias. A Hortensia, por su compañía, por comprarnos la merienda y por dejarnos el ordenador cada vez que la Wi-Fi no funcionaba. A Ali, por sus consejos sobre PCRs y sobre cosas que a uno le preocupan en su día a día. A Chema, nuestro médico y gracias al cual he podido acabar esta tesis con esos bonitos encabezados. Y en los últimos meses a Montse y Tathiana, por su simpatía.

Al Norte al completo, empezando por Miguel, quien me ha asesorado a la hora de diseñar algún que otro experimento, me ha corregido cualquier cosa escrita en inglés y me ha ayudado a darle un título tan bonito a esta tesis. A Cris, una de las primeras personas que conocí aquí ya que llegamos a la vez, por sus consejos y su buen saber escuchar. A Irene, que aunque hace mucho que se fue del laboratorio, hizo que mi llegada fuera mucho más fácil. A Alba, otra de mis primeras compañeras, que junto con Irene y Rocío hacía que salir tarde del laboratorio no fuera tan malo porque nos esperaban unas cañas en el bar de abajo. A Lidia, que aunque también hace tiempo que se fue, sigo acordándome de ella al ver las etiquetas rosas con su nombre.

A los “*Urzainquis*”; a Ana, por haber sido siempre tan cariñosa conmigo y a la pequeña Marina, siempre tan alegre.

A la gente de High Tech, todos los que han sido y los que son ahora. Aquí tengo que hacer mención especial a Pablo, por enseñarnos tantas cosas sobre la vida y por esas conversaciones a la hora de la comida tan… tan… no lo tengo claro! A Elena y Ali por su simpatía y buenos ratos. A Dani, porque aunque llegó hace relativamente poco tiempo, se ha convertido en uno de los imprescindibles y porque además sabe combinar colores. A David, uno de los *frikis* mayores y creo que al que menos entiendo de todos. Gracias por intentar enseñarme conceptos de juegos, aunque no sea capaz de retener muchos de ellos.

A Amalia, porque es imposible aburrirse con ella y más imposible aún hacer que se enfade. Por sus curiosas historias y por ofrecerse siempre a echarte una mano cuando lo necesitas. A Vane (con sus uñas siempre tan originales), Iria, Ana y Amada.

Al laboratorio de Cecilia y todos los residentes: Itxaso, Anita, Bea, Carlos, Fede, Vero, Santi, Tamara y Ana. Al laboratorio de citometría y al de rutina.

Terminando con la gente de la Princesa no puedo olvidarme de Mari Ángeles ("*la secre*"), por encargarse de todas nuestras gestiones y nuestros paquetes y por ponernos guapos cuando tenemos algo importante. También tengo que agradecer al hombre que repone el café de la máquina, porque sin él no seríamos personas (bueno, ni nosotros ni nadie en todo el hospital) y al servicio de informática, por haberme hecho aprender más de ordenadores de lo que me hubiera gustado. También a Pepe, por alimentarlos al salir del laboratorio y preferir echar a todos sus clientes antes que a nosotros y a nuestros gritos.

A mis compañeros del CNIC, especialmente a Marta por enseñarme a manejar ratones y por surtirme de todo tipo de reactivos cada viernes. A Ana, por su buen humor y su constante sonrisa. A María Laura, mi primera compañera de habitación en un congreso y mi biblioteca de papers y a Olga, con quien compartí mis inicios en la Princesa y me enseñó a hacer inhibidores de proteasas. A Dani y Irene, con los que espero compartir alguna otra excursión, siempre que no haya agua de por medio. A Cris, Francesc, Carolina, Vera y Danay.

A la gente del Santa Cristina, porque aunque ahora nos pillan un poco lejos, sabemos que siempre podemos reunirnos para celebrar cualquier paper o proyecto.

A mi tutor académico, el Dr. José González Cataño, por la corrección de la tesis doctoral.

Fuera del laboratorio quiero dar las gracias a Benito, por aguantarme y dejarme que le aguante, por las horas de pelis, de cenas y de piscina y por muchas cosas más. A Marta, por estar ahí todos estos años, por nuestros bailes, nuestras comilonas y nuestras vueltas por el plenilunio buscando pantalones. A Ana, que desde el máster ha estado cerca en todo momento, ayudándome en lo que he necesitado y con la que tan buenos momentos he pasado. También a mis amigos de Úbeda y de Navalosa, a mis *clonos*, a mis *postus*, y a mis compis de biología, porque aunque no nos veamos tan a menudo, estemos repartidos por toda Europa y cada uno nos dediquemos a una cosa diferente, seguimos en contacto y siempre hay un rato para vernos y hablar de cómo van nuestras vidas.

A toda mi familia y a la de Alberto y en especial a mis padres y a mi hermana que son los que han sufrido mis años tanto en la carrera como en la tesis más de cerca. Porque sé que a veces no ha sido tan fácil convivir con una estudiante predoctoral, ni con sus horarios, ni con su extraño trabajo en el que da de comer a células.

Para terminar, tengo que agradecer a Alberto, por su paciencia y cariño. Y porque aunque aún no tiene claro cuál es mi trabajo, ha aguantado como un campeón todos mis dramas científicos y siempre ha hecho el esfuerzo de buscarme y llevarme al laboratorio a cualquier hora y cualquier día. Además de ser mi apoyo diario para seguir adelante.

A todos vosotros, una vez más, gracias.

Summary

Summary

T cell activation depends on the ability of the T cell receptor (TCR) to recognize specific antigens presented in the context of the major histocompatibility complex (MHC) on the antigen-presenting cell (APC). The binding of the TCR to MHC promotes the formation of the immune synapse (IS). In this process, the TCR and its associated molecules localize to a central area of the T-cell-APC contact, the central supramolecular activating complex (cSMAC). Adhesion molecules relocate to the peripheral supramolecular activating complex (pSMAC). Essential proteins in this process are the Src family kinase members (Lck and Fyn). Lck phosphorylates the immunoreceptor tyrosine-based activation (ITAM) motifs of the TCR/CD3 complex leading to the recruitment of key molecules for the downstream signalling pathways and the IS formation. The formation of the IS also triggers changes in the tubulin cytoskeleton, including the translocation of the centrosome or microtubule (MT)-organizing centre (MTOC), to the IS, which is accompanied by the Golgi Apparatus, multivesicular bodies and mitochondria. These changes facilitate the polarized secretion of cytokines and exosomes toward the APC. MTOC polarization orchestrates active MT growth and forms the core of a dense MT network that regulates vesicular traffic at the IS.

Aurora A is a serine/threonine kinase that plays a critical role in centrosome and spindle dynamics during mitosis. During centrosome maturation, Aurora A promotes MT assembly by recruiting nucleation and stabilization factors. Due to its role in controlling MT dynamics, we hypothesized that Aurora A may play a role in the activation of T lymphocytes during IS formation. We found that Aurora A is activated upon TCR stimulation and localizes at the IS during contact. Moreover, inhibition of Aurora A with pharmacological agents or genetic deletion in human or mouse T cells severely disrupts the dynamics of microtubules and CD3-bearing vesicles at the IS. Specific targeting of Aurora A impairs activation of the TCR/CD3 complex, preventing early T cell activation and downstream expression of CD69, CD25 and IL-2. Aurora A inhibition causes delocalized clustering of Lck at the IS and decreases phosphorylation levels of tyrosine kinase Lck, thus indicating Aurora A is required for maintaining Lck active. These findings establish Aurora A as a major regulator of early signaling and the tubulin cytoskeleton during T cell activation.

Resumen

Resumen

La activación de las células T depende de la capacidad del receptor de células T (TCR) para reconocer antígenos específicos en el contacto del complejo mayor de histocompatibilidad (MHC) de las células presentadoras de antígeno (APC). La unión del TCR al MHC promueve la formación de la sinapsis inmunológica (IS). En este proceso, el TCR y las moléculas que se asocian a él se localizan en el área central de la región de contacto entre la célula T y la APC, en lo que se conoce como el complejo de activación supramolecular central (cSMAC). Las moléculas de adhesión se trasladan al complejo de activación supramolecular periférico (pSMAC). Algunas de las proteínas esenciales en este proceso son los miembros de la familia de proteínas Src (Lck y Fyn). La proteína quinasa Lck fosforila los motivos de activación de inmunorreceptores basados en tirosina del complejo TCR/CD3 permitiendo el reclutamiento de moléculas esenciales para la ruta de activación del TCR y la formación de la IS. La formación de la IS también induce cambios en el citoesqueleto de tubulina, incluyendo la translocación del centrosoma o el centro organizador de microtúbulos (MTOC), hacia la IS, acompañado por el aparato de Golgi, los cuerpos multivesiculares y las mitocondrias. Estos cambios facilitan la secreción polarizada de citoquinas y exosomas hacia la APC. La polarización del MTOC dirige el crecimiento activo de microtúbulos (MT), constituyendo el núcleo de una densa red de MT que regula el tráfico vesicular en la SI.

La proteína Aurora A es una serina/treonina quinasa que desempeña un papel crítico en la dinámica del centrosoma y del huso mitótico durante la división celular. Durante la maduración del centrosoma, Aurora A promueve el ensamblaje de MT mediante el reclutamiento de factores nucleadores y estabilizadores de los mismos. Debido a su papel en el control de la dinámica de MT, postulamos que Aurora A podría ejercer un papel importante en la activación de células T durante la formación de la SI. Encontramos que Aurora A se activa tras la estimulación del TCR y se localiza en la IS durante el contacto celular. Por otro lado, tanto la inhibición farmacológica como la depleción génica de Aurora A en células T humanas o de ratón altera severamente la dinámica de MT así como el transporte a la IS de microvesículas que contienen CD3. El bloqueo de Aurora A impide la activación del complejo TCR/CD3, interrumpiendo la activación temprana de las células T así como la expresión de los genes CD69, CD25 y IL-2. La inhibición de Aurora A causa la deslocalización de tirosina quinasa Lck en la región de la SI y disminuye sus niveles de fosforilación, lo que indica que Aurora A es necesaria para mantener a Lck en su forma activa. Estos hallazgos demuestran que Aurora A es una molécula reguladora importante en la señalización temprana y del citoesqueleto de tubulina durante la activación de los linfocitos T.

Index

List of abbreviations

List of abbreviations

ACD: Asymmetric Cell Division
ADAP: Adhesion and Degranulation-promoting Adapter Protein
APC: Antigen Presenting Cell
BSA: Bovine Serum Albumin
BF: Bright Field
CaM: calmodulin
Cbp: Csk Binding Protein
Csk: C terminal Src Kinase
CDC42: Cell Division Cycle 42
CRAC: Ca^{2+} release-activated channels
cSMAC: central Supramolecular Activation Cluster
D-box: Destruction box
DMSO: Dimethyl Sulfoxide
DC: Dendritic Cell
EB: End-Binding protein
ERK: Extracellular signal-Regulated Kinase
GA: Golgi Apparatus
GFP: Green Fluorescence Protein
GM-CSF: Granulocyte Macrophage Colony-Stimulating Factor
G418: Geneticin
HA: Hemagglutinin
HDAC6: Histone Deacetylase 6
ICAM: Intercellular Adhesion Molecule
ITAM: Immunoreceptor Tyrosine-based Activation motifs
Ig: Immunoglobulin
IFN: Interferon
IFT: Intraflagellar Transport
IL: Interleukin
IP3: 1,4,5-triphosphate
IS: Immunological Synapse
kDa: KiloDalton
LAT: Linker of activated T cells
Lck: Lymphocyte-specific protein tyrosine kinase
LPS: Lipopolysaccharide
mAb: Monoclonal Antibody
MAPK: Mitogen-Activated Protein Kinases
MAL: Myelin And Lymphocyte protein
MHC: Major Histocompatibility Complex
MT: Microtubule
MTOC: Microtubule-Organizing Center
OVA: Ovalbumin
PAG: Phosphoprotein Associated with Glycosphingolipid-enriched microdomains
PBLs: Peripheral Blood Lymphocytes
PBMCs: Peripheral Blood Mononuclear Cells
PBS: Phosphate Buffered Saline
PCM: Pericentriolar Matrix
PIP2: Phosphatidylinositol-4,5-bisphosphate
PKC: Protein Kinase C
PLCγ1: Phospholipase C, gamma 1
Plk-1: Polo-like Kinase 1
pSMAC: peripheral Supramolecular Activation Cluster
SEB: Superantígeno B
SEE: Superantígeno E
SFK: Src Family Kinase
siRNA: small interfering RNA
TACC: transforming acidic-coiled-coil
TCR: T Cell Receptor
TIRFm: Total Internal Reflection Fluorescence microscopy
TGN: *Trans*-Golgi Network
Unc-119: Uncoordinated 119
VCAM: Vascular Cell Adhesion Molecule
VLA: Very Late Antigen
WASp: Wiskott–Aldrich syndrome protein and SCAR homologue
WB: Western Blot
WT: Wild Type
ZAP70: ζ chain-associated protein kinase 70
γ-TURC: γ-Tubulin Ring Complex

List of figures

List of figures

Introduction

Results

Discussion

Introduction

1. Introduction

1.1 Immune and adaptive immunity

Immune responses protect the organism against infections through cell- and molecular- based mechanisms. These mechanisms are subdivided in two arms of the immune response: innate and adaptive. Both responses are executed by cells of different linages and are interdependent. Innate immune system acts providing immediate defence against pathogens by recognizing and responding to them in a generic way. Innate immune system activates the adaptive immune system through the process known as antigen presentation. Adaptive immunity is a highly specialized system, composed by several cell types and complex processes. This mechanism allows to respond to a specific pathogen, generating immunological memory for future infections. The axis of the adaptive immune response resides in lymphocytes. B lymphocytes are responsible for humoral immunity, providing defense through secretion of antibodies. By contrast, T lymphocytes are involved in cell-mediated immunity. There are two different population of T lymphocytes, cytotoxic $CD8^+$ and helper $CD4^+$ T lymphocytes. $CD8^+$ lymphocytes are involved in eliminating cells producing foreign antigens, such as virus-infected cells and other intracellular microorganisms. By contrast, the $CD4^+$ T lymphocytes provide an important link between adaptive immunity and effectors of innate immunity mechanisms, promoting the proliferation and differentiation of other lymphocytes and activating and recruiting cells of the innate immune response (Fig. I1).

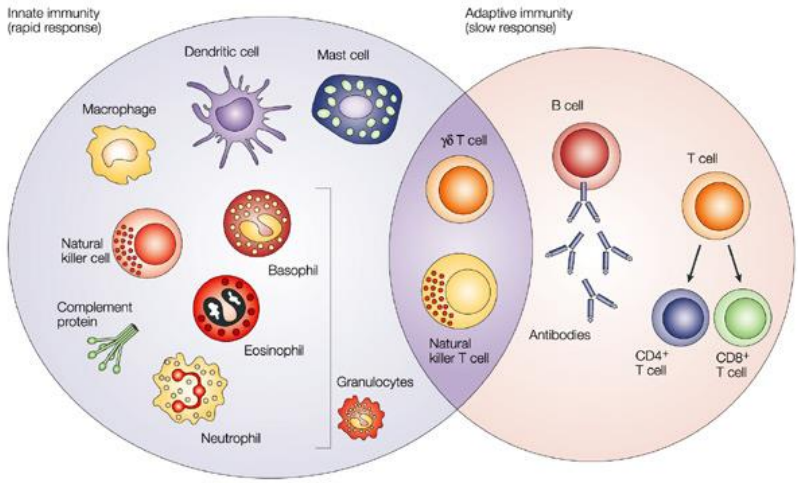

Figure I1. Different components of the immune system. The innate immune response is the first line of defence against infection. It is composed by several cellular components such as dendritic cells, mast cells, macrophages, natural killer cells and granulocytes (basophils, eosinophils and neutrophils) and soluble factors including complement proteins. The adaptive immune response acts later but in a specific way. It is composed by B lymphocytes that produce antibodies, and $CD4^+$ and $CD8^+$ T lymphocytes that carry out the cellular response. Natural killer T cells and γδ T cells are cytotoxic lymphocytes that are in the middle of innate and adaptive immunity (Dranoff, 2004).

1.2 ¿What is the immune synapse?

The contact between the T cell and the antigen presenting cell (APC) is termed the immune synapse (IS) and this structure acts as a transient, cell-to-cell communication structure between the T cell and the APC, which is a hallmark of the adaptive immune response (Monks et al, 1998). This intimate contact promotes the proliferation and differentiation of the lymphocytes involved in the contact. The first encounter of a T lymphocyte with an antigen bearing sufficient affinity for its T cell receptor (TCR) to trigger its activation takes place at lymph nodes that drain most peripheral tissues. It depends on the interaction of the T cell with an APC that presents the antigen associated to its major histocompatibility complex (MHC) molecules. APCs can be myeloid cells, such as dendritic cells or macrophages; lymphoid, e.g. B lymphocytes, or non-immune cells, such as target cells that have been infected by virus or bacteria or are transformed into tumorigenic cells, activated endothelial cells and some others (Friedl et al, 2005). T cells scan the surface of the APC and if the affinity of the TCR for the peptide-MHC complex is sufficient, the TCR undergoes conformational changes that activate different signaling pathways, leading to cytoskeletal reorganization and organelle polarization to the contact area with the APC. The stability of the IS is sustained by the TCR-dependent transactivation of adhesion molecules, e.g. integrins, which maintain the IS over time and seal the extracellular space between the T cell and the APC. In this manner, the T:APC space adopts cleft shape, not unlike those observed in neuronal synapses. The IS structure is classically described as an eye-shaped molecular assembly. It is formed by a central SMAC (cSMAC; supramolecular activation clusters) that contains TCR with associated molecules (TCR signalosomes). The cSMAC is surrounded by the peripheral SMAC (pSMAC), which comprises adhesion molecules such as integrins (Davis & van der Merwe, 2006). Moreover, the distal SMAC (dSAMC) is enriched with proteins with large extracellular domains such as phosphatases that may have an inhibitory role during the IS formation (Davis & Dustin, 2004). This structure establishes an intimate contact between the T cell and the APC that increases the relative concentration of secreted molecules, thereby facilitating the exchange of signals between them (Fig. I2).

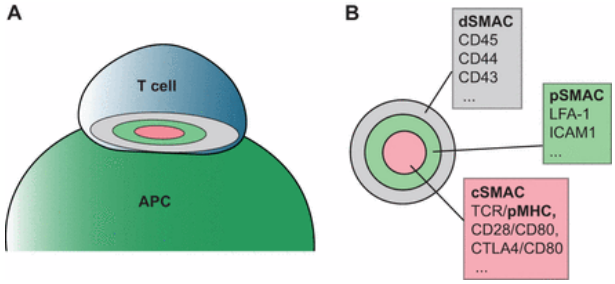

Figure I2. Diagram of the IS in the contact area between a T cell and an APC. (a) T cell activation promotes the segregation of different molecules in the contact area between both cells during the IS formation. **(b)** Diagram showing the 'bull's eye' pattern of several distinct concentric domains, which are known as supramolecular activation clusters (SMACs). The cSMAC (central, pink) is enriched with TCR microclusters, co-stimulatory receptors and protein-tyrosine kinases. The pSMAC (peripheral, green) contains integrins, such as LFA-1 and its ligand ICAM1, and cytoskeletal linker protein. The dSMAC (distal, grey) includes protein-tyrosine phosphatase CD45 and glycoproteins CD44 and CD43 (Yu et al, 2013).

1.3 T cell-APC contact: Initiating the IS

The formation of the IS involves that the membrane of the T cell and that of the APC are in close proximity to each other. The plasma membrane is not entirely homogeneous; separate domains can be defined according to their different composition of lipids and proteins (Brown, 1998). In terms of lipids, the plasma membrane is formed by different specific domains distinguished by their solubility or insolubility in non-ionic detergents. Insoluble, cholesterol-rich microdomains are classically termed 'rafts' (Simons & Ikonen, 1997). Since different adaptors and signaling intermediates display a preference for localizing in raft or non-raft domains, lipid-based regions can be considered as platforms for signaling molecules involved in T cell activation. In this view, these platforms boost, or block signaling; and these signals are coordinated by the action of different lipid-associated proteins that are the backbone of these specific microdomains. The coalescence of specialized membrane microdomains at the IS requires the dynamic rearrangement of the actin and tubulin cytoskeletons. Both cytoskeletal systems are heavily involved in the movement and segregation of membrane and intracellular components. For example, they participate in the accumulation of the TCR at the IS that accounts for a higher clustering of the TCR than that predicted by models of passive diffusion. In this regard, passive lateral diffusion of receptors is actin-dependent. A model of actin-dependent TCR accumulation envisions the pSMAC as a contractile actin-myosin ring that allows retrograde flow of actin and centripetal movements that direct the TCR/CD3 nanoclusters to the center of the IS (Ilani et al, 2009). Nanoclusters merge into microclusters before reaching the cSMAC (Lillemeier et al, 2010; Varma et al, 2006).

A proposed model is that TCR/CD3 is translocated into specific cholesterol-enriched microdomains, where it is activated by Lck (He & Marguet, 2008; Swamy et al, 2016). CD28, a major co-stimulation receptor that binds to CD80 and CD86 also concentrates at the cSMAC, controlling the ability of PKCθ to activate transcription factors, e.g. NF-κB (Yokosuka *et al.*, 2010).

The cognate recognition of peptide-MHC (p-MHC) by the αβTCR subunits of the TCR-CD3 complex promotes a conformational change in the heterodimers containing the CD3ε subunit (CD3 γε and δε) prior to the phosphorylation on its own immunoreceptor tyrosine-based activation motif (ITAM) and the three ITAMs at each CD3ζ subunit of the homodimers that are part of the CD3 complex (Figure I3). Nck is rapidly recruited to the TCR/CD3 complex upon exposure of a proline-rich, Nck-binding sequence (PRS) in CD3ε. Nck then binds to the adaptor protein Src homology 2 (SH2) domain-containing leukocyte protein of 76 kD (SLP76) and Vav, which in turn promotes the re-organization of the actin cytoskeleton (Gil et al, 2002). In addition to this conformational change, ITAM phosphorylation by the Src-family kinase Lck and/or Fyn enables the recruitment of proteins containing SH2 domains, such as ZAP70. CD3 and ZAP70 coupling predates the recruitment of CD4 or CD8 co-receptors, which are bound to Lck. CD4 or CD8 remain in close proximity to the TCR-CD3 complex, enabling lateral binding to the corresponding MHC (CD4-MHCII; CD8-MHCI). This interaction stabilizes the TCR-p-MHC interaction, while Lck keeps phosphorylating ITAMs that are being recruited to the macromolecular complex (Gascoigne et al, 2011).

Active ZAP70 phosphorylates LAT, which is a scaffold protein bearing multiple tyrosine residues. Phosphorylated LAT acts as docking site for different proteins. LAT forms two spatially segregated pools; one appears at the plasma membrane and it is involved in the amplification of the initial TCR signal. A second pool localizes to intracellular compartments (Bonello et al, 2004). LAT interacts with SLP76, which recruits multimolecular complexes that converge on the cytoskeletal regulators CDC42/Rac, Nck and Vav, thereby controlling the remodeling of T cell actin cytoskeleton (Martin-Cofreces et al, 2014; Pauker et al, 2012) (Fig. I3)). One molecule of these complexes is PLCγ1, which binds to LAT at phospho-Y132 and hydrolyzes phosphatidylinositol 4,5-bisphosphate (PIP2) to produce inositol 1,4,5-triphosphate (IP3) and diacylglycerol (DAG). DAG is an activator of different PKCs (serine/threonine kinases) while IP3 causes a sustained increase in intracellular Ca2+ concentrations from endogenous reservoirs, which is crucial for NFAT activation (Balagopalan et al, 2010). Production of DAG is a critical step for the propagation of signals emanating from the TCR and centrosome polarization to the IS (Quann et al, 2009).

DAG binds to and activates PKD2. PKD2 also requires PKC-dependent phosphorylation on S707 and S711 for its complete activation. This process promotes the amplification of PKC and PKD2 activation and mediates the production of cytokines that stimulate T cell proliferation and T cell-dependent inflammation, such as interleukin 2 (IL-2) and interferon gamma (IFNγ), respectively (Navarro et al, 2012). Additionally, DAG participates in the activation of Ras through binding to the serine/threonine kinase Raf-1. Ras activation initiates the mitogen-activated protein kinases signaling cascade (MAPK). This results in the phosphorylation and activation of the serine/threonine kinases ERK1 and ERK2, which in turn phosphorylate and activate transcription factors, e.g. ELK-1, SAP-1 and SAP-2. As a result, ERK1 and 2 regulate the expression of early activation genes such as c-Fos and c-Jun in T cells. Furthermore, ERK1 and 2 also play a role in microtubule (MT) remodeling through the regulation and phosphorylation of stathmin (Filbert et al, 2012). RSK (Ribosomal S6 kinase) is also regulated by ERK1 and 2, promoting cell cycle progression and cytokine production in T cells. Finally, other proteins regulated by the ERK1/2 pathway are MNK1 and MNK2, which participate in the phosphorylation of the eukaryotic translation initiation factor eIF4E (Navarro & Cantrell, 2014; Romeo et al, 2012) (Fig. I3)).

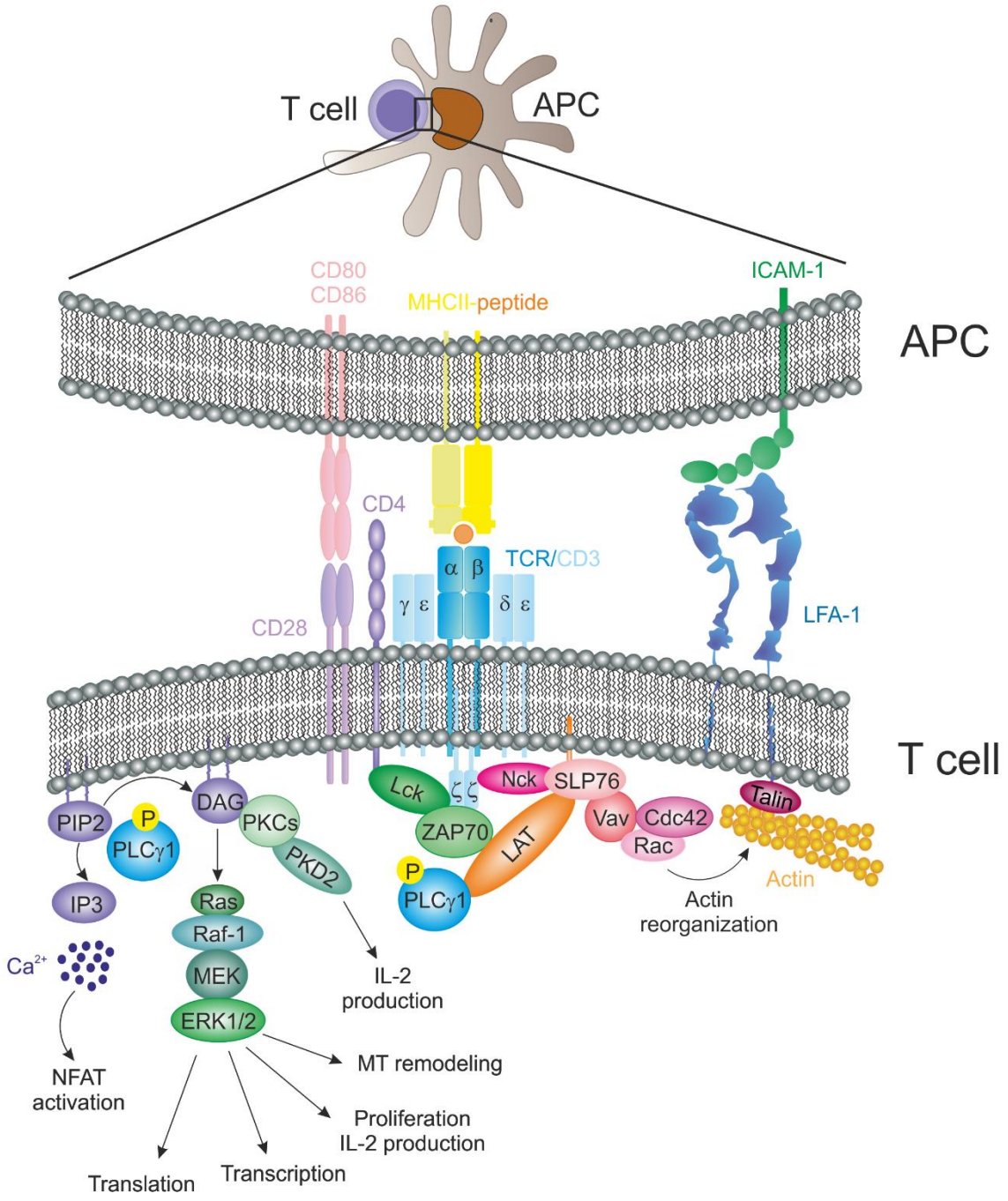

Figure I3. Membrane microdomains in T cell activation. TCR-activation pathways. Upon TCR recognition of a peptide-charged MHC, the TCR/CD3 complex undergoes conformational changes (not depicted). These conformational changes initiate its activation, allowing Nck binding to CD3ε and actin polymerization. TCR/CD3 conformational changes also favor the phosphorylation of the intracellular ITAMS of the CD3ε and CD3ζ subunits by Lck. Phosphorylated ITAMs are docking sites for the SH2 domains of ZAP70, which accumulates at the TCR/CD3 complexes and phosphorylates LAT in different tyrosine residues. LAT acts as a signaling amplifying platform, where PLCγ clusters and activates. PLCγ generates second messengers for TCR signaling, like IP3 and DAG from PIP2. IP3 activates calcium intracellular flux. DAG helps to the activation of different signaling mediators such as PKC and Ras, to trigger PKD2 and MAPK signaling cascades to induce the expression of late activation genes like IL-2. Nck and LAT act in concert to recruit SLP76, Vav, Cdc42 and Rac1, to reorganize actin cytoskeleton at the IS.

1.4 Intracellular traffic of TCR/CD3, LAT and Lck

The concentration of TCR/CD3 complexes at the IS comes from two sources. One is lateral membrane mobility. The other is the recycling of the complexes via endosomes (Figure I4). In general, the endosomal system is used by the cells to maintain a metabolic steady-state, enabling the rapid reutilization of pre-synthesized molecules. Endosomes are characterized by the localization of different Rab GTPases bound to their membrane, e.g. Rab11. These molecular switches act as spatial and temporal coordinators of recycling (Baetz & Goldenring, 2013). Endosomes also contain signaling molecules and adaptor proteins. Finally, they are essential for plasma membrane replenishment at the IS. This is a crucially important event, because the interaction between the T cell and the APC through the IS continuously triggers TCR/CD3 internalization. However, for sustained signaling to take place, the amount of TCR/CD3 complexes at the T cell surface of the IS need to be relatively constant (Varma et al, 2006), hence the internalized fraction needs to be renewed immediately (Das et al, 2002). Not surprisingly, the endosomal TCR/CD3 pool constitutes an important fraction of the total amount of TCR/CD3 that is recycled back to the IS (Fig. I4). The amount of internalization/recycling events at the IS functionally results in heavy and localized vesicular trafficking, leading to the definition of the IS as a focal point of endocytosis/exocytosis.

Although actin dynamics may contribute to TCR/CD3 complex concentration at the IS, mainly due to retrograde flow (Beemiller et al, 2012), the recycling pool is mostly driven by MT and MT-based motors. Moreover, dynein, a minus-end directed MT motor protein, accumulates at the pSMAC, where it associates with ADAP (Adhesion and Degranulation promoting Adaptor Protein). This interaction may generate the pulling force needed to polarize the centrosome to the IS (Combs et al., 2006). This can be graphically described as “reeling a fish”, in which the dynein-ADAP complex acts as a fixed reel, the MTs would be the line and the centrosome would be the fish. However, dynein/dynactin activity was also found essential for sustained T cell activation, which likely means that dynein is not only involved in the reeling of the centrosome, but also in its long-term maintenance in the contact zone (Hashimoto-Tane et al, 2011; Martin-Cofreces et al, 2008).

On the signaling front, continuous internalization and recycling of TCR/CD3 depends on the phosphorylation of a di-leucine motif present on the CD3γ chain mediated by PKC, which is then recruited by the clathrin adaptor protein AP-2 (Monjas et al, 2004). TCR/CD3 complexes that enter this pathway are directed to recycling endosomes positive for Rab4 and Rab11. Rab4-endosomes are early endosomes involved in the rapid shuttling of internalized receptors to the plasma membrane in a MT-independent manner. On the other hand, endosomes marked by Rab11 aggregate in more distal locations inside the cell, following a slower route and moving along the MT in order to return to the plasma membrane. Other Rab GTPases, e.g. Rab35, are also involved in the regulation of endosomal trafficking as well as in actin polymerization through WASp (Wiskott–Aldrich syndrome protein and SCAR homologue). WASp activates Arp2/3 complex and also interacts with tubulin cytoskeleton in both early and late endosomes,

conjoining both networks to promote efficient endosome shuttling back to the IS (Finetti et al, 2015) (Fig. I4).

TCR/CD3-containing endosomes can also be degraded by fusion with lysosomes (endolysosomal system). This is important to modulate TCR-dependent signaling. TCR/CD3 internalization and subsequent degradation requires a TCR ligand, and it also involves Lck and ZAP-70. Lck is also implicated in a constitutive TCR internalization by phosphorylating clathrin heavy chain (Crotzer et al, 2004). Despite these data, there is also evidence of tyrosine kinase-independent TCR internalization and downregulation.

Regarding the type of membrane-dependent mechanism involved in TCR/CD3 internalization, it has been proposed that non-engaged, bystander TCRs are internalized in clathrin-coated pits, while engaged TCRs are internalized in a cholesterol-enriched domains-dependent manner (Monjas et al, 2004). More recently, GPCR-interacting β-arrestin-1, which is a multiple-subunit receptor without intrinsic enzymatic activity, has been identified as a new ligand that can bind to phosphorylated ITAMs. This fact places TCR/CD3 complexes also in the GPCRs-driven, arrestin-dependent internalization pathway. TCR/CD3 ligation promotes its PKC-dependent phosphorylation at S163, which in turn promotes β-arrestin-1 recruitment. In this manner, bystander, co-internalized TCRs are directly recycled back to the plasma membrane, while engaged, internalized TCRs are targeted to lysosomes for degradation (Fernandez-Arenas et al, 2014).

In contrast to TCR/CD3 vesicles, which are controlled by VAMP3, the endosomal recruitment and docking of LAT to the cortical region of the IS depend of the v-SNARE protein VAMP7. It is, however, important to note that CD3 vesicles may also interact with VAMP7. Endosomal pools of LAT are localized in different subpopulations of recycling endosomes positive for Rab27 and Rab37 (Fig. I4). The main difference between CD3- and LAT-containing vesicles is that LAT vesicles do not fuse with the plasma membrane. This suggests that early phosphorylation of LAT upon TCR activation depends on the clustering of the LAT pool at the plasma membrane, rather than on the LAT subset at endosomes. The latter pool is likely more important to stabilize signaling mediators close to the TCR (Larghi et al, 2013; Soares et al, 2013a). Analysis of end-binding protein 1 (EB1) by TIRFm (total internal reflection fluorescence microscopy) showed that MT growing mediated by EB1 favors the movement of cortical vesicles underneath the TCR/CD3 microclusters at the plasma membrane. EB1 also favors the proximity of LAT- and TCR/CD3-harbouring vesicles at the IS, thereby facilitating the sustained activation of LAT and PLCγ1 upon TCR triggering (Martin-Cofreces et al, 2012). Moreover, a Rab11b- and MAL-positive endosomal pool containing Lck also contributes to T cell activation. In this pool, MAL enables the association of Lck to the plasma membrane at the IS, whereas Rab11b interacts with myosin 5B through the adaptor protein uncoordinated 119 (Unc-119), promoting the movement of the vesicles from the peri-centrosomal region to the IS (Martin-Cofreces et al, 2014; Soares et al, 2013b) (Fig. I4)).

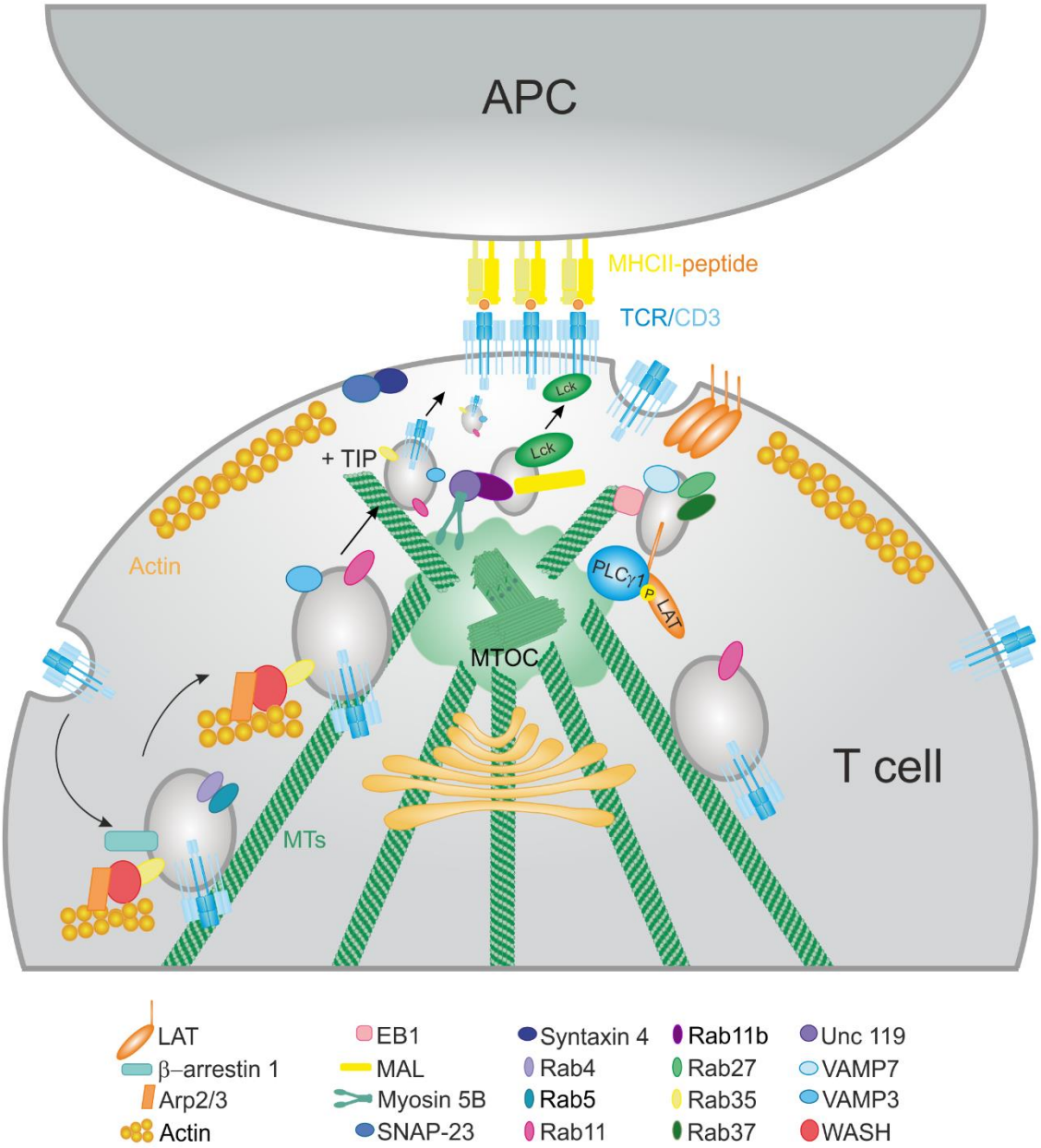

Figure I4. Intracellular traffic and activation at the IS. TCR recycling is important for a sustained T cell signalling. TCR complex is endocytosed by the formation of Rab4- and Rab11-bearing vesicles. They are transported along the MTs towards the MTOC or centrosome. Once in the proximity of the IS they fuse in a VAMP3-dependent manner. Lck and LAT also have an intracellular pool that docks at the IS. Lck vesicles are transported in a myosin II-dependent manner in vesicles bearing Rab11b and Unc119, and its release to the plasma membrane depends on MAL protein. LAT vesicles, marked with Rab27 and Rab37, move to the subcortical region and its accumulation and dynamics there depend on their interaction with EB1 and the tubulin cytoskeleton.

1.5 The centrosome as an organelle-organizing center

In different immune cell types, cytoskeletal remodeling underlies functional polarization. This process is important for many highly specialized and polarized cells, such as the neurons, in which the localization of the centrosome determines the number of neurites that initially sprout from the cell body, and which of

these becomes the axon (de Anda et al, 2005). Microtubule-organizing centre (MTOC) reorientation also promotes the movement of other cellular organelles such as the Golgi Apparatus (GA), the mitochondria and the recycling and secretory apparatus. These events also occur in T cells in response to antigen recognition by the TCR. TCR triggering in a polarized, migrating T cell trumps migratory polarity, and the leading edge evolves into a structure containing radially symmetric lamellipodium that spreads over the APC (Dustin et al, 2010). The MTOC relocates to the cSMAC, along with many other cellular components and organelles (Huse et al, 2008). MTOC polarization promotes a directional secretion of cytokines and vesicles towards the APC, which is very important for the specificity of the $CD4^+$ T cell-dependent response (Mittelbrunn et al, 2011). Moreover, MTOC translocation is crucial for the function of cytotoxic T lymphocytes and NK cells, enabling the polarized secretion of granules containing perforin, granzymes and cathepsins that kill target cells (Stinchcombe & Griffiths, 2007).

The Src family of Tyr-kinase proteins, e.g. Lck, is involved in centrosome translocation and docking to the membrane upon TCR activation. An early study demonstrates that Lck-dependent ITAM phosphorylation in the TCR/CD3 complex was essential for centrosome polarization (Lowin-Kropf et al, 1998). However, later evidence shows that Lck-deficient cells do polarize the centrosome around the nucleus, but cannot maintain the centrosome at the IS, suggesting that this protein is not involved in centrosome translocation per se, but it participates in its stabilization at the IS (Tsun et al, 2011). On the other hand, Fyn-deficient cells do not polarize the centrosome properly; interestingly, Fyn does not compensate the lack of Lck, which indicates that both proteins are important for centrosome translocation and docking (Martin-Cofreces et al, 2006).

Another important factor is DAG (Figure I5). DAG is produced by PLCγ1 at the IS during its formation, promoting the recruitment of several proteins containing DAG-binding C1 domains to the plasma membrane. MTOC polarization is preceded by accumulation of DAG at activated TCR microclusters, suggesting that DAG guides centrosome positioning. Indeed, the absence of DAG blocks centrosome translocation (Huse, 2012). T cells likely use both DAG and PIP3 to decouple lamellipodial dynamics from centrosome movement. The clustering of DAG and PIP3 conversion by lipid phosphatases may be important for the transition between migratory and synaptic morphologies (Huse, 2012). Some of the DAG-binding proteins are members of PKC family, which are involved in many TCR-induced responses such as proliferation and secretion of cytokines (Baier & Wagner, 2009). There is an early accumulation of PKCε and PKCη at the IS, which is followed by the subsequent accumulation of PKCθ at the peripheral actin ring and the polarization of the centrosome (Quann et al, 2011). The differences in the timing of recruitment of these proteins can be explained by their affinities for DAG; PKCε and PKCη bind to DAG with higher affinity than PKCθ (Huse et al, 2013). Therefore, affinity for DAG and the interaction with other lipid or proteins could potentially tune the localization of different PKCs.

On the other hand, accumulation of DAG at the IS engages the MT-based dynein motor complex (Quann et al, 2009). Dynein is a multisubunit protein composed by two heavy chains that contain the motor

and MT binding domains and several accessory light chains that provide structural integrity and support interactions with other proteins. One of these interacting proteins is dynactin, a multi-subunit complex that enhances dynein processivity and controls its localization (Fu & Holzbaur, 2014; Kikkawa, 2013). The recruitment of SLP-76 and ADAP into the integrin ring at the pSMAC facilitates dynein movement to the IS (Combs et al, 2006). The dynein/dynactin complex is involved in the polarization of the MTOC to the IS in human T cells (Fig. I5). Disruption of dynein/dynactin complex prevents the correct localization of the centrosome (Martin-Cofreces et al, 2008), while ADAP depletion prevents both dynein accumulation and MTOC translocation (Combs et al, 2006). ADAP interacts with MTs and also with dynein, suggesting that accumulation of ADAP at the pSMAC generates tension along MTs that support the MTOC reeling mechanism toward the IS (Combs et al, 2006). This suggests that dynein/dynactin complex may help dock the MTOC to the IS by interacting with Fyb/ADAP (Martin-Cofreces et al, 2014) (Fig. I5). However, in mouse primary T cells, depletion or inhibition, of dynein is not enough to block the translocation of the MTOC; although it slows the dynamics of TCR/CD3 microclusters (Hashimoto-Tane et al, 2011). These results suggest that a dynein-independent pathway may also mediate MTOC reorientation; or that these mechanisms differ from human to mouse lymphocytes.

Coupling between actin and MT networks seems essential for MTOC translocation (Martin-Cofreces et al, 2011; Obino et al, 2016). Several proteins involved in coupling MT and actin cytoskeletons include the scaffolding molecule IQGAP1 and the Diaphanous formins. These molecules do participate in MTOC polarization (Gomez et al, 2007). A proposed model suggests that dynein may pull the MT cytoskeleton, while myosin II may push it from behind, although the role of myosin II still remains unclear (Liu et al, 2013). Therefore, much work is still needed to elucidate the cross-talk between actin and tubulin-based motors in MTOC polarization.

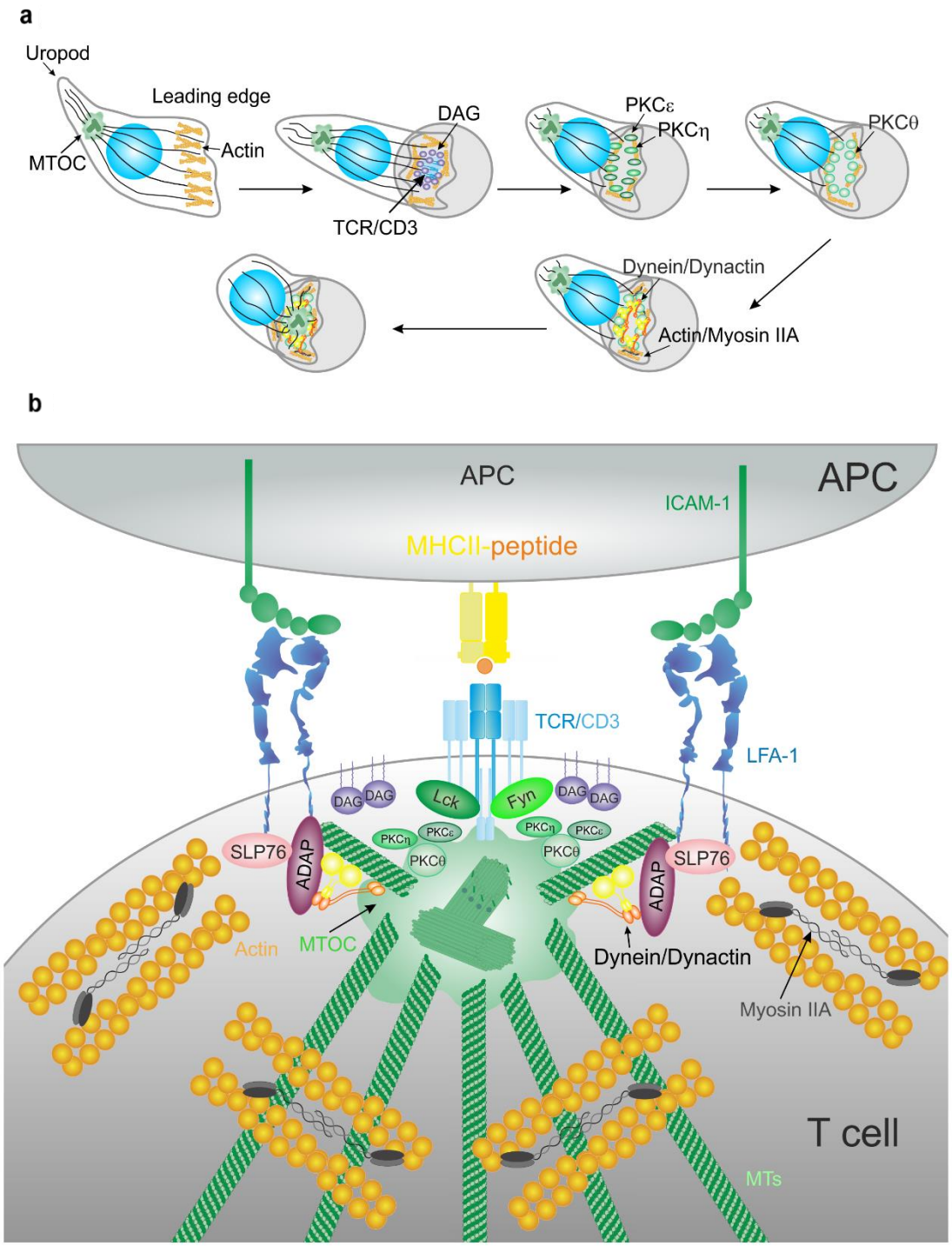

Figure I5. Centrosome translocation and docking at the IS. (a) Contact between the APC and T cell triggers a rapid translocation of the MTOC towards the IS (2-5 min). Migrating lymphocytes show a polarized shape. Cognate contact with a specific APC promotes clustering of TCR/CD3 complexes and production of local DAG. PKCε and η cluster to DAG and helps actin polymerization. PKCθ clusters to actin cytoskeleton and regulates its dynamics. Dynein/dynactin complexes and Myosin IIA helps the coalescence of TCR/CD3 microcluster and MTOC translocation to the IS in formation. **(b)** Activation of TCR/CD3 through the phosphorylation of the ITAMs by Lck and Fyn members of src family of kinases promotes MTOC translocation to the IS. This movement depends on the dynein/dynactin complex and also requires the interaction of ADAP with the integrins to generate the pulling force towards the IS.

1.6 The Aurora family

The Aurora family of serine/threonine kinases comprises three members in humans—Aurora A, B and C—which are encoded by three different genes (Carmena & Earnshaw, 2003) and are key regulators of different mitotic processes (Barr & Gergely, 2007). Auroras contain a specific aurora kinase domain with a regulatory threonine residue in the activation loop, which phosphorylation promotes kinase activation. Auroras also present a D-box domain (destruction box), which mediates their proteasome-dependent degradation and a N-terminal regulatory domain involved in substrate binding and subcellular location (Lukasiewicz & Lingle, 2009) (Fig. I6). Aurora A plays a critical role for proper cell cycle progression and in centrosome and spindle dynamics during mitosis, whereas Aurora B regulates the kinetochore attachment to the MTs and cytokinesis (Hochegger et al, 2013). Aurora C is the least studied member of the family and seems to have a role during meiosis (Yang et al, 2015).

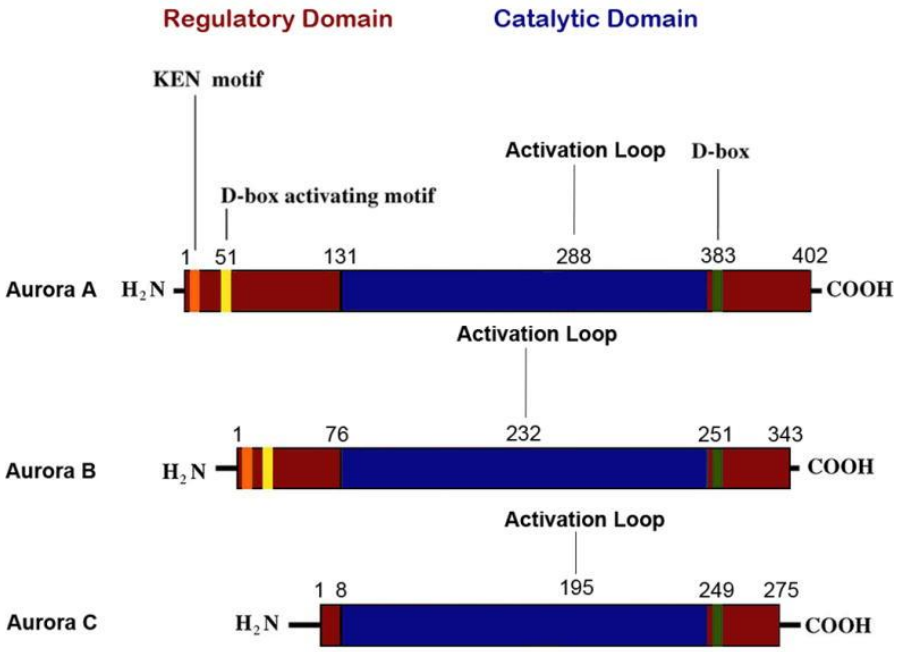

Figure I6. Structure and domains of the Aurora kinases family. Members of Aurora family are composed by three domains: regulatory, catalytic and destruction box. Key residues are represented (Goldenson & Crispino, 2015).

Aurora A is self-activated by autophosphorylation at T288 in its T loop, helped by cofactors including Bora, TPX2, Ajuba and PAK1 (Barr & Gergely, 2007; Bischoff et al, 1998; Gopalan et al, 1997). The mechanism of activation by cofactors is well established in case of TPX2. TPX2 induces the autophosphorylation of Aurora A but also prevents dephosphorylation of the activating residue by the protein phosphatase PP1 (Bayliss et al, 2003). Moreover, TPX2 targets Aurora A to the mitotic spindle MTs for assembly and maintenance of the mitotic spindle (Kufer et al, 2002). Polo-like kinase 1 (Plk-1) and CDK11 are also involved in Targeting of Aurora A to the centrosomes for their proper maturation (Barr &

Gergely, 2007; Petretti et al, 2006). During late S/early G2 Aurora A exchanges continuously between the centrosomes and a cytoplasmatic pool (Berdnik & Knoblich, 2002). However, there is an Aurora A expression and activity peak in late G2 and the protein is concentrated at centrosomes (Carmena & Earnshaw, 2003; Lukasiewicz & Lingle, 2009). Although Aurora A localization in centrosomes and in the mitotic spindle during mitosis is universally accepted, its location in interphase is not clear. Some of the observed localizations are in the centrosome or, in *Xenopus* egg extract, along the MTs (Lukasiewicz & Lingle, 2009; Sardon et al, 2008).

Aurora A has several functions related to cell division. It promotes mitotic entry by phosphorylating CDC25B, which in turns activates Cyclin B/Cdk-1 complex at the centrosomes (Cazales et al, 2005; Dutertre & Prigent, 2003). Moreover, Aurora A phosphorylates and activates Plk-1 which regulates many others proteins involved in cell cycle progression (Lee et al, 2013; Seki et al, 2008) (Fig. I7).

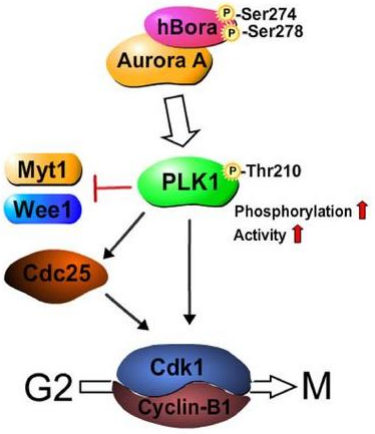

Figure I7. Regulation of mitotic entry by Aurora A. During G2/M transition, Aurora A activates Plk-1 which in turns is going to direct the phosphorylation of several substrates involved in cell cycle progression **(**Modified from Lee et al, 2013).

Aurora A is also involved in centrosome separation after duplication at the early mitosis. Although Aurora A seems not be implicated during centrosome duplication, its absence impedes their separation, resulting in a monopolar spindle (Barr & Gergely, 2007). However, in some cases there is a bipolar spindle that are disorganized when Aurora A function is blocked (Peset et al, 2005). It is consistent with that there are two distinct pathways for centrosome separation: a nuclear-envelope-dependent pathway and a nuclear-envelope-independent one (Barr & Gergely, 2007). In late G2 phase, during centrosome maturation, the pericentrosomal matrix (PCM) directs the MT nucleation through the recruitment of MT nucleating factors such as the gamma-tubulin ring complex (γ-TURC) (Hannak et al, 2001). This recruitment allows the incorporation of αβ-tubulin dimers into new formed MTs (Wiese & Zheng, 2006). It has been established an evolutionary conserved role for Aurora A in centrosome maturation (Hannak et al, 2001; Mori et al, 2007; Sardon et al, 2008) and although the effect caused by Aurora A depletion in different species is not exactly the same, some similarities exist. In this sense, Aurora A depletion in *Caenorhabditis elegans* disrupts the accumulation of γ–tubulin, resulting in a decrease of centrosomal MT levels (Hannak et al, 2001). Furthermore, after nuclear envelope breakdown, centrosome activity increases through the action of the Ran-GTP gradient that emanates from the condensed chromosomes (Gruss et al, 2001). It has been

described that Aurora A activity enhances the Ran-GTP dependent pathway both at the centrosome and in the cytoplasm through the phosphorylation of factors that participate in this pathway (Sardon et al, 2008). This process may be mediated by some proteins that are substrates of Aurora A and targets of Ran-GTP such as TPX2 or Maskin (Gruss et al, 2001; Gruss & Vernos, 2004).

Moreover, Aurora A is also linked to mitotic MT dynamics and stability through the transforming acidic-coiled-coil-containing (TACC) family proteins. TACC proteins interact with the ch-TOG/XMAP215 family of centrosomal proteins which are involved in stabilization of MTs and control their plus-end dynamics (Barr & Gergely, 2007) (Fig. I8).

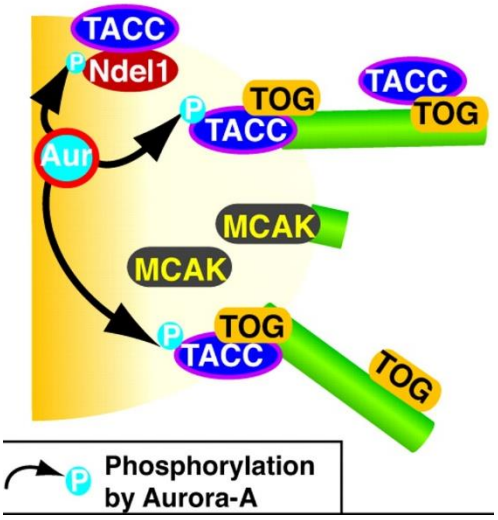

Figure I8. Control of MT stability by Aurora A. TACC is phosphorylated by Aurora A directly or through Ndel1 in the centrosomes. TACC binds to MTs when they are complexed with the MT-stabilising protein ch-TOG/XMAP215. This interaction protects the MTs from the MKAC-induced destabilization (Modified from Barr & Gergely, 2007).

Objectives

2. Objectives

Based on the role of Aurora A in controlling MT dynamics, we postulate that Aurora A may allow the maturation of the centrosome in the stimulated T lymphocytes during the IS, promoting the proper activation of T cells.

In order to challenge our hypothesis, our main aims were:

1) Assess the specific location of Aurora A in T cells during the IS

2) Study the role of Aurora A in cytoskeletal dynamic and in vesicular traffic

3) Analyse the effect of Aurora A inhibition in TCR signalling pathway

4) Control of Lck activity by Aurora A

Materials and methods

3. Materials and methods

3.1 Reagents and antibodies

- Human Fibronectin (FN) and Poly-L-Lys (PLL) from Sigma.
- Enterotoxins E (SEE; 0.3 µg/mL) and B (SEB; 5 µg/mL) from Staphylococcus aureus were from Toxin Technology.
- HA (Hemagglutinin) peptide (200 µg/mL) from Lifetein LLC.
- Recombinant human Lck, histidine tagged from MBL.
- DMSO (Dimethyl Sulfoxide) fron Sigma-Aldrich.
- Cell Tracker Blue CMAC (7-amino-4-chloromethylcoumarin; 0.1µM) from Molecular Probes-Invitrogen. Blue excitation/emission spectra (353/466 nm maxima) is a fluorescent dye well suited for monitoring cell movement or location. This dye is well retained, allowing for multigenerational tracking of cellular movements. The blue excitation/emission spectra are ideal for multiplexing with green and red fluorescent dyes and proteins. Cells were incubated with CMAC in serum free RPMI 1640 + GlutaMAXTM – I + 25mM HEPES for 30 min at 37º C. Non-internalised dye was removed by washing twice with PBS and once with RPMI 1640 + GlutaMAXTM – I + 25mM HEPES with serum.
- Phalloidin conjugated to Alexa Fluor 647 (1:100) from Thermofisher Scientific. Phalloidin is a toxin which binds and stabilizes F-actin.
- Prolong Gold anti-fade mounting medium from Molecular Probes-Invitrogen.
- Aurora A inhibitor (MLN8237; 10 µg/ml) and Aurora B inhibitor (AZD1152; 100 nm/ml) from Selleckchem.
- Anti-human CD3; clon HIT3a (5 µg/ml; eBioscience) and anti-human CD28; clon CD28.2 (2µg/ml; BD Pharmingen)
- Anti-mouse CD3ε; clon 2C11 (10 µg/ml; BD Pharmingen) and anti-mouse CD28; clon 37.51 (5 µg/ml; BD Pharmingen)
- Murine IL-7 (5 ng/ml; PreproTech)
- Human IL-2 (50 U/ml) from National Institutes of Health AIDS Research and Reference Reagent Program.
- Goat anti-Armenian hamster IgG (10 µg/ml) from Jackson ImmunoResearch
- Antibodies used are in the table below:

Primary				
Antibody	**Host species**	**Specificity**	**Manufacturer**	**Use**
OKT3	Mouse	CD3ε	Biolegend	IF
Anti-P-LAT	Rabbit	LAT Y132	Abcam	WB
Anti-LAT	Rabbit	LAT	Santa Cruz	WB
Anti-Tubulin DM1A	Mouse	Tubulin	Sigma	WB
Anti-Tubulin-FITC	Mouse	Tubulin	Sigma	IF
Anti-β-Actin	Mouse	β-Actin	Sigma	IF, WB
Anti-P-ERK 1/2	Rabbit	ERK 1/2 T202/204	Calbiochem	WB
Anti-ERK 1/2	Mouse	ERK	Invitrogen	WB
Anti-P-Src	Rabbit	Lck Y394	Invitrogen	WB
Anti-Lck	Rabbit	Lck	Cell Signaling	IF, WB
Anti-Lck	Rabbit	Lck	Millipore	IP
Anti-P-PKCθ	Rabbit	PKCθ T538	Cell Signaling	WB
Anti-PKCθ	Mouse	PKCθ	Cell Signaling	WB
Anti-PKCθ Sc-13/18	Goat	PKCθ	Santa Cruz	IF
Anti-P-CD3ζ	Rabbit	CD3ζ Y83	Abcam	WB
448	Mouse	CD3ζ	Dr. B. Alarcón	WB
Anti-P-PLCγ1	Rabbit	PLCγ1 Y783	Cell Signaling	WB
Anti-PLCγ1	Rabbit	PLCγ1	Cell Signaling	WB
Anti-P-Aurora A	Mouse	Aurora A T288	Abcam	IF
Anti-Aurora A	Rabbit	Aurora A	Abcam	WB
Anti-V5	Mouse	V5 tag	Invitrogen	IP, WB
Anti-Rac1	Mouse	Rac1	BD Pharmingen	Pull-down, WB
Anti-GST	Mouse	GST	Dr. B. Alarcón	Pull-down, WB
Secondary				
Antibody	**Host species**	**Specificity**	**Manufacturer**	**Use**
GAM-488/568/647	Goat	IgG de ratón	Invitrogen	IF
GAR-488/568/647	Goat	IgG de conejo	Invitrogen	IF
DAM-488/568/647	Donkey	IgG de ratón	Invitrogen	IF
DAR-488/568/647	Donkey	IgG de conejo	Invitrogen	IF
DAG-488/568/647	Donkey	IgG de cabra	Invitrogen	IF
GAM-HRP	Goat	IgG de ratón	Pierce	WB
GAR-HRP	Goat	IgG de conejo	Pierce	WB
DAG-HRP	Donkey	IgG de cabra	Pierce	WB

3.2 Cells

- The human Jurkat-derived T-cell line J77 (Vαl.2 Vβ8+ TCR) and the lymphoblastoid B-cell lines Raji (Burkitt lymphoma) and Hom2 (HLA-DR1 EBV-transformed) were cultured in RPMI 1640 + GlutaMAX–I + 25 mM HEPES (Gibco-Invitrogen) supplemented with 10% fetal bovine serum (Hyclone, Thermofisher). The human Jurkat-derived CH7C17 cells (Vβ3+ transgenic TCR, specific for HA peptide) were grown in the same medium supplemented with 400 μg/ml hygromycin B (Roche Diagnostics) and 4 μg/ml puromycin (Invitrogen).

- CH7C17 clones expressing EB1-GFP were generated by CH7C17 transfection and post-selection with G418 (1 mg/ml).

- HEK293T cells were cultured in DMEM medium (Invitrogen) supplemented with 10% fetal bovine serum, 50 IU/ml penicillin and 50 μg/ml streptomycin.

- Human peripheral blood mononuclear cells (PBMCs) were isolated from buffy coats obtained from healthy donors by separation on a Biocoll gradient (Biochrom) according to standard procedures. Monocytes were separated from PBMCs by a 30 minute adherence step at 37 °C in RPMI supplemented with 10% fetal calf serum. Non-adherent cells were washed off and CD4+ T cells were purified from PBMCs using MACS (magnetic-activated cell sorting; Miltenyi Biotech). Non-adherent cells were obtained after 30 min of the adhesion step at 37 °C. In order to generate SEE-responsive human T lymphoblasts, PBMCs were cultured five days in the presence of SEE (0.1 μg/ml) and then, phytohemagglutinin (5 μg/ml) was added for 2 days. To favor its proliferation, IL-2 (50 U/mL) was added later to the medium every 2 days for a time period of 8 days. These studies were performed according to the principles of the Declaration of Helsinki and approved by the local Ethics Committee for Basic Research at the Hospital La Princesa (Madrid); informed consent was obtained from all human volunteers. These studies were performed according to the principles of the Declaration of Helsinki and approved by the local Ethics Committee for Basic Research at the Hospital La Princesa (Madrid); informed consent was obtained from all human volunteers.

3.3 Mice

The Aurora A conditional model has been described (Perez de Castro et al, 2013). These mice carry an Aurka(lox) conditional allele and the RERTert allele expressing an inducible Cre recombinase. After the appropriate crosses, we obtained the experimental Aurka(lox/lox); RERT(ert/ert) and control Aurka(+/+); RERT(ert/ert) mice used in this study. Cre activation upon tamoxifen treatment induces conversion of the

Aurka(lox) allele to the Aurka(Δ) allele. The Aurora kinase A (AurkA)-inducible mouse model has been reported recently (Piazzolla et al, 2014). This model was generated using the tetracycline-inducible single-copy transgenic system (Beard et al, 2006), and carries the M2-rtTA gene inserted within the Rosa26 allele and a cassette containing the Aurora A cDNA under the control of the doxycycine-responsive promoter (tetO) inserted downstream of the Col1a1 locus. The final mouse model, Col1a1tetO-Aurka/+; Rosa26rtTA/rtTA, overexpresses exogenous Aurora A upon doxycycline treatment in a wide range of proliferative and non-proliferative tissues and cells.

Both Aurora A mouse models were maintained in a mixed background (129/Sv, CD1, C57BL/6J, and FVB/N). Mice were housed in the pathogen-free animal facility of the Centro Nacional de Investigaciones Oncológicas (Madrid) in accordance with the animal care standards of the institution. These animals were observed on a daily basis, and sick mice were killed humanely in accordance with the Guidelines for Humane Endpoints for Animals used in biomedical research. All animal protocols were approved by the Instituto de Salud Carlos III Committee for Animal Care and Research.

Mouse $CD4^+$ T cells were obtained from single-cell suspensions of the spleen and mesenteric lymph node (MS-LN). The cell suspensions were incubated with biotinylated antibodies against CD8, CD16, CD19, CD24, CD117, major histocompatibility complex (MHC) class II (I-Ab), CD11b, CD11c and DX5, and were subsequently incubated with streptavidin microbeads (MACS; Miltenyi Biotec). $CD4^+$ T cells were negatively selected in an auto-MACS Pro Separator (Miltenyi Biotec). Cells were then labeled with antibodies to CD4 and CD25 and analyzed by flow cytometry to confirm their purity and resting status. For conditional knockout and knockin studies, mouse $CD4^+$ T cells were cultured with tamoxifen for 96 h (Aurora A gene deletion model) or doxycycline for 20 h (Aurora A overexpression model) in RPMI 1640 + GlutaMAX–I + 25 mM HEPES (Gibco-Invitrogen) supplemented with 10% fetal bovine serum (Hyclone, Thermofisher), 50 IU/ml penicillin, 50 µg/ml streptomycin, and 5ng/mL murine IL-7.

3.4 Plasmids, siRNAs and transfection

The plasmid encoding GFP-EB3 was generously provided by Dr. A. Akhmanova (Utrecht University; Utrecht, The Netherlands) (Grigoriev & Akhmanova, 2010) and the plasmid encoding Aurora A-GFP was reported previously (Perez de Castro et al, 2011). T cell lines were transfected with specific double-stranded siRNA against human Aurora Kinase A 3'UTR (CCCUCAAUCUAGAACGCUA) (Plotnikova et al, 2012) or a scramble negative control (CUAGGGUGCCGAGUGUGUU). For transfection, T cell lines were centrifuged at 1200 rpm for 5min and washed with HBSS (Hank's balance salt solution; Lonza) and resuspended in Opti-Mem I (GIBCO-Invitrogen) ($15x10^6$ cells in 400 µl). Plasmid encoding GFP-EB3 (5 µg) or Aurora A-GFP (5 µg) was added to cells, and transfection was performed with the gene-pulser III system from Bio-Rad Laboratories (240 V, 975 mΩ, aprox 27 ms). After electroporation, cells were cultured

in 9 ml RPMI 1640 + GlutaMAXTM–I + 25mM HEPES medium. After 4 h, 500 µL of fetal bovine serum was added to the cell medium. Experiments were performed 24 h after transfection. The plasmids encoding Aurora A-V5 wild type (WT) or kinase dead mutant (KD) (24µg) were transfected with lipofectamin (Invitrogen) in HEK293T cells. Experiments were performed 24 h after transfection.

3.5 T cell activation

3.5.1 Human TCR stimulation

T cells were incubated for the indicated times with latex microbeads (6.4 µm diameter) conjugated to anti-CD3 antibody (10 µg/ml) and anti-CD28 antibody (5µg/ml).

3.5.2 Mouse TCR stimulation

T cells were incubated with anti-CD3 antibody (10 µg/ml) and anti-CD28 antibody (5µg/ml) for 15 (4ºC) followed by incubation with goat anti-Armenian hamster IgG for 15 minutes (4ºC).

3.5.3 Antigen stimulation

Raji cells were pulsed with 0.3 µg/ml SEE (30 min) and mixed with J77 cells (1:5); alternatively, Hom2 cells pulsed with 200 µg/ml HA peptide (2 h) or with 5 µg/ml SEB (30 min) and were mixed with CH7C17 cells (1:5) in HBSS. Where indicated, cells were pretreated with MLN8237 (10 µM) or AZD1152 (100 nM) or vehicle for 45 min at 37 ºC in HBSS prior to stimulation with the corresponding APC or anti-CD3 and anti-CD28 antibodies. Cells were centrifuged at low speed for the indicated times at 37ºC to favor the formation of conjugates.

3.6 Cell lysis and immunoblotting

Cells were lysed in 50 mM Tris–HCl pH 7.5 containing 1% NP40, 0.2% Triton X-100, 150 mM NaCl, 2 mM EDTA, 1.5 mM $MgCl_2$, and phosphatase and protease inhibitors. Lysates were spin at 14000 rpm (4 °C, 10 min) to remove debris and nuclei. Proteins were resolved by SDS–PAGE and transferred to nitrocellulose membranes. After blocking with TBS (Tris-buffered saline) containing 0.2% TWEEN and 5% BSA, membranes were blotted with primary antibodies (o/n at 4 ºC) and peroxidase-labeled secondary antibodies (30 min) and detected with the ImageQuant LAS-4000 chemiluminiscence&fluorescence imaging system (Fujifilm).

3.7 Cell conjugate formation, immunofluorescence and IS analysis.

Raji B cells or Hom2 B cells were washed once with HBSS and loaded with the CMAC cell tracker (10 µM) and with SEE or SEB for 30 min or HA peptide for 2 h at 37 ºC. T cells (1×10^5 cells) were mixed with the corresponding APC (1:1) and plated onto Poly-L-Lys-coated slides (50 µg/ml; 1h at 37ºC). Cells

were allowed to settle for 20 min at 37 °C, fixed with 4% paraformaldehyde and 0.12mM sucrose in PHEM (60 mM PIPES, 25 mM Hepes, 5 mM EGTA, 2 mM $MgCl_2$), and permeabilized for 5 min at room temperature with 0.2% Triton X-100 in immunofluorescence solution (PHEM containing 3% BSA, 100 µg/ml γ-globulin and 0.2% azide). Cells were blocked for 30 min with immunofluorescence solution and stained with the indicated primary antibodies (5 µg/ml) followed by Alexa Fluor 488, 568 or 647-labeled secondary antibodies, alexa-conjugated phalloidin (5 µg/ml) or FITC-conjugated anti-α-tubulin (0.1 µg/ml). Cells were mounted on Prolong Gold and analyzed with a Leica SP5 confocal microscope (Leica) fitted with a HCX PL APO 63x/1.40-0.6 oil objective, and images were processed and assembled using Image J software (http://rsbweb.nih.gov/ij/) and Photoshop software. For quantification in individual ISs, we used a home-made plugin for Image J software (http://rsbweb.nih.gov/ij/) called '*Synapse Measures*'. By comparing fluorescence signals from multiple regions of the T cell, APC, IS, and background fluorescence, the program yields accurate measurements of localized immunofluorescence. A detailed description of *Synapse Measures*, including the algorithms used, is described (Calabia-Linares et al, 2011).

3.8 Immunoprecipitation, mass spectrometry and analysis of phosphorylation

For Lck immunoprecipitation assay, human lymphoblast pretreated with MLN8237 (10 µM) or vehicle (DMSO) for 30 min, were activated with Raji preloaded with SEE for 2 min at 37 ºC. Then, cells were lysed for 40 min at 4ºC in extraction buffer with 50 mM Tris–HCl pH 7.5 containing 0.5% NP40, 150 mM NaCl, 2 mM EDTA, 1.5 mM $MgCl_2$, and phosphatase and protease inhibitors. Lysates were spun at 14000 rpm (4°C, 10 min) to remove debris and nuclei. The anti-Lck antibody was allowed to bind with Protein G-conjugated sepharose beads (GE Healthcare) overnight at 4ºC and then mixed with the extracts. The mixture was left in stirring at 4ºC for 2 hours and then beads were washed ten times with the same buffer used for lysis without detergents. As a control, we used beads preincubated with the extracts. For Aurora A immunoprecipitation, Aurora A-V5 WT or KD transfected HEK293T cells were lysed with RIPA buffer with 1% Triton X-100, 0.5% deoxycholate (Sigma Aldrich), 0.1% SDS in Tris buffer saline and sonicated (3x30 s pulses). The anti-V5 antibody was mixed with the extracts, and left in stirring at 4 ºC for 2 h and then Protein G-conjugated sepharose (GE Healthcare) was added for 1 h in stirring at 4 ºC. Bead were washed three times with the buffer kinase with 20mM Hepes pH 7.4 containing 150mM KCl, 10mM $MgCl_2$, 1mM EGTA, 0.5mM DTT and phosphatase and protease inhibitors and once with buffer kinase plus NaCl 0.5mM. Beads were incubated with 0.5µg of recombinant Lck in buffer kinase plus 10mM ATP during 30 min at 30 ºC. For proteomic analysis, the samples were trypsin-digested using the whole proteome in-gel digestion protocol (Bonzon-Kulichenko et al, 2011). The peptides produced by digestion were vacuum-dried and redissolved in 1% trifluoroacetic acid for desalting in reversed-phase C-18 extraction cartridges (Oasis, Waters Corporation, Milford, MA, USA). High-resolution parallel reaction monitoring of phosphorylated peptides was carried out on an Easy nLC 1000 nano-HPLC apparatus (Thermo Scientific,

San Jose, CA, USA) coupled to a hybrid linear ion trap-orbitrap (Orbitrap Elite, Thermo Scientific). Peptides were suspended in 0.1% formic acid and then loaded onto a C-18 reversed-phase nano-column (75 µm I.D., 50 cm) and separated in a continuous gradient consisting of 8-30% B for 15 min and 30-90% B for 2 min (B = 90% acetonitrile, 0.1% formic acid) at 200 nl/min. Peptides were ionized using a Picotip emitter nanospray needle (New Objective, Woburn, MA, USA). Each MS run consisted of enhanced FT-resolution spectra (30,000 resolution) in the 390–1600 m/z range followed by data-independent MS/MS spectra of 11 parent ions acquired along the chromatographic run. The AGC target value in the Orbitrap for the survey scan was set to 1,000,000. Fragmentation in the linear ion trap was performed at 35% normalized collision energy with a target value of 10,000 ions, and the dynamic exclusion was set to 0.5 min. Data analysis was performed with Xcalibur 2.2 (Thermo Scientific).

3.9 Time-lapse confocal and total internal reflection fluorescence (TIRF) video microscopy.

Raji APCs ($5x10^5$; SEE-pulsed or unpulsed) were allowed to adhere to fibronectin-coated coverslips in Attofluor open chambers (Molecular Probes-Invitrogen) at 37 ºC in a 5% CO_2 atmosphere. The cells were maintained in 1 ml HBSS (1% fetal bovine serum, 25 mM HEPES). T cells were added (1:1 ratio) and a series of fluorescence and differential interference contrast frames were captured using a TCS SP5 confocal laser scanning unit attached to an inverted epifluorescence microscope (DMI6000) fitted with an HCX PL APO 63x/1.40-0.6 oil objective. Images were acquired and processed with the accompanying confocal software (LCS; Leica) and Image J software (http://rsbweb.nih.gov/ij/). For TIRF microscopy (TIRFm), T cells stably expressing EB3-GFP or transfected with EB3-GFP and CD3ξ-mCherry were allowed to settle onto glass bottom dishes (No 1.5 Mattek; Ashland, MA, US) coated with anti-CD3 (10 µg/ml) and anti-CD28 (3 µg/ml). Recording was initiated 3 minutes after cells were plated, and cells were visualized with a Leica AM TIRF MC M system mounted on a Leica DMI 6000B microscope coupled to an Andor-DU8285_VP-4094 camera fitted with a HCX PL APO 100.0x1.46 OIL objective. For mCherryActin expressing T cells, recording was initiated upon addition of cells to the glass bottom dishes. Images were processed with the accompanying confocal software (LCS; Leica). The laser penetrance used was 150 or 200 nm for both laser channels (488 and 561 nm), using the same objective angle. Time-lapse settings were optimized for each type of experiment and are specified throughout the text. Synchronization was performed with the accompanying Leica software, and images were processed with Leica software, matlab and Image J software (http://rsbweb.nih.gov/ij/).

3.10 Quantitative real-time PCR

RT–PCR was performed with 1 μg of RNA isolated with Trizol RNA reagent (Invitrogen, Eugene, OR, USA) from $CD4^+$ T cells obtained from healthy donors. mRNA levels of IL-2, CD25 and CD69 were determined in triplicate using the Power SYBR Green PCR master mix from Applied Biosystems (Warrington, UK). Expression levels were normalized to the expression of glyceraldehyde-3-phosphate dehydrogenase (GAPDH). Primer sequences are listed in table below.

Oligos	5´- 3´ Forward Sequence	5´- 3´ Reverse Sequence
GAPDH	AGCCACATCGCTCAGACAC	GCCCAATACGACCAAATCC
IL-2	AAGTTTTACATGCCCAAGAAGG	AAGTGAAAGTTTTTGCTTTGAGCTA
CD69	CAAGTTCCTGTCCTGTGTGC	GAGAATGTGTATTGGCCTGGA
CD25	CAGCCCCAGCTCATATGCA	TGAGGCTTCTCTTCACCTGGAA

Results

4. Results

4.1 Localization of Aurora A at the IS

To assess the specific location of activated Aurora A, we conjugated human CD4$^+$ T cells from peripheral blood from healthy donors with beads coated with stimulatory anti-CD3 and anti-CD28 antibodies, and stained with anti-phospho-specific antibody against the Aurora-T288 residue, that detects active Aurora A. In these experiments, T288-phosphorylated endogenous Aurora A was found in two different pools, one in the centrosome and the other at the T cell-bead contact region (examples of conjugates at different stages of the process are shown, Fig. R1a); the low signal of activated Aurora A in non-stimulated control conjugates was not detected at the IS (Fig. R1a). Pretreatment of peripheral-blood-derived human CD4$^+$ T cells with the specific Aurora A inhibitor MLN8237 blocked the phosphorylation of Aurora A (Fig. R1a). Quantitative analyses showed that phosphorylated Aurora A is accumulated at the IS in stimulated CD4$^+$ T cells, and that this is prevented by MLN8237 treatment (Fig. R1b).

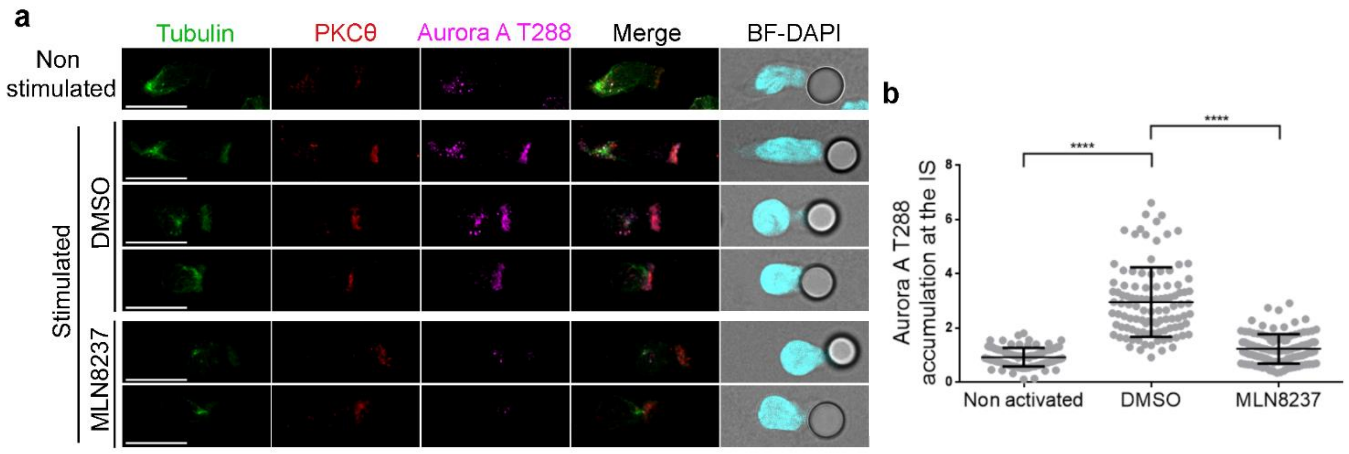

Figure R1. Aurora A is located at the IS contact area and is activated upon TCR triggering. **(a)** Maximum Z projection of a confocal stack of human primary CD4$^+$ T cells pretreated with vehicle (DMSO) or Aurora A inhibitor (MLN8237, 10 µM) and conjugated with anti CD3/CD28-coated beads. Images show three representative conjugates in DMSO and two in MLN8237-treated cells at different stages of cell conjugation. Cells were fixed and stained for PKCθ (red), T288-phosphorylated Aurora A (magenta) and α-tubulin-FITC (green). Bright field with DAPI frames are included. Bar, 10 µm. **(b)** Quantification of T288-phosphorylated Aurora A accumulation at the IS contact area in conjugates as in **a** from three independent experiments (n=93 in non activated, n=105 in DMSO, n=109 in MLN8237). Data represent means ± SD. Means were compared with a t-test. (**** $p < 0.0001$).

In order to confirm the specificity of the T288-Aurora A antibody, we transfected J77 T cells with specific siRNAs for Aurora A for silencing it. Staining of phosphorylated endogenous Aurora A upon TCR stimulation was abolished, confirming the specific binding of the antibody (Fig. R2).

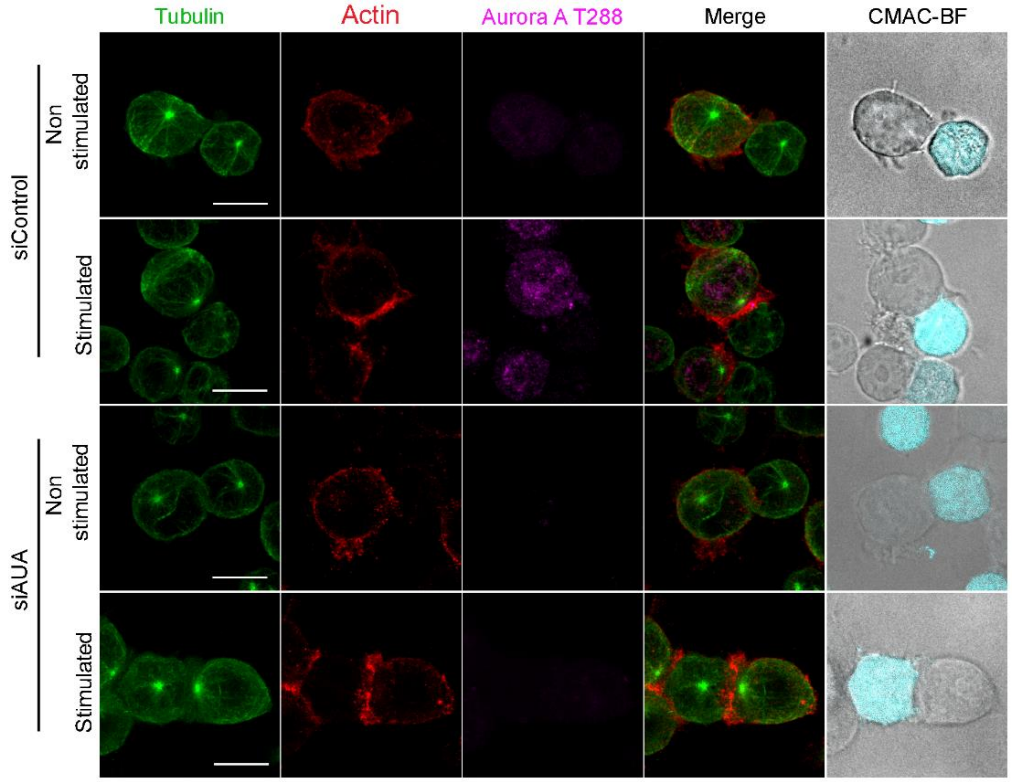

Figure R2. Specific silencing of Aurora A. Maximum Z stack projection of a confocal XYZ-stack of Jurkat T cells transfected with a specific siRNA against Aurora A (siAUA) or a scrambled negative control (siControl) and conjugated with SEE-pulsed Raji B cells. Cells were incubated for 30 min, fixed and stained for α-tubulin (green), T288-phosphorylated Aurora A (magenta) and actin (red). A merged fluorescence image is shown. The right-hand image shows Raji cells labeled with CMAC cell tracker (cyan) and bright field. Bar, 10 µm.

Active Aurora A also localized at the IS in conjugates of naïve mouse OTII T lymphocytes with primary dendritic cells pulsed or not (control) with OVA peptide (Fig. R3). These results clearly show that TCR triggering promotes the activation of Aurora A and its recruitment to the IS.

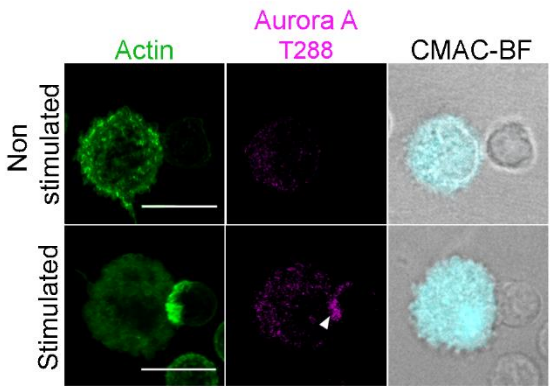

Figure R3. Active Aurora A is located at the IS in mouse CD4$^+$ T cells. Maximum Z projections of confocal stacks of transgenic OTII CD4$^+$ cells conjugated with OVA peptide-pulsed bone-marrow-derived dendritic cells (DC). Cells were incubated for 30 min, fixed and immunostained for T288-phosphorylated Aurora A (magenta) and actin (green). The right-hand image shows CMAC cell tracker labeling of DCs (cyan) and bright field. Bar, 10 µm.

To parse the localization of activated Aurora A with respect to total Aurora A, we transfected primary CD4⁺ T cells with Aurora A-GFP WT or Aurora A-GFP KD (kinase dead mutant) and then conjugated the transfected cells with stimulatory anti-CD3/CD28-coated beads (Fig. R4a). Quantitative analysis of Aurora A-GFP or active Aurora A (Aurora A T288) accumulation demonstrated that it is mainly found at the IS (Fig. R4b). However, Aurora A KD accumulation at the IS is significantly decreased, compared to WT (Fig. R4b). Moreover, overexpression of the Aurora A-GFP KD mutant, dispersed the remaining active protein (Fig. R4b). Thus, the phosphorylated active form of Aurora A is specifically recruited to the IS.

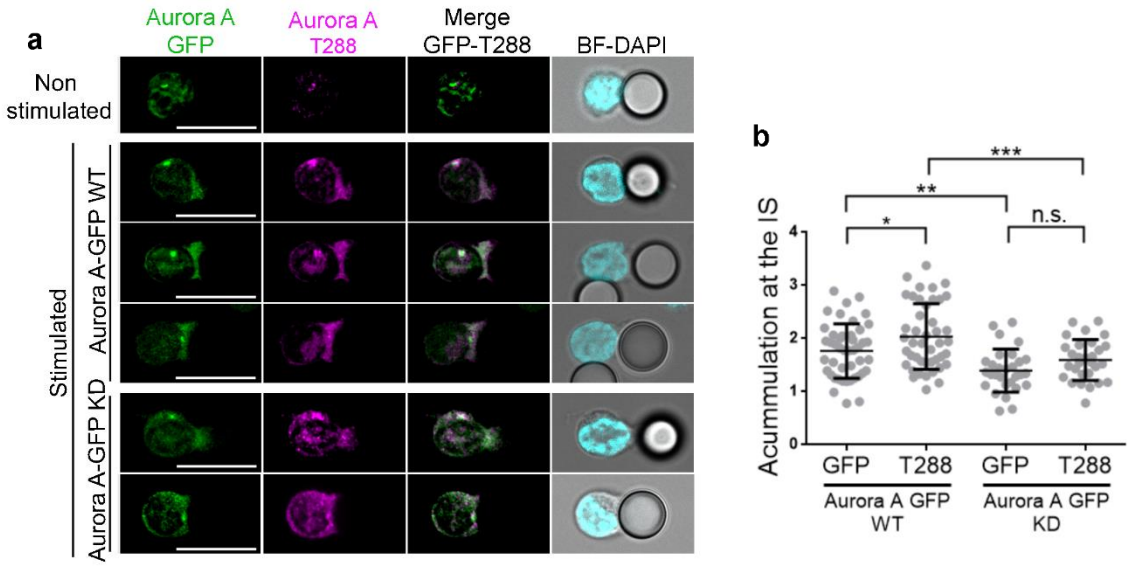

Figure R4. Both Aurora A-GFP and active Aurora A localize at the IS. (a) Maximum Z projection of a confocal stack of human primary CD4⁺ T cells transfected with Aurora A-GFP WT or Aurora A-GFP KD (green) and conjugated with anti CD3/CD28-coated beads. Cells were incubated for 30 min, fixed and stained for T288-phosphorylated Aurora A (magenta). Bright field with DAPI frames are included. Bar, 10 µm. **(b)** Quantification of T288-phosphorylated Aurora A and transfected Aurora A accumulation at the IS contact area in conjugates as in **a** from three independent experiments (n=45 in Aurora A-GFP WT, n=29 in Aurora A-GFP KD). Data represent means ± SD. Means were compared with a t-test. n.s., non-significant. (* $p < 0.05$), (** $p < 0.01$), (*** $p < 0.001$).

4.2 Aurora A in MT dynamics and in MTOC translocation

Aurora A plays an important role in the dynamics of the centrosome during mitosis (Berdnik & Knoblich, 2002; Hannak et al, 2001). To ascertain its possible function in microtubule dynamics and centrosomal polarity during T cell activation, we analyzed the dynamics of the microtubular network in CH7C17 T cells transiently transfected or stably expressing an EB3-GFP fusion protein (EB3 cells; Fig. 5a and Supplementary Movie 1). EB3 and EB1 (End-Binding proteins) are plus-tip-tracking proteins that are also found in the pericentrosomal matrix and promote MT growth (Etienne-Manneville, 2010). Cells were settled on anti-CD3/CD28-coated chambers and time-lapse confocal 3D

imaging was performed by XYZ-stack acquisition. The stimulating surface allows IS-like formation, associated centrosome polarization and MT polymerization (Martin-Cofreces et al, 2012). EB3 cells were pre-treated or not (vehicle) with MLN8237 for 30 min before imaging. Maximal projection of the XYZ-stack (Fig. R5a and Supplementary Movie 1) revealed that the relative amount of EB3-GFP incorporated into microtubule plus-ends (TIPs) was clearly decreased in Aurora A-inhibited cells. This effect was measured in 3D as the ratio of EB3-GFP fluorescence incorporated in TIPs with respect to the whole cell fluorescence using Imaris software, confirming that Aurora A-inhibited cells polymerize microtubules less efficiently (Fig. R5b and Supplementary Movie 1). The amount of polymerized MT observed along the time-course was clearly decreased in MLN8237-treated cells (Fig. R5a).

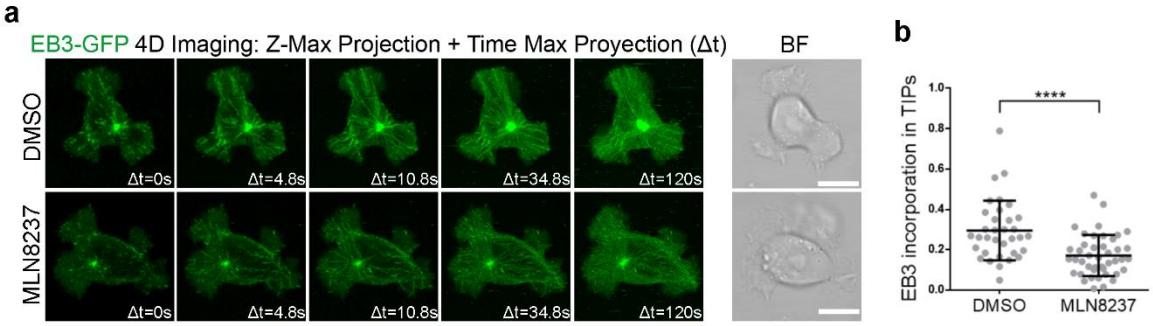

Figure R5. Microtubule dynamics at the IS is impaired by Aurora A chemical inhibition. **(a)** Imaging of EB3-GFP-expressing CH7C17 T cells, pretreated with DMSO or MLN8237 and settled on corresponding anti-CD3/CD28-coated glass-bottom chambers. Maximal projection of XYZ-stacks for fluorescence and single bright field (BF) images are shown. Bars, 10. (**b**) Ratio of EB3-GFP fluorescence incorporated in TIPs from XYZ-stack from three independent experiments (0s; n=34 in DMSO, n=43 in MLN8237). Data represent means ± SD. Means were compared with a Mann-Whitney test. (**** $p < 0.0001$).

To further assess the function of Aurora A in primary naïve T cells, we used a mouse model of conditional Aurora deficiency. $CD4^+$ cells were isolated from lymph nodes and spleens of experimental [Aurka(lox/lox); RERT(ert/ert)] (KO mice) and control [Aurka(+/+); RERT(ert/ert)] (WT mice), treated with tamoxifen and IL-7 for 96 h to suppress Aurora A expression (Fig R6a). These cells were transfected with a plasmid encoding EB3-GFP, and then activated with anti-CD3/CD28 stimulating monoclonal antibodies (Fig. R6b and c and Supplementary Movie 2). We found that Aurora A-deficient T cells had significantly less EB3 incorporation in microtubule +TIPs than their WT counterparts (Fig. R6b and c and Supplementary Supplementary Movie 2). Furthermore, the effect of Aurora A deficiency was similar to the effect of the MLN8237 inhibitor on WT cells, while the inhibitor did not have additional effects on Aurora A KO cells, suggesting that these and previously recorded effects of the inhibitor were Aurora A-specific.

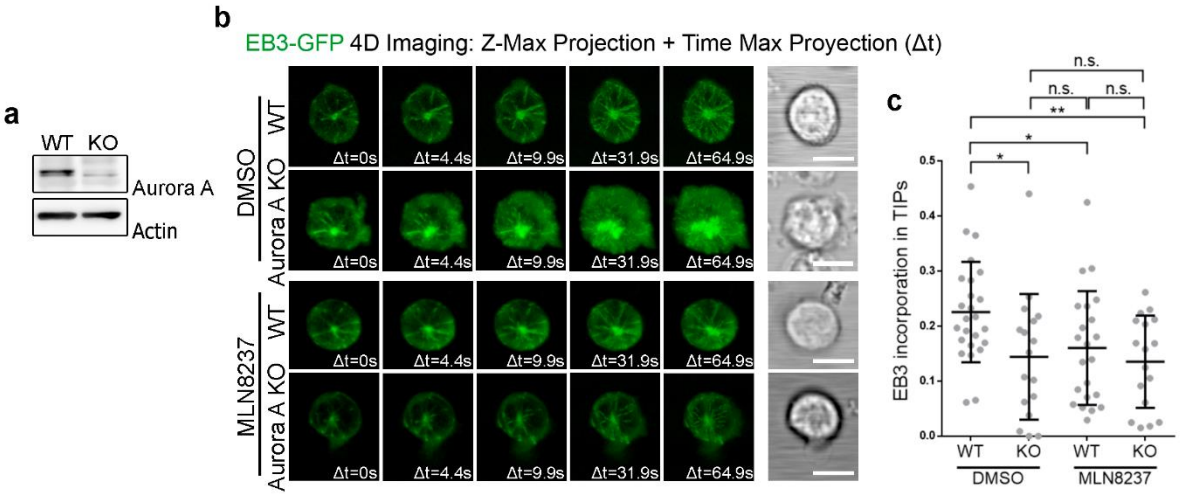

Figure R6. Aurora A gene ablation impairs EB3 incorporation in MT +TIPs. (a) Immunoblot analysis of Aurora A protein expression in CD4$^+$ T cells WT and KO. **(b)** Imaging of EB3-GFP-expressing Aurora A-deficient and control CD4$^+$ T cells, pretreated with DMSO or MLN8237 and settled on corresponding anti-CD3/CD28-coated glass-bottom chambers. Maximal projection of XYZ-stacks for fluorescence and single bright field (BF) images are shown. Bars, 10 or 5 µm, respectively. **(c)** Ratio of EB3-GFP fluorescence incorporated in TIPs from XYZ-stack from three independent experiments (0s; n=25 in WT, n=17 in KO, n=22 in WT MLN8237 and n=17 in KO MLN823). Data represent means ± SD. Means were compared with a Mann-Whitney test. n.s., non-significant. (* $p < 0.05$), (** $p < 0.01$).

We next tracked the dynamics of microtubule growth using EB3-GFP imaging and TIRF microscopy in cells settled on anti-CD3/CD28-coated surfaces to improve the XY spatial and time resolution (Dixit & Ross, 2010; Grigoriev & Akhmanova, 2010; Manneville, 2006). EB3 cells were treated with MLN8237 or DMSO (vehicle) for 30 min before imaging, and images were taken every 300 ms. MLN8237-treated EB3-GFP cells had fewer EB3-decorated tips emerging from the centrosome, indicating impaired microtubule growth (Fig. R7a and b and Supplementary Movies 3 and 4). MT growth was similarly impaired in Aurora-KO primary CD4$^+$ T cells, displaying fewer and slower growing microtubules than control cells (0.140 +/-0.037 µm.s-1 and 0.190 +/-0.023 µm.s-1, respectively; mean +/- SD) (Fig. R7c and d and Supplementary Movies 5 and 6). These results thus show that the microtubule network at the immune synapse is disrupted in T cells with defective Aurora A activation.

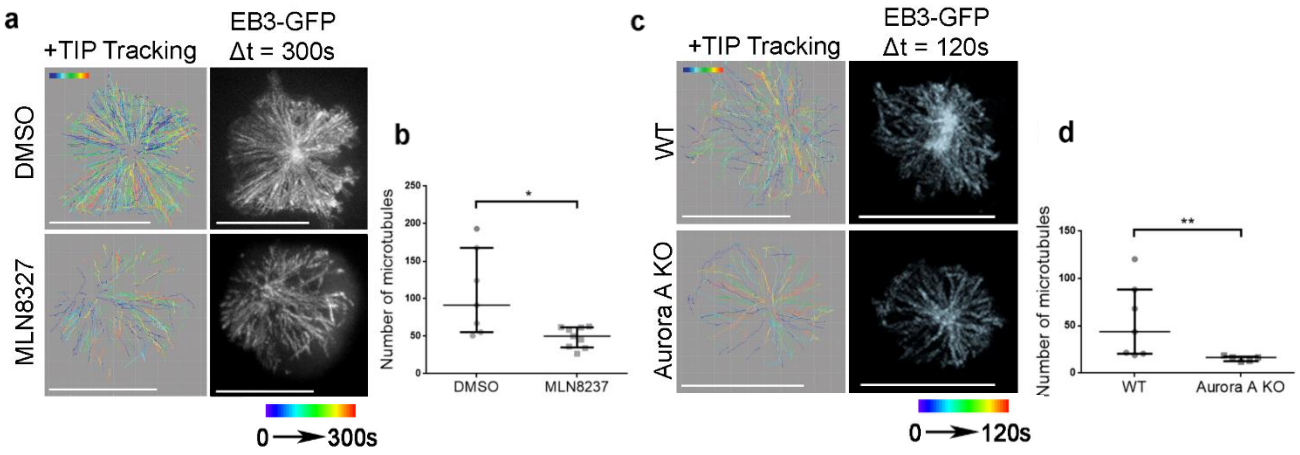

Figure R7. Aurora A gene ablation impairs MT dynamics at the IS. (a) Map of the trajectories of EB3-GFP decorated microtubule plus tips in human CH7C17 T cells pretreated with DMSO or MLN8237 and settled on anti-CD3/CD28-coated glass-bottom chambers. Images were taken every 300 ms under a TIRF microscope at a penetrance of 150 nm. MT tips were tracked with Imaris software over 5 min. Maximal projections of the time-lapse from representative cells are shown. Bar, 10 µm. **(b)** Quantification of the number of microtubule plus tip tracks presented in **a** from three independent experiments (n=7 in DMSO, n=9 in MLN8237). **(c)** Map of the trajectories of EB3-GFP decorated microtubule plus tips in Aurora A-deficient and control WT $CD4^+$ T cells and settled on anti-CD3/CD28-coated glass-bottom chambers. Images were taken every 300 ms under a TIRF microscope at a penetrance of 150 nm. MT tips were tracked with Imaris software over 2 min. **(d)** Quantification of the number of microtubule plus tip tracks presented in **c** from three independent experiments (n=6). Error bars represent interquartile rage. Medians were compared with a Mann-Whitney test. n.s., non-significant. (* $p < 0.05$), (** $p < 0.01$).

To assess the localization of the MTOC and the EB3-GFP fluorescence by 3D and orthogonal projections of the XYZ-stacks in EB3 cells. Cells were settled on anti-CD3/CD28-coated surfaces during 3 min and maximal fluorescence, corresponding to MTOC was analyzed (Fig. R8a and b). MTOC is detected close to the stimulating surface (Fig. R8a) and there is not significant changes in the translocation in MLN8237 treated cells (Fig. R8b). This can be also observed by comparing bottom and top slices of the XYZ-stacks (Fig. R8c). Moreover, no significant change on MTOC translocation in Jurkat T cells pre-treated or not with MLN8237 and conjugated with Raji B cells was observed either at 10 or 30 min of activation (Fig. R8d).

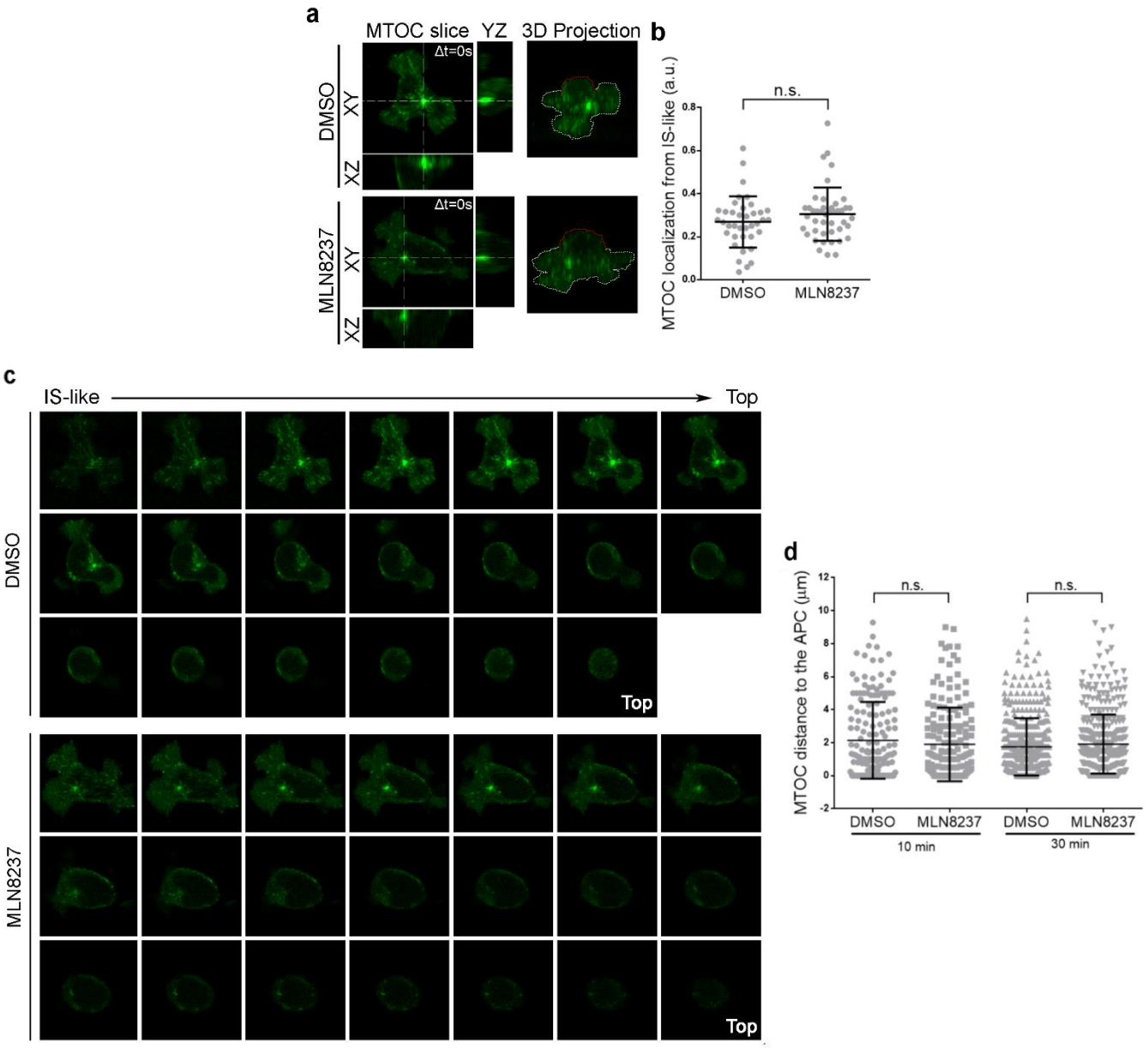

Figure R8. Aurora A inhibition does not affect MTOC translocation to the IS. (a) Orthogonal and 3D projections from XYZ-stacks. Dotted white or red lines indicate contact with substrate or media, respectively. **(b)** Ratio of the MTOC location from the IS-like from three independent experiments (n=38 in DMSO, n=44 in MLN8237). **(c)** Single slices from the XYZ-stack of 4D imaging of EB3-GFP transfected human CH7C17 T cells treated with DMSO or MLN8237 and platted onto anti-CD3/CD28 stimulating antibodies (time 0s). **(d)** Distance from the T cell MTOC to the APC contact area in conjugates of T cells with SEE-pulsed APCs from three independent experiments (10 min; n=166 in DMSO, n=168 in MLN8237; 30 min; n=412 in DMSO, n=394 in MLN8237). Data represent means ± SD from 3 independent experiments. Means were compared

We also analyzed the localization of the MTOC and the EB3-GFP fluorescence by 3D and orthogonal projections of the XYZ-stacks in mouse $CD4^+$ T cells. Cells from WT and Aurora A KO mice were transfected with the plasmid encoding EB3-GFP and then settled on anti-CD3/CD28-coated surfaces during 3 min. MTOC and EB3-GFP tracking of MTs was also observed at the bottom of the

cells (Fig. R9a and b). Despite the effect of Aurora A-depletion on MT dynamics, no significant change on MTOC translocation was detected in mouse CD4$^+$ T cells (Fig. R9b).

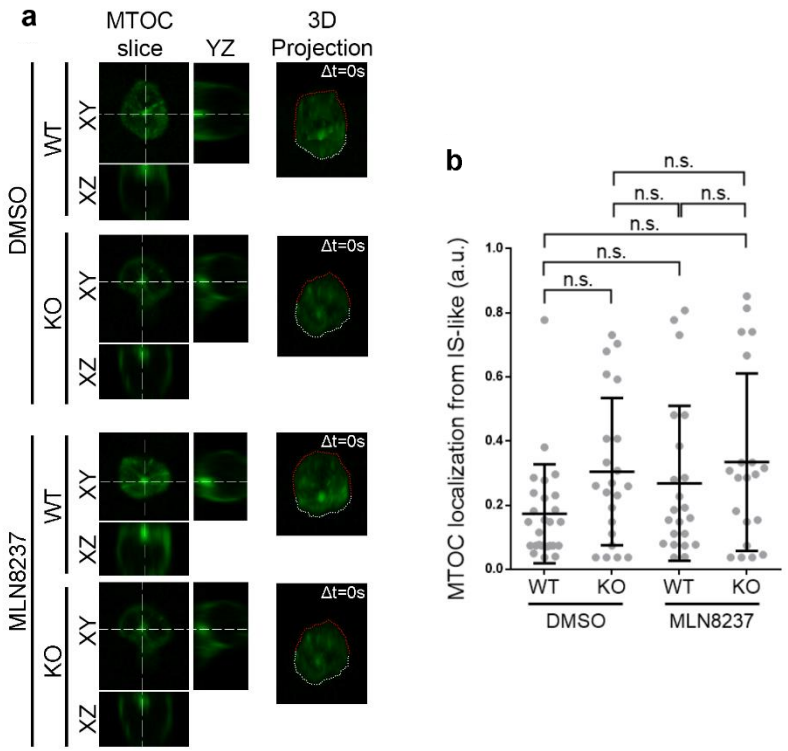

Figure R9. Aurora A gene ablation does not affect the MTOC translocation to the IS. (**a**) Orthogonal and 3D projection from XYZ-stacks of WT and KO mouse cells, pre-treated with DMSO or MLN8237 (time 0s). Dotted white or red line indicates contact with substrate or media in the 3D projection, respectively. **(b)** Ratio of the MTOC location from the IS-like from three independent experiments (n=26 in WT, 22 in KO and WT+MLN and n=20 in KO+MLN). Data represent means ± SD. Means were compared with a Mann-Whitney test. n.s., non-significant. (* $p < 0.05$), (** $p < 0.01$).

As control, to determine if the percentage of J77 T cells conjugated with SEE-pulsed Raji is affected by Aurora A inhibition, we incubated J77 cells pretreated or not with the MLN8237 inhibitor with Raji cells during 30 min. Targeting of Aurora A did not alter the number of conjugates formed with SEE-pulsed Raji cells (Fig. R10), indicating that inhibition of Aurora A did not result in a global defect in cytoskeleton dynamics.

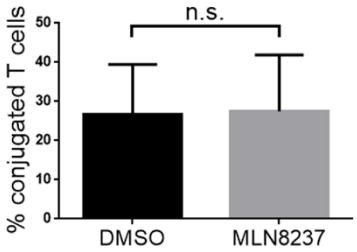

Figure R10. Aurora A blockade does not affect the percentage of conjugates formation. Quantification of the percentage of T J77 T cells, pre-treated with DMSO or MLN8237, conjugated with SEE-pulsed Raji B cells, from three independent experiments.

4.3 Aurora A in CD3ζ-bearing vesicles traffic at the IS

In order to analyze the accumulation of TCR/CD3 complexes at the IS, Jurkat T cells pre-treated or not with the Aurora A inhibitor were conjugated with non stimulated or SEE- pulsed Raji cells during 30 min. The impaired MT growth observed in Aurora A-targeted T cells did not affect the localization of the surface

TCR/CD3 complexes at the IS, since TCR/CD3ε was comparably clustered at the IS of untreated and MLN8237-treated T cell (Fig. R11a and b).

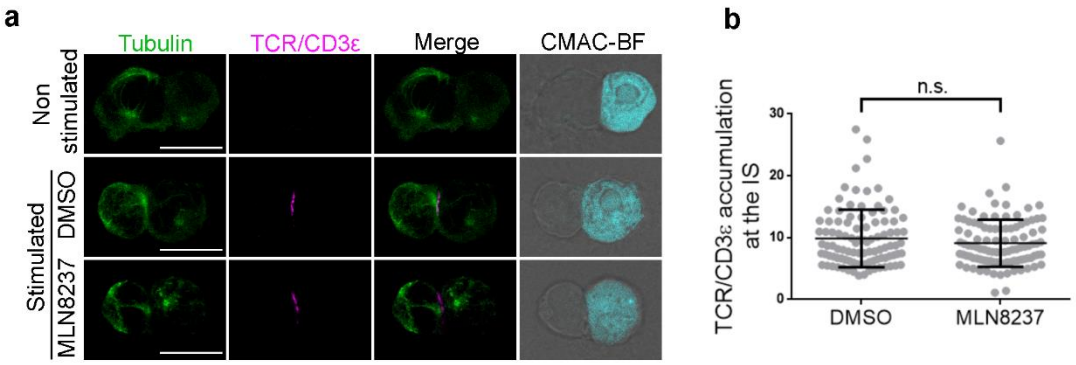

Figure R11. Accumulation of TCR/CD3ε at the IS is not affected by Aurora A inhibition. (a) Maximum Z projections of confocal stacks of Jurkat T cells pretreated with vehicle (DMSO) or Aurora A inhibitor (MLN8237) and conjugated with SEE-pulsed Raji B cells. Cells were incubated for 30 min, fixed, and stained for α-tubulin (green) and TRC/CD3ε (magenta). The right-hand image shows CMAC cell tracker labeling of Raji B cells (cyan) and bright field. Bar, 10 µm. **(b)** Graph shows quantification of TRC/CD3ε clustering at the IS from as in **a** from three independent experiments. Means ± SD is shown. t-test was used to compare means (n=101 in DMSO and in MLN8237).

We next assessed the dynamics of CD3ζ-bearing vesicles at the IS. CD3ζ traffics through endosomal compartments towards the IS (Yudushkin & Vale, 2010). These vesicles move associated to microtubules and support the sustained activation of the T cell at the IS (Martin-Cofreces et al, 2012; Soares et al, 2013a). The vesicles enter and leave the TIRF plane, some of them moving toward the position of the centrosome at the center of the IS-like structure, probably along the microtubules. To analyze the dynamics of these vesicles, Jurkat T cells expressing CD3ζ-Cherry were treated with DMSO or MLN8237, settled onto anti-CD3/CD28, and analyzed by TIRFm. Images were taken every 100 ms (200 nm penetrance) and the trajectories of detected vesicles were tracked. Treatment of EB3 cells with MLN8237 decreased the number of vesicles at the IS-like structure and disrupted the movement of those that were present (Fig. R12a and b and Supplementary Movies 7 and 8). Moreover, the number of vesicles at the IS-like structure and their movement is also disrupted in Aurora A KO mouse $CD4^+$ T cells (Fig. R12c and d and Supplementary Movie 9). The effect of Aurora A inhibition on microtubule dynamics therefore impeded the movement of vesicles toward the IS structure, a finding confirmed by the reduced speed of vesicles.

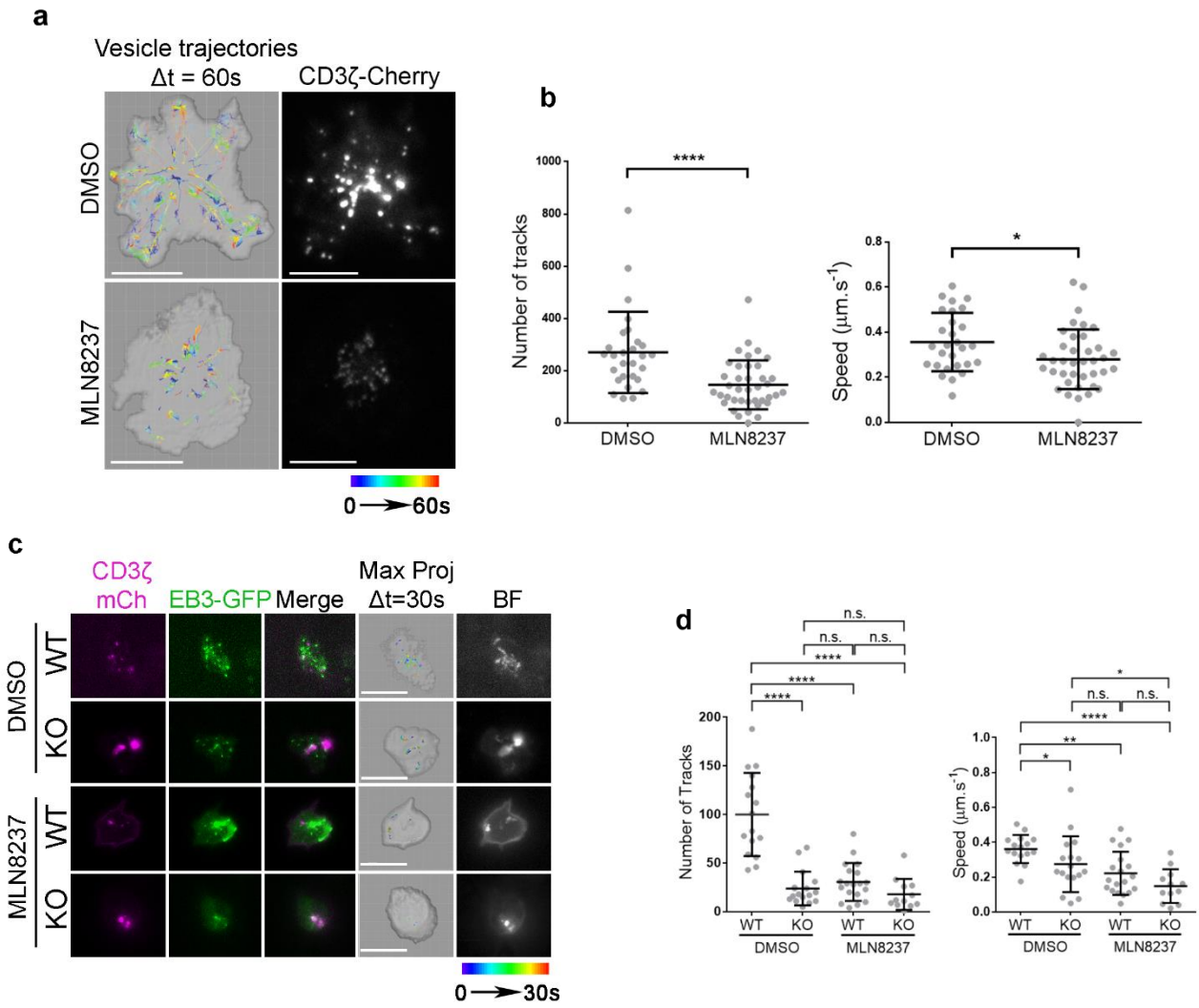

Figure R12. Trafficking of CD3-bearing vesicles at the IS is impaired by Aurora A chemical inhibition or gene ablation. (a) Map of the trajectories of CD3ζ-cherry bearing vesicles in human CH7C17 T cells pre-treated with vehicle (DMSO) or MLN8237 inhibitor and settled on corresponding anti-human or anti-mouse stimulating anti-CD3/CD28-coated glass-bottom chambers. Images were taken every 100 ms under a TIRF microscope at a penetrance of 200 nm with 561 nm laser; vesicles were tracked with Imaris software over 60 s and maximal projections of the time-lapse are shown for tracks. A representative cell is shown for each case. Fluorescence images from CD3ζ-mCherry are also shown. **(b)** Quantification of the number of vesicle tracks, as well as the speed of vesicles from cells analyzed in **a** from three independent experiments (n=28 in DMSO, n=39 in MLN8237). **(c)** Map of the trajectories of CD3ζ-cherry bearing vesicles in Aurora A-deficient and control $CD4^+$ T cells and settled on corresponding anti-human or anti-mouse stimulating anti-CD3/CD28-coated glass-bottom chambers. Images were taken every 110 ms under a TIRF microscope at a penetrance of 200 nm with 561 nm laser; vesicles were tracked with Imaris software over 30 s and maximal projections of the time-lapse are shown for tracks. A representative cell is shown for each case. Fluorescence images from CD3ζ-mCherry and EB3-GFP are also shown. **(d)** Quantification of the number of vesicle tracks, as well as the speed of vesicles from cells analyzed in **c** from three independent experiments (n=16 in WT, n=17 in KO, n=19 in WT MLN8237, n=12 in KO MLN8237). Data represent means ± SD. Means were compared with a Mann-Whitney Test. n.s., non-significant. (* $p < 0.05$), (** $p < 0.01$), (*** $p < 0.001$), (**** $p < 0.0001$).

4.4 Aurora A in TCR-driven actin dynamics

To further analyze the role of Aurora A in the control of cytoskeletal dynamics at the IS, we assessed the effect of Aurora A inhibition on the activation-dependent interaction of TCR/CD3 with the actin-cytoskeleton associated protein Nck. This interaction is enabled by the conformational change in the TCR/CD3ε complex upon antigenic triggering (Gil et al, 2002). Aurora A inhibition had no effect on CD3ζ-Nck association in pull down assays (Fig. R13a). This is in agreement with a surface recruitment and accumulation of TCR/CD3ε to the IS in Aurora A-inhibited cells (Fig R11a and b). Using a similar approach, we assessed whether Aurora A impairment affects the activation of the small GTPase Rac1, a hallmark for TCR-dependent actin polymerization (Gomez & Billadeau, 2008). Likewise, no effect was detected in Rac1 pull-down assays with the GST-PAK-CD (p21-activated kinase CRIB-Domain (Sander et al, 1998)) in stimulated $CD4^+$ T cells when using MLN8327 inhibitor (Fig. R13b).

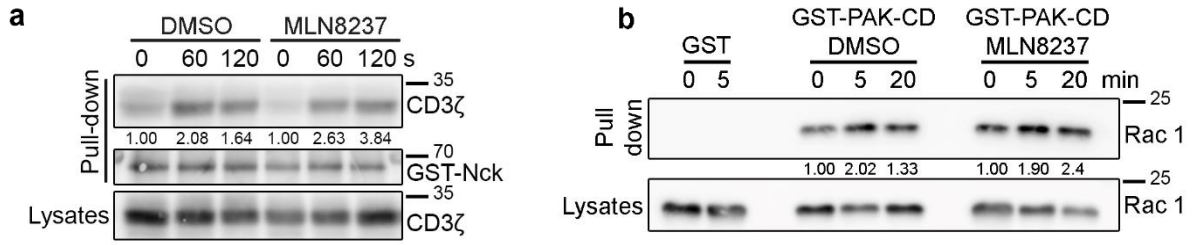

Figure R13. Aurora A inhibition does not affect actin cytoskeleton dynamics. (a) Immunoblot of a pull-down assay of GST-Nck fusion protein from cell lysates of control (DMSO; vehicle) or Aurora A inhibitor (MLN8237)-pretreated human T lymphoblasts. Activation was performed with soluble anti-CD3ε antibodies for indicated times. CD3ζ and GST are shown. CD3ζ content in whole cell lysates is indicated in the bottom row. **(b)** Immunoblot of Rac1 pull-down assay of GST and GST-PAK-CD from cell lysates of DMSO or MLN8237-pretreated Jurkat T cells activated with SEE-pulsed Raji B cells (APCs) for the indicated times. Loading control for Rac1 in whole cell lysates is shown.

Furthermore, the Aurora A inhibitor did not affect the spreading of mCherry-β-actin-expressing T cells on anti-CD3/CD28-coated coverslips, measured either as the total occupied surface or as the rate of membrane extension on the coverslip (Fig. R14a and b). This finding correlated with a similar distribution of mCherry-β-actin at the pSMAC and cSMAC in control and Aurora A-inhibited cells. Aurora A inhibition also had no effect on the total area occupied by adhered cells or their lamellae (Fig. R14b). Similarly, actin accumulation at the IS in Jurkat T cell-Raji conjugates was not significantly affected by inhibition of Aurora A (Fig. R14c and d).

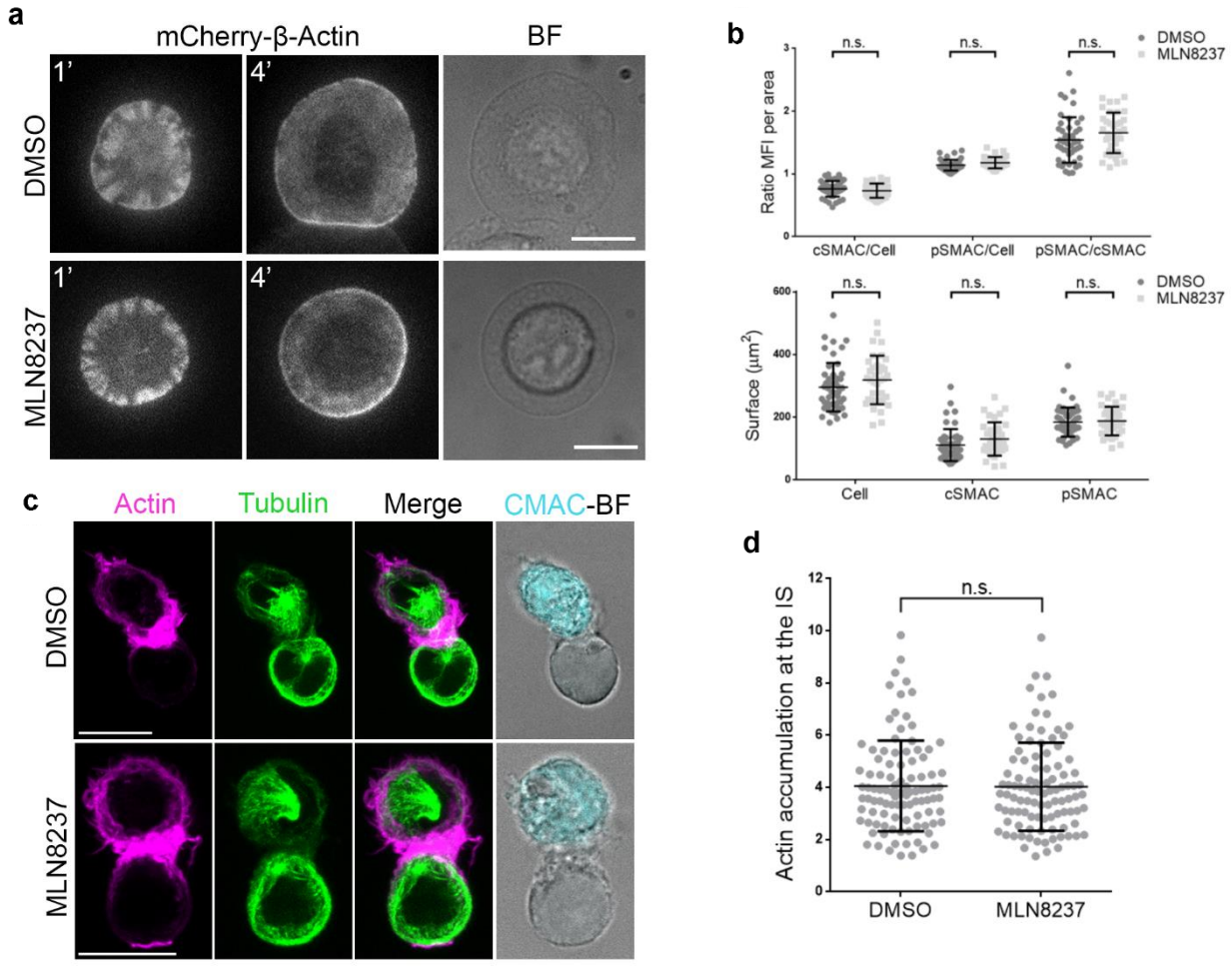

Figure R14. Actin spreading and distribution during the IS is not affected by Aurora A inhibition. (a) Images from TIRFm time-lapse analysis of mCherry-β-Actin-expressing Jurkat T cells spreading over anti-CD3/CD28-coated glass-bottom chambers. Cells were pretreated with DMSO or MLN8237. Images were taken every 100 ms for 5 min at 90 nm penetrance. A corresponding bright field image is shown. Bar, 10 µm. **(b)** Quantification of the area occupied by the whole cell (lamella), the actin-rich area (pSMAC), the central area (cSMAC), and the distribution of mean fluorescence intensity per area (ratios cSMAC:cell; pSMAC:cell and cSMAC/pSMAC) from cells in **a** from three independent experiments (n=48 and n=36). Cells were fixed after spreading (4 min) and fluorescence images were taken. Data represent means ± SD. Means were compared with a t-test. **(c)** Maximum Z projections of confocal stacks from DMSO- or MLN8237-pretreated Jurkat T cells conjugated with SEE-pulsed Raji B cells. Cells were incubated for 30 min, fixed, and stained for α-tubulin (green) or actin (magenta). The right-hand image shows CMAC cell tracker labeling of APCs (cyan) and bright field. Bar, 10 µm. **(d)** Quantification of actin accumulation at the IS contact area in conjugates as in **c** from three independent experiments (n=100). Data represent means ± SD. Means were compared with a t-test.

We therefore analyzed the formation of the actin ring in mCherry-β-actin-expressing Jurkat T cells-Raji conjugates using time lapse 3D confocal imaging. Actin accumulation and ring formation was similar in control and MLN8237-treated cells (Fig. R15a and b and Supplementary Movie 10). Aurora A therefore appears to specifically affect the tubulin cytoskeleton at the IS, without affecting actin-based dynamics.

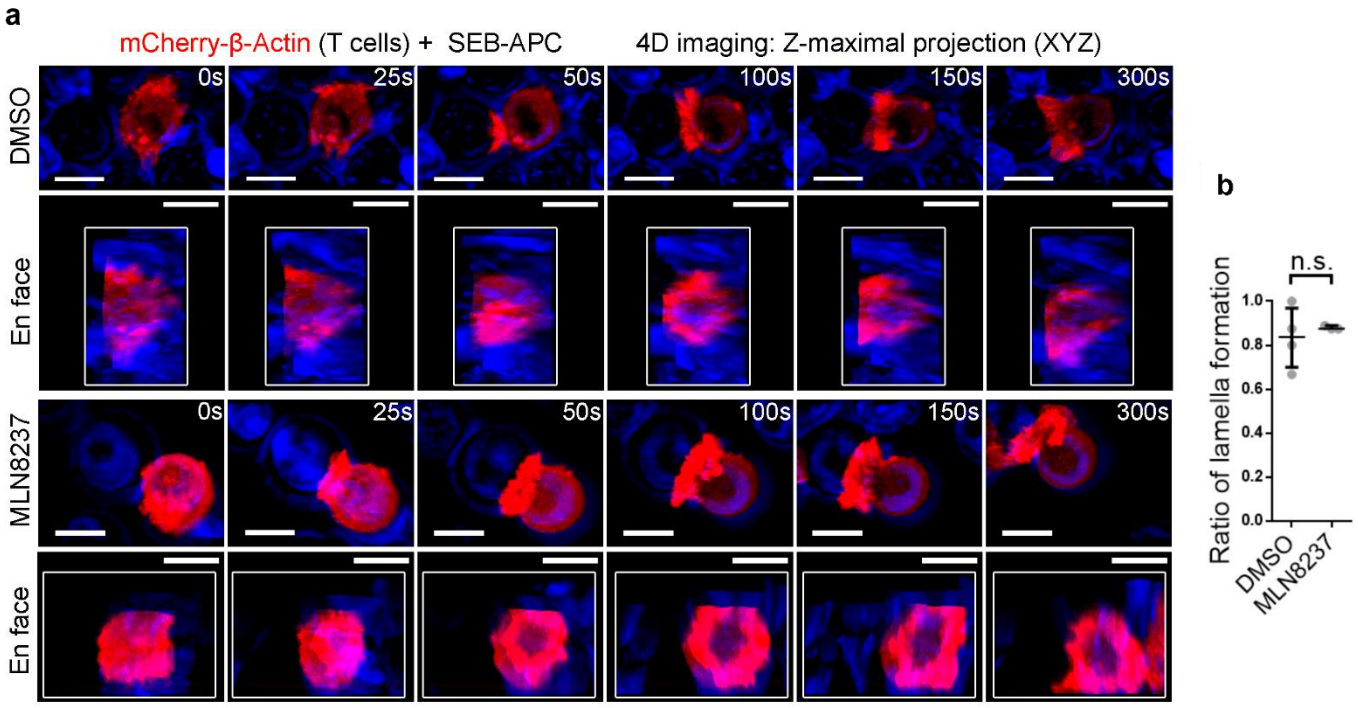

Figure R15. Inhibition of Aurora A does not affect actin accumulation at the IS. (a) Image sequence for IS formation between mCherry-β-actin-expressing T cells and SEB-APCs treated with DMSO or MLN8237. XYZ-stacks were acquired every 25 s (Maximal projections of XYZ-stacks and 3D reconstructions with Imaris Software are shown; a representative experiment out of 5 is shown). **(b)** Ratio of T cells forming lamella upon contact with an APC from **a** from three independent experiments. Data represent median ± interquartile range. Medians were compared with a Mann-Whitney test (DMSO: 28 cells (n=4); MLN8237: 25 cells (n=3)). n.s., non-significant.

4.5 Aurora A in early TCR signalling

To assess the possible role of Aurora A in TCR signaling, we analyzed the phosphorylation of several canonical downstream molecules that are phosphorylated in response to cognate interactions in SEE-stimulated Jurkat T cells (Fig. R16a and b). The phosphorylation of specific residues in CD3ζ (Y83), LAT (Y132), PLCγ1 (Y783), PKCθ (T538) and ERK1/2 (T202/Y204) was greatly diminished upon Aurora A inhibition with MLN8237.

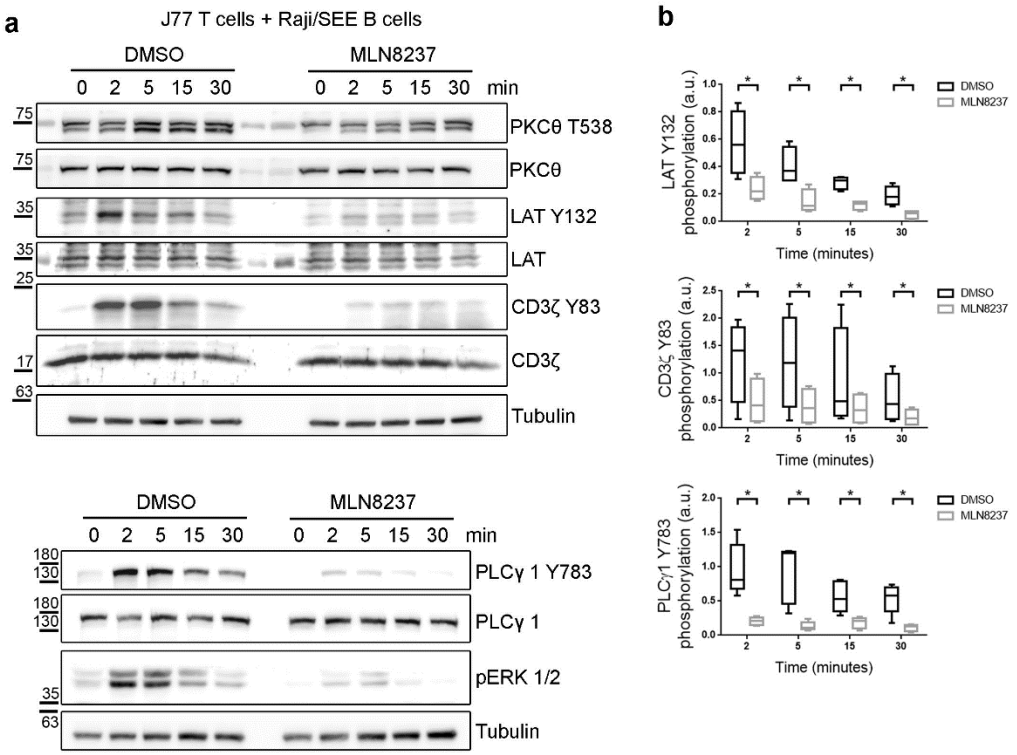

Figure R16. Aurora A inhibition impairs TCR signaling pathways in Jurkat T cells. (a) Immunoblots showing phosphorylation of the indicated molecules in lysates of J77 Jurkat T cells pretreated with vehicle (DMSO) or Aurora A inhibitor (MLN8237) and conjugated for the indicated times with SEE-pulsed Raji B cells. **(b)** Quantification of blots as in **a** from four-six independent experiments. Error bars represent interquartile range. Medians were compared with a Friedman test.

To corroborate these results in primary CD4$^+$ T cells, we analyzed the phosphorylation of those proteins through the activation with anti-CD3/CD28-coated beads (Fig. R17a and b). The phosphorylation of specific residues was also greatly diminished upon Aurora A inhibition with MLN8237.

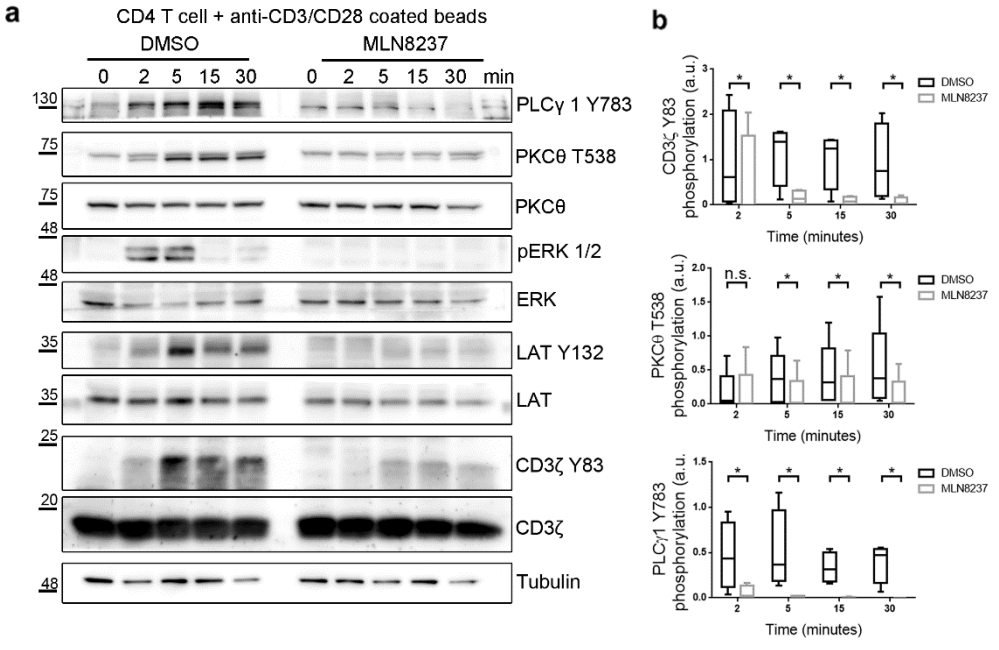

Figure R17 Aurora A inhibition impairs TCR signaling pathways in primary CD4⁺ T cells. (a) Immunoblots showing phosphorylation of the indicated molecules in lysates of DMSO- or MLN8237-pretreated primary human CD4⁺ T cells conjugated for the indicated times with anti-CD3/CD28-coated beads. **(b)** Quantification of blots as in **a** from four-six independent experiments. Error bars represent interquartile range. Medians were compared with a Friedman test (* $p < 0.05$). n.s., non-significant. a.u., arbitrary units.

The role of Aurora A in TCR signaling was also confirmed in a MHC/peptide-specific system, in which MLN8237-treated CH7C17 Jurkat T cells were stimulated with Hom2 lymphoblastoid B cells pre-loaded with HA peptide (Fig. R18a and b).

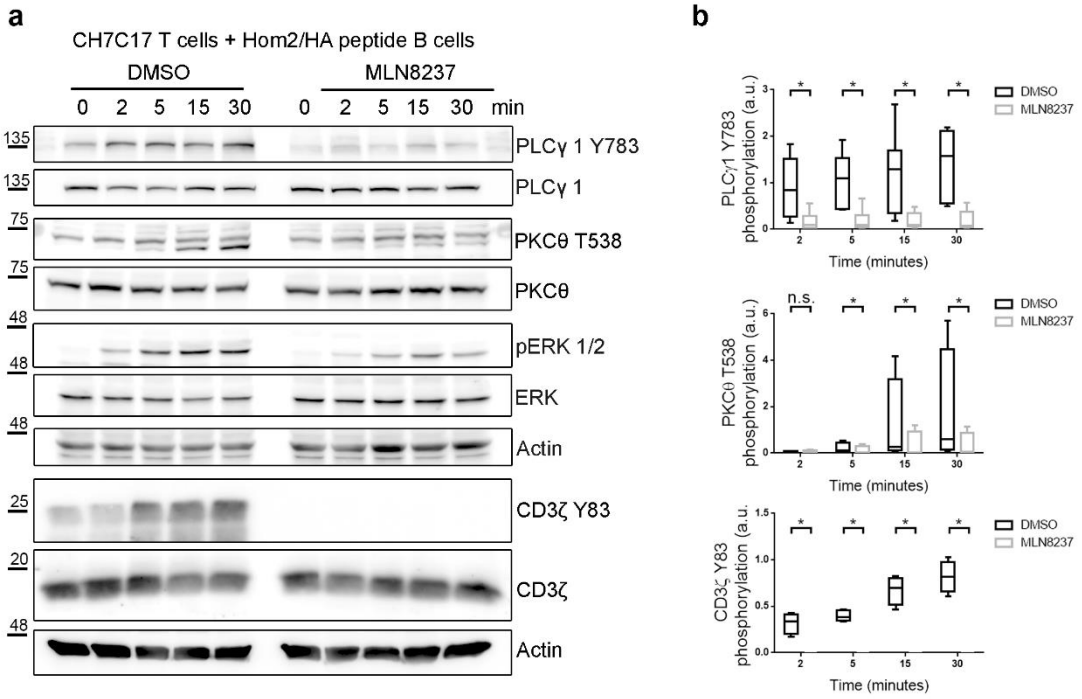

Figure R18. Aurora A inhibition impairs TCR signaling in a MHC/peptide-specific system. (a) Immunoblots showing phosphorylation of the molecules indicated in lysates of CH7C17 Jurkat T cells pretreated with DMSO or MLN8237 and conjugated for the indicated times with HA-peptide-pulsed Hom2 B cells. **(b)** Quantification of blots as in **a** from four-six independent experiments. Error bars represent interquartile range. Medians were compared with a Friedman test (* $p < 0.05$). n.s., non-significant. a.u., arbitrary units.

In order to ascertain that the inhibitor was dose-dependent, Jurkat T cell pre-treated with DMSO or with different concentrations of MLN8237 during 30 min were incubated with SEE-preloaded Raji B cell during 10 min (Fig. R19a and b). The results showed that TCR impairment was bigger at higher concentration of MLN8237 inhibitor, confirming that the inhibition of Aurora A is dose dependent.

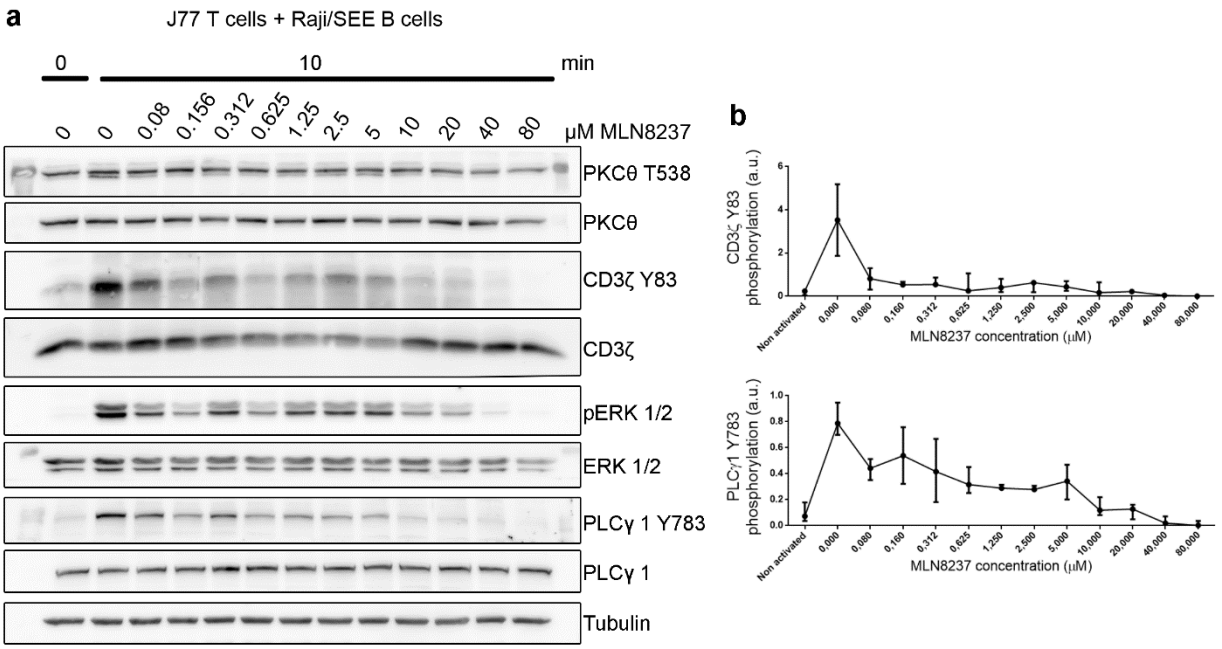

Figure R19. Dose-response effect of the Aurora A inhibitor MLN8237 on T cell activation. (a) Immunoblots showing phosphorylation of the indicated molecules in lysates of J77 Jurkat T cells pretreated with vehicle (DMSO) or Aurora A inhibitor (MLN8237) at the concentrations indicated and conjugated for 10 minutes with SEE-pulsed Raji B cells. **(b)** Quantification of blots as in **a** from three independent experiments. Error bars represent interquartile range.

As a control of MLN8237 specificity, we added the inhibitor just before the activation of Jurkat T cells with SEE-Raji cells and the same effect was observed (Fig. R20).

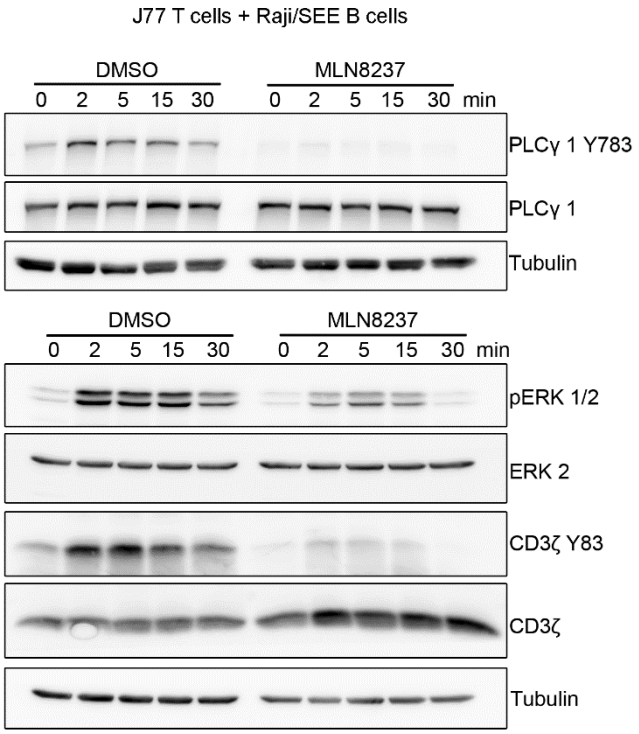

Figure R20. Addition of MLN8237 just before T cell activation impairs TCR signaling. Immunoblots showing phosphorylation of the indicated molecules in lysates of J77 Jurkat T cells conjugated for the indicated times with SEE-pulsed Raji B cells in presence of DMSO or MLN8237.

By extensively washing the inhibitor before activation, the phosphorylation levels of these specific residues were restored, indicating that the effects of the inhibitor were reversible (Fig. R21).

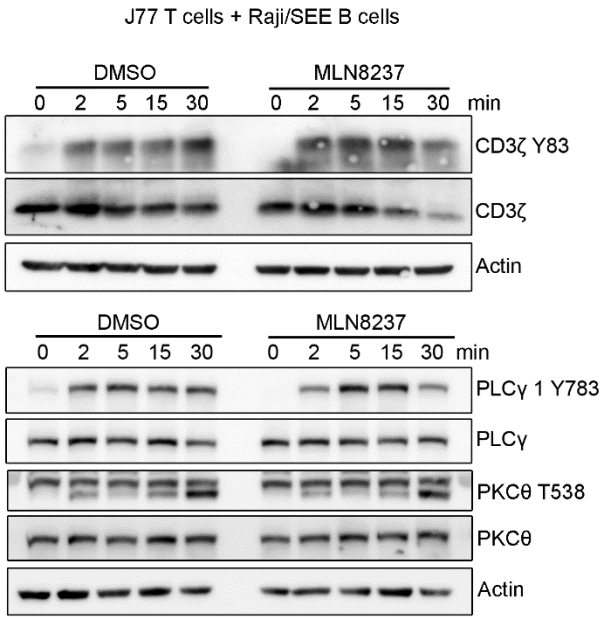

Figure R21. MLN8237 is a reversible inhibitor. Immunoblots showing phosphorylation of the indicated molecules in lysates of J77 Jurkat T cells pretreated with DMSO or MLN8237 for 30 min, extensively washed and conjugated for the indicated times with SEE-pulsed Raji

MLN8237 shows a 200 fold higher selectivity for Aurora A over Aurora B (Manfredi et al, 2011); nonetheless, to rule out a possible role of Aurora B, we treated Jurkat T cells with AZD1152 (100 nM), which is 3,700 times more selective for Aurora B (Yang et al, 2007). AZD1152 had no effect on the phosphorylation of T cell proteins (Fig. R22), confirming that proper T cell activation critically depends of the isoform A, but not B, of Aurora kinase.

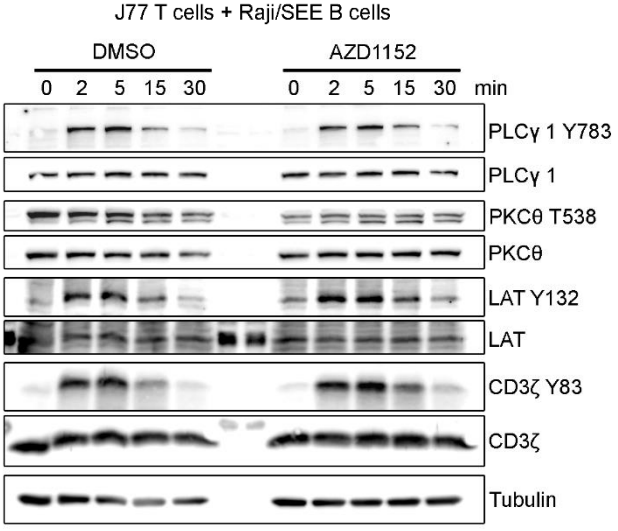

Figure R22. TCR signaling is not affected by Aurora B inhibition. Immunoblots showing phosphorylation of the indicated molecules in lysates of J77 Jurkat T cells pretreated with vehicle (DMSO) or Aurora B inhibitor (AZD1152, 100 µM) and conjugated for the indictaed times with SEE-pulsed Raji B cells.

This was further confirmed in conjugates of Aurora A-silenced Jurkat T cells and SEB-preloaded Hom2 B cells as APCs. The activation of CD3ζ-dependent molecules was defective in Aurora A-silenced cells, with below-normal LAT phosphorylation on residue Y132, likely responsible for the concomitant decreases in PLCγ1 (Y783) and PKCθ (T538) phosphorylation (Fig. R23).

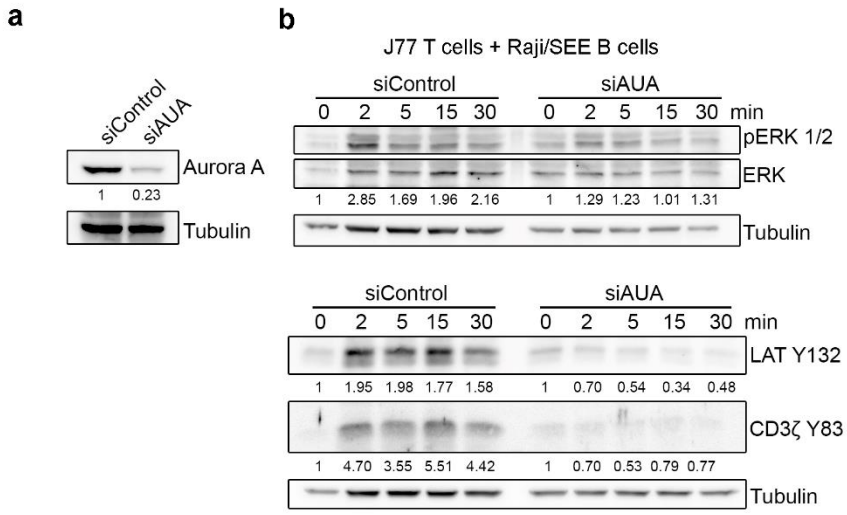

Figure R23. TCR signaling is impaired by silencing of Aurora A. (a) Immunoblot analysis of Aurora A protein expression in Jurkat T cells transfected with a specific siRNA against Aurora A (siAUA) or a scrambled negative control (siControl). **(b)** Immunoblots showing phosphorylation of the indicated molecules in lysates of J77 Jurkat T cells transfected with the siAUA or siControl and conjugated for the indicated times with SEE-pulsed Raji B cells**.**

To determine the role of Aurora A in late events of T cell activation, we examined the mRNA expression of IL-2, CD25 and CD69. Human $CD4^+$ T lymphocytes were treated with MLN8237 and AZD1152 or vehicle for 30 min, and stimulated with anti-CD3/CD28 antibodies for 3 h. Inhibition of Aurora A impaired the up-regulation of IL-2, CD25 and CD69 mRNA determined by RT-PCR (Fig. R24), indicating a defect in late T cell activation. In contrast, Aurora B inhibition had no effect on the mRNA production of these genes, supporting a specific role for Aurora A and its regulated pathways in T cell activation.

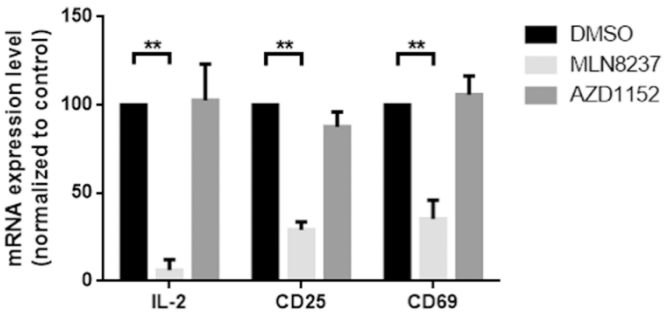

Figure R24. IL2, CD69 and CD25 expression is impaired by Aurora A inhibition. IL2, CD69 and CD25 mRNA levels in primary human $CD4^+$ T cells pretreated with DMSO, MLN8237 (10 µM) or the Aurora B inhibitor AZD1152 (100 nM) and activated by settling on anti-CD3/CD28-coated plates for 4 h. mRNA levels from four-six independent experiments were normalized to the housekeeping gene GAPDH and the levels of the target mRNA in non-stimulated cell levels. Error bars represent interquartile rage. Medians were compared with a Mann-Whitney test. (** $p < 0.01$).

Pharmacologic inhibition of Aurora A also impaired early T cell activation in mouse naive $CD4^+$ T cells polyclonally stimulated with anti-CD3/CD28 (Fig. R25).

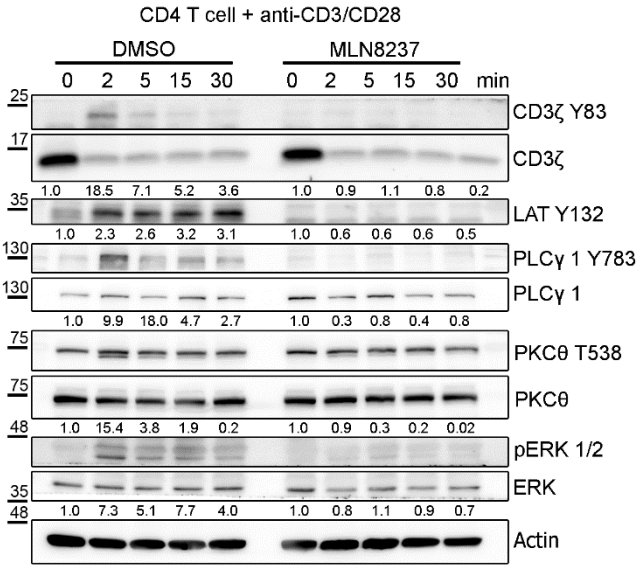

Figure R25. Aurora A inhibition impairs TCR signaling in mouse CD4⁺ T cells. Immunoblots showing phosphorylation of the indicated molecules in cell lysates of WT mouse CD4⁺ T cells pretreated with vehicle (DMSO) or Aurora A inhibitor (MLN8237) and activated for the indicated times with anti-CD3/CD28 antibodies.

To further assess the function of Aurora A in primary naive T cells, we deleted Aurora A expression in CD4⁺ cells from the conditional Aurora KO mice and activated them with anti-CD3/CD28 antibodies. Tamoxifen-induced suppression of Aurora A expression in Aurka(lox/lox); RERT(ert/ert) cells correlated with clear decreases in the phosphorylation of CD3ζ (Y83), LAT (Y132), PLCγ1 (Y783), PKCθ and ERK1/2 (T202/Y204) (Fig. R26a and b).

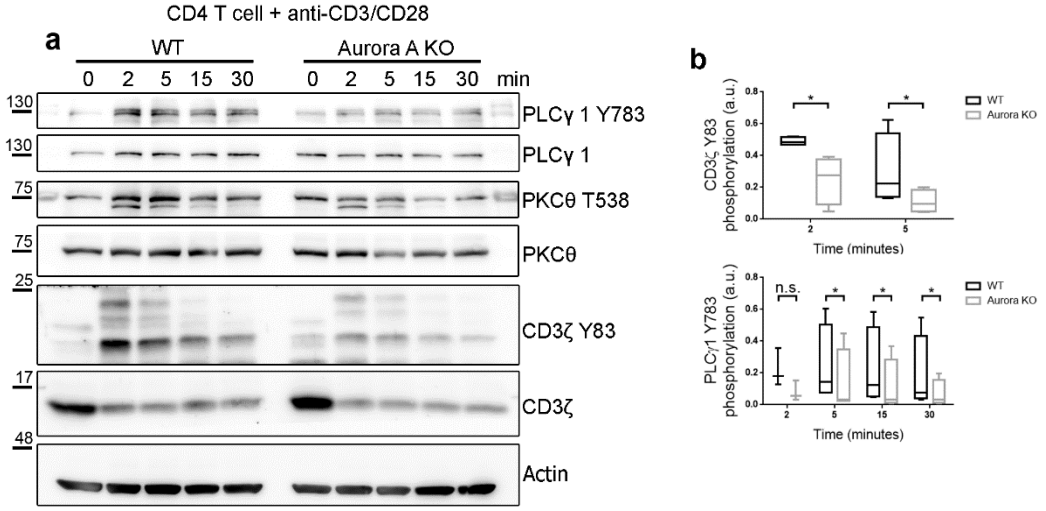

Figure R26. Aurora A gene ablation blocks TCR signaling pathways. (a) Immunoblots showing phosphorylation of the indicated molecules in cell lysates of Aurora KO and control CD4⁺ T cells conjugated for the indicated times with anti-CD3/CD28 antibodies. **(b)** Quantification of data from four independent experiments as in **a**. Error bars represent interquartile range. Medians were compared with a Friedman test (* $p < 0.05$). n.s., non-significant. a.u., arbitrary units.

In complementary experiments, we examined a transgenic mouse model of Aurora A overexpression (Piazzolla et al, 2014). Naive CD4⁺ T cells isolated from lymph nodes and spleens of Col1a1tetO-Aurka/+; Rosa26rtTA/rtTA mice (Aurora KI) and controls were treated with doxycycline and IL-7 for 24 h, followed

by activation with anti-CD3/CD28 antibodies. Doxycycline treatment increased Aurora A expression in the conditionally transgenic cells (Fig. R27a), correlating with increased levels of TCR-dependent signaling (Fig. R27b and c).

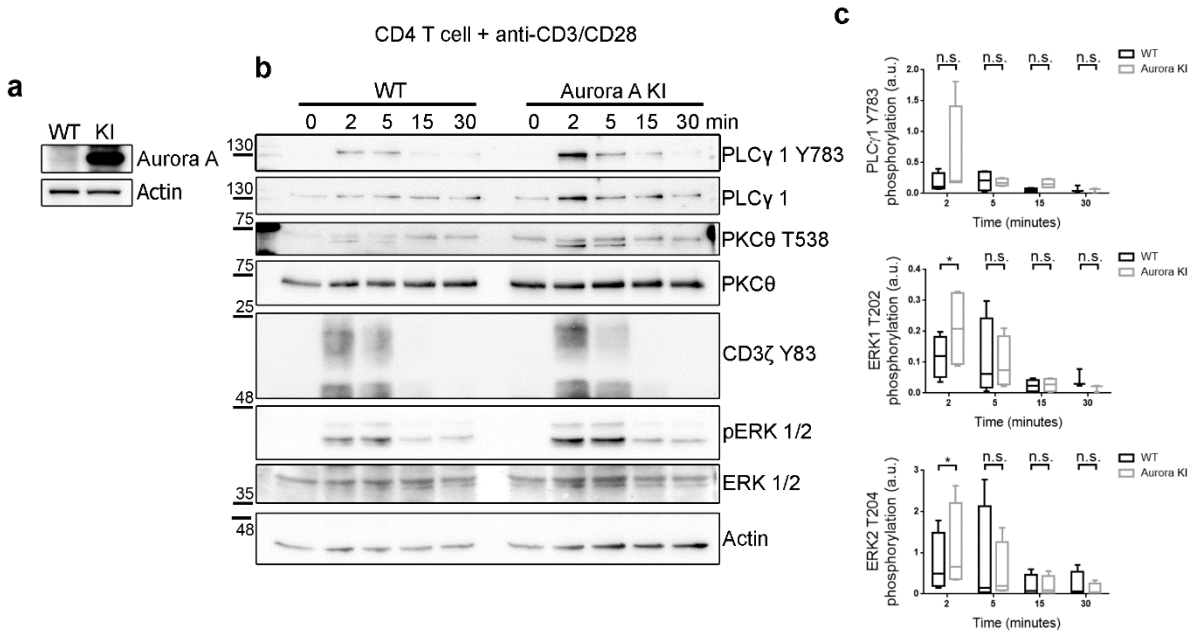

Figure R27. Overexpression of Aurora A increase levels TCR molecules phosphorylation. (a) Immunoblot analysis of Aurora A protein expression in CD4$^+$ T cells isolated from Col1a1tetO-Aurka/+; Rosa26rtTA/rtTA mice and treated with doxycycline for 20 h to induce Aurora A expression (KI). Control cells (WT) were maintained without doxycycline. Actin is shown as a loading control. **(b)** Immunoblots showing phosphorylation of the indicated molecules in cell lysates of Aurora KI CD4$^+$ T cells conjugated for the indicated times with anti-CD3/CD28 antibodies. **(c)** Quantification of data from four independent experiments as in **b**. Error bars represent interquartile rage. Medians were compared with a Friedman test (* p value < 0.05). n.s., non-significant. a.u., arbitrary units.

4.6 Mechanism through Lck regulation

To study the mechanism underlying the earliest T cell activation defects in the absence of Aurora A, we assessed the possible regulation of the Src kinase Lck by Aurora A. Lck phosphorylates CD3 ITAMs at tyrosine residues upon TCR trigering and shows autophosphorylation activity towards its Y394 residue, an activatory residue (Nika et al, 2010). By quantitative analysis of Lck accumulation at the IS we have detected a significant reduction in Lck relocation to the IS contact area, as a result of Aurora A inhibition in Jurkat T cells (Fig. R28a and b). In accordance with a perturbed Lck localization, pharmacologic inhibition of Aurora A in human primary CD4$^+$ T cells impaired Lck autophosphorylation at Y394, a marker of its activity (Fig. R28c and d). Notably, these experiments showed that Lck-Y394 phosphorylation was impaired prior to TCR stimulation, suggesting a role of Aurora A in the maintenance of the pre-activated pool of Lck (Nika et al, 2010).

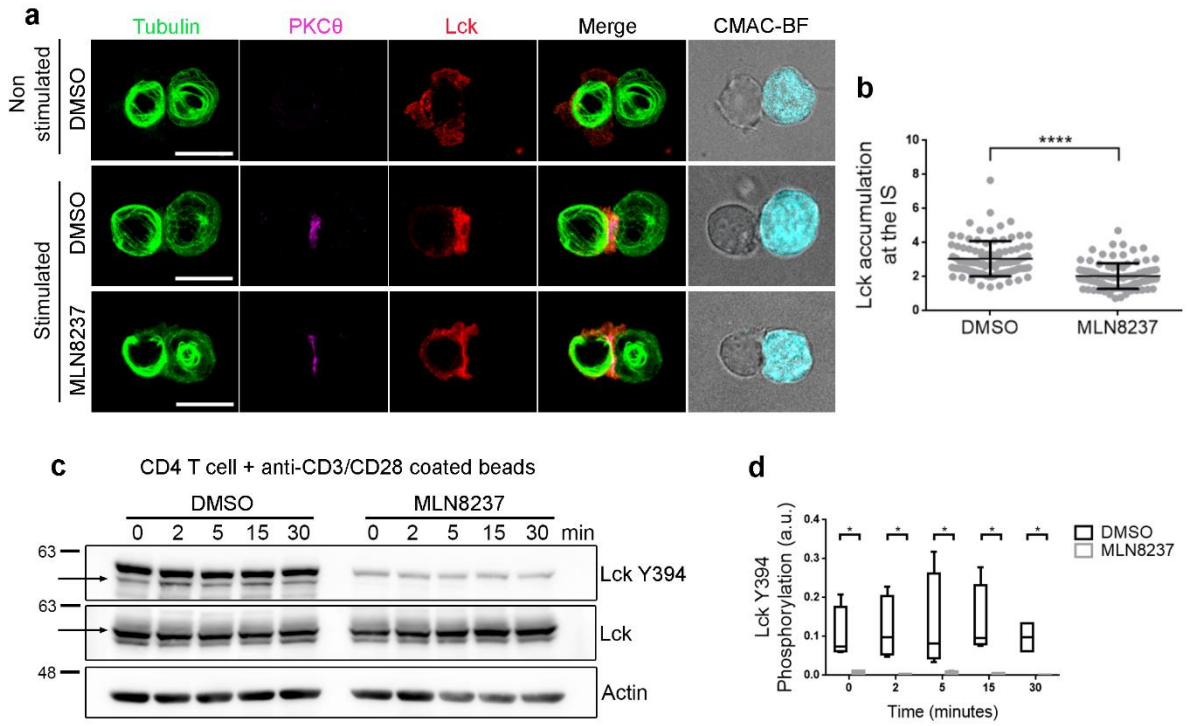

Figure R28. Aurora controls localization and phosphorylation of the tyrosine kinase Lck. (a) Maximum Z projection of XYZ-stack of human Jurkat T cells pretreated with vehicle (DMSO) or Aurora A inhibitor (MLN8237) and conjugated with SEE-preloaded Raji B cells (APCs; 30 min). Cells were fixed and stained for α-tubulin-FITC (green), PKCθ (magenta) and Lck (red). Bright field images are included. Bar, 10 µm. **(b)** Quantification of Lck accumulation at the IS in conjugates as in **a** from three independent experiments (n=96 in DMSO, n=94 in MLN8237). Data represent means ± SD. Means were compared with a t-test; (**** P<0.0001)**. (c)** Immunoblot of Lck phosphorylation at Y394 in primary human $CD4^+$ T cells. Cells were pretreated with DMSO or MLN8237 and conjugated for the indicated times with anti-CD3/CD28-coated beads. Total Lck and actin are included as loading controls. Arrows point Lck band**. (d)** Quantification of data from four independent experiments as in **c**. Error bars represent SD. Medians were compared with a Friedman test (* P<0.05).

To analyze whether the effect of Aurora A on Lck activation is dependent on the intracellular traffic of Lck (Soares et al, 2013a) and taking into account that Lck recruitment at the IS is also driven by its association with CD4 (Li et al, 2004), we decided to assess T cell activation in a Lck-deficient cell line (J.CAM1 (Goldsmith & Weiss, 1987; Straus & Weiss, 1992)) reconstituted with full-length Lck-GFP or murine CD4-Lck chimeric proteins. CD4-Lck is mainly localized at the plasma membrane (Anton et al, 2008; Xu & Littman, 1993) . A murine CD4 lacking its cytosolic tail and fused to GFP was used as a negative control (Krummel et al, 2000) (Fig. R29; CD4-ΔCyt-GFP). We found that Lck-GFP expression rescued CD3 phosphorylation and thus T cell activation in J.CAM1, whereas MLN8237 treatment prevented such an effect. Rescue of J.CAM1 signaling with CD4-Lck chimaera was also prevented with the Aurora A inhibitor. Therefore, Aurora A activity is needed for Lck activity independently of its intracellular trafficking during IS formation.

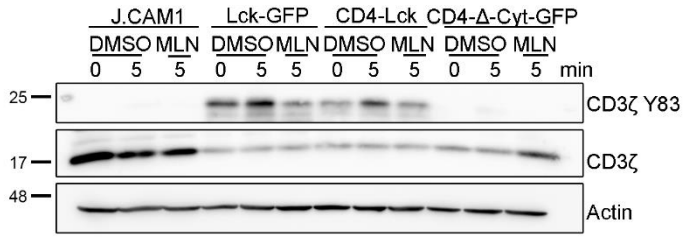

Figure R29. Membrane Lck is affected by Aurora A inhibition. Immunoblots of CD3ζ phosphorylation in lysates of J.CAM1 T cells transfected with Lck-GFP, CD4-Lck or CD4-ΔCyt-GFP, pretreated with DMSO or MLN8237 and conjugated for 5 min with SEE-pulsed APCs.

Immunoprecipitation of Lck from T lymphoblasts followed by mass spectrometry analysis revealed that Aurora A inhibition resulted in decrease of Lck phosphorylation at the activation residue Y394 in resting and stimulatory conditions (Fig. R30).

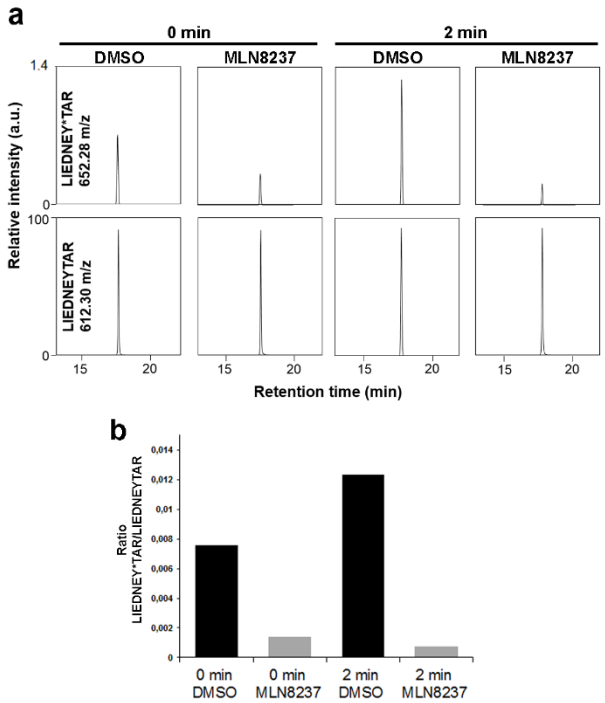

Figure R30. Lck phosphorylation at Y394 decreases by Aurora A inhibition. T cell lymphoblasts pretreated with DMSO or MLN8237 were activated or not with SEE-pulsed APCs (2 min) and subjected to immunoprecipitation using an anti-Lck antibody. The immunoprecipitates were subjected to mass spectrometry analysis. **(a)** MS/MS extracted ion chromatograms of the Y394-phosphorylated and non-modified forms of Lck peptide LIEDNEYTAR. **(b)** Phosphorylated:non-modified peak ratios.

This was further corroborated by in vitro kinase assays of purified recombinant Lck protein by immunoprecipitated Aurora A proteins. While wild type (WT) Aurora A protein keeps Lck phosphorylated at residue Y394, a kinase dead mutant (KD) form of Aurora is unable to maintain Lck phosphorylation at Y394 (Fig. R31). Treatment with the Aurora A inhibitor corroborated the KD results (Fig. R31). Together these results highlight the relationship of Aurora A-mediated signal spreading at the IS with Lck location, phosphorylation, and therefore, regulation.

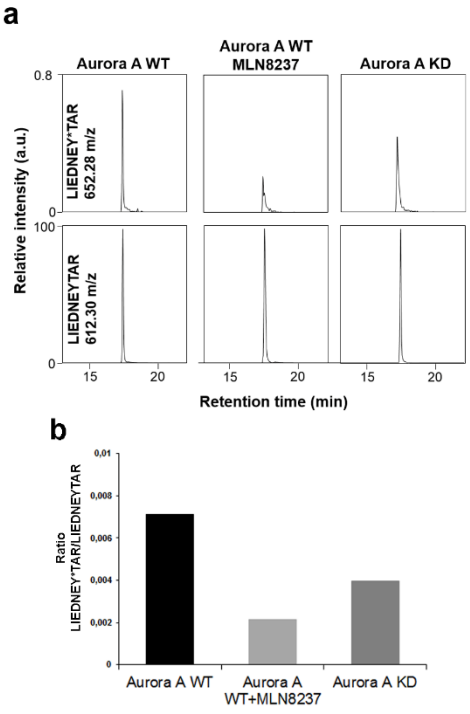

Figure R31. Aurora A keeps Lck phosphorylated before TCR stimulation. Recombinant Lck was incubated with Aurora A WT (in the absence or presence of MLN8237) or Aurora A KD immunoprecipitated from nocodazole-treated (16 h), transfected HEK293 cells. Lck and Aurora were incubated for 30 min in presence of ATP and the mixture analyzed by mass spectrometry. **(a)** MS/MS extracted ion chromatograms of the Y394-phosphorylated and non-modified forms of Lck peptide LIEDNEYTAR. **(b)** Phosphorylated:non-modified peak ratios.

Discussion

5. Discussion

In this study we have analyzed the influence of a well-known cell cycle regulator, Aurora A kinase, in T cell activation. Our results provide novel evidence that Aurora A is a key regulator of early TCR-dependent signaling pathways and controls signaling vesicle and microtubular dynamics. However, the direct interaction of TCR/CD3 with Nck and actin polymerization at IS are not affected by Aurora A inhibition. Aurora A localizes at the IS and appears activated upon antigen- and superantigen-driven T cell activation. Early activation of Aurora A seems to be essential for TCR downstream signaling leading to LAT and PLC activation. In addition, our data provide mechanistic insight into how Aurora A acts as master regulator of T cell activation by controlling Lck phosphorylation and clustering at the IS.

5.1 Aurora A localization and activation at the IS

During $CD4^+$ and $CD8^+$ T cell activation, the secretory elements, including the GA, ER (endoplasmic reticulum), endolysosomal system and secretory vesicles are rapidly translocated with the centrosome to the IS (Bustos-Moran et al, 2016; Martin-Cofreces et al, 2014). This specific localization promotes a fast and direct secretion of diverse molecules from the trans-Golgi network (TGN) and the endosomal compartment to the plasma membrane, regulating the polarized secretion of exosomes or IL-4 cytokine in $CD4^+$ and perforin and granzymes from lytic granules in $CD8^+$ T cells (Bustos-Moran et al, 2016; Huse et al, 2008; Kienzle & von Blume, 2014). Several studies have proposed a relationship between GA and Aurora A function and localization. During mitosis, the GA undergoes fragmentation to properly segregate into the daughter cells. The inhibition of the GA fragmentation at the G2 stage blocks the recruitment and activation of Aurora A at the centrosomes (Cervigni et al, 2011). Also, there is evidence of a role for the GA in the regulation of spindle formation during mitosis. The GA matrix protein GM130 recruits importin α to the GA membranes, promoting the release of the spindle assembly factor TPX2. TPX2 activates Aurora A, stimulating local MT nucleation (Fig. D1) (Wei et al, 2015). GM130 may control MT polymerization from the GA also in cells in interphase. To do this, it recruits AKAP450 to the cis-Golgi (Rivero et al, 2009). AKAP450 promotes tubulin nucleation through the binding to CGP subunits of the γ-Tubulin ring complex (γ-TURC) at the centrosome (Takahashi et al, 2002), which seems a shared mechanism for polymerization at the cis-Golgi. The structure of MTs is clearly different at the centrosome and the GA, since they show a radial array in the first organelle and a more tangential disposition at the GA (Zhu & Kaverina, 2013). In this regard, silencing of AKAP450 or over-expression of a dominant-negative, AKAP450-centrosomal domain prevents T cell activation and centrosome polarization to the

IS (Robles-Valero et al, 2010). Therefore, centrosome-resident AKAP450 is required for T cell activation, but the relative contribution of GA-resident AKAP450 remains to be determined. Although Aurora A inhibition does not prevent centrosome polarization, tubulin nucleation is impaired. The possible tubulin-nucleation activity of the GA has not been determined in T cells. Since Aurora A is activated by TPX2 and this process is mediated by GM130 during spindle formation in mitosis, these observations indicate that Aurora A could be involved in MT polymerization from the GA during the IS, further supporting a conserved mechanism between cell division and IS formation (Fig. D1).

A recent study showed that, during G2 phase, the GA fragmentation promotes Src protein activation at the TGN. This is relevant because Src phosphorylates Aurora A on residue Y148; which is required for Aurora A to localize to centrosomes and become active (Fig. D1a) (Barretta et al, 2016). Therefore, the translocation of the GA during the first step of the IS might be involved in the activation of Aurora A in this region. Some proteins that regulate Aurora A function in other systems, e.g. TPX2 or Src, which also participate in the formation of the IS, may form feedback loops that connect the regulation of different phenomena, e.g. activation of Aurora A by Src during mitosis and Lck regulation by Aurora A during the IS (Fig. D1).

Some works reveal a non-mitotic role for Aurora A, such as ciliary disassembly, with different mechanisms of activation. This process requires interaction with Ca^{2+}/calmodulin (CaM) (Plotnikova et al, 2012). The IS formation has been compared with the cilia formation, since a set of proteins are implicated in both processes, such as IFT (intraflagellar transport) proteins for transport of vesicles, AKAP450 or HDAC6, both regulators of microtubules (Bustos-Moran et al, 2016). During the IS, Ca^{2+} release-activated channels (CRAC) are opened after TCR activation, promoting proper IS formation by regulating actin organization (Hartzell et al, 2016). Similarly to the relationship between Ca^{2+} and Aurora A activation in primary cilia formation, this interaction could imply a role of Ca^{2+} in Aurora A activation during IS formation.

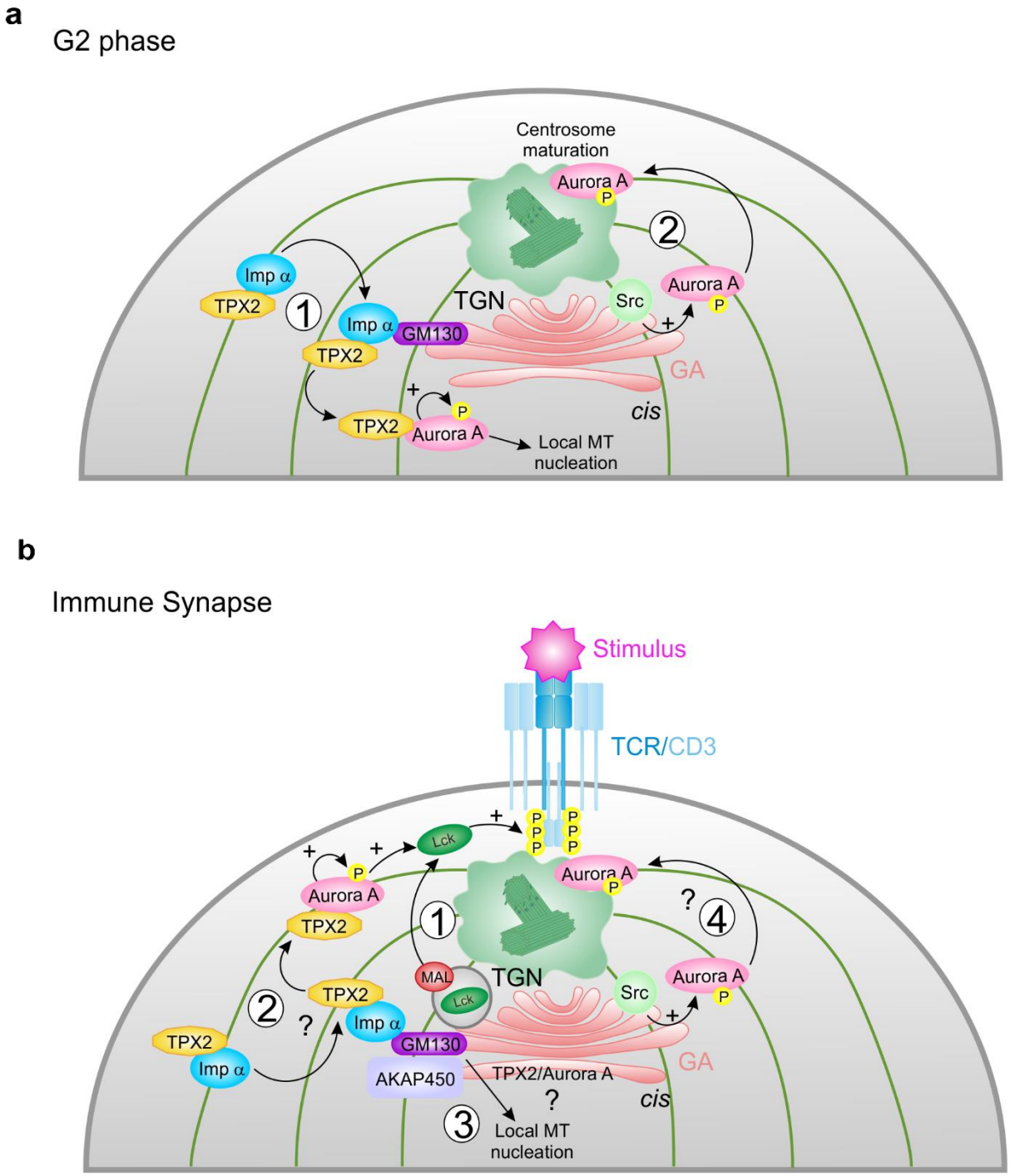

Figure D1. Activation of Aurora A during the IS by proteins from GA. **(a)** Regulation of Aurora A activity during G2 phase. (1) Interaction of GM130 with importin α promotes the release of TPX2 and the consequent Aurora A autophosphorylation, promoting local MT polymerization. (2) Aurora A phosphorylation by Src allows Aurora A localization at the centrosome for proper centrosomal maturation. **(b)** Possible model of Aurora A regulation during the IS. (1) Translocation of vesicles containing Lck from TGN to membrane is directed by MAL. (2) Activation of Aurora A by TPX2 release next to the IS area. (3) Local MT polymerization from GA through Aurora A activation mediated by GM130 and AKAP450. (4) Activation of Aurora A at the centrosome through Src activation. GA, Golgi apparatus; Imp α, importin α; MT, microtubule; TCR, T cell receptor; TGN, trans-Golgi network.

5.2 Microtubule polymerization and vesicular traffic

Aurora A contributes to centrosome maturation through the recruitment of MT nucleation factors. However, its absence does not prevent the formation of the centrosomal microtubule aster but instead affects the density of the aster formed in other systems (Sardon et al, 2008). Our TIRFm analysis demonstrates that Aurora A controls growing MT arising from the MTOC upon TCR activation while having no apparent effect on MTOC translocation at the IS. In addition, during the M phase Aurora A is required for the recruitment of adaptor proteins like NEDD1 for the correct formation of the mitotic spindle. Previous work on proteins implicated in MT regulation such as EB1 or HDAC6 (Martin-Cofreces et al, 2012; Serrador et al, 2004) showed a defect in late T cell activation. The role of these proteins in MT cytoskeleton dynamics and T cell activation seemed to be mainly related to the maintenance of the TCR signal rather than its initial activation. Aurora A might regulate late T cell activation through a similar mechanism. Our data indicate that the decrease in the number of MTs nucleated near the contact area may affect polarized secretion from this area and vesicular trafficking at the IS and throughout the T cell. Hence, Aurora A inhibition prevents movement of CD3ζ vesicles around the MTOC almost completely, possibly reflecting a global effect on vesicle trafficking. Also, since CD3 is tightly regulated by its cycle of degradation and recycling (Monjas et al, 2004), the absence of this pool of CD3ζ vesicles at the c-SMAC may explain why the TCR signal cascade is not properly propagated. It has been proved that there is a pool of phosphorylated CD3ζ that instead of going to a degradation pathway keeps accumulated at the endosomal compartment ready to maintain CD3ζ phosphorylation signaling (Yudushkin & Vale, 2010). Although Aurora A inhibition has no effect in TCR/CD3ε subunit surface clustering at the IS, the transport of vesicles of the CD3ζ subunit is clearly impaired. Taking into account the presence of this phosphorylated CD3ζ pool at the endosomal compartment, Aurora A might have an effect mainly over this recycling of the active CD3ζ and therefore over TCR signal propagation.

5.3 Actin cytoskeleton

Although Aurora A contributes to actin cytoskeleton dynamics in mitosis and during mammary cell migration, no such effect was observed during IS formation by spreading T cells. Aurora A-mediated phosphorylation of LIM kinase 1 (LIMK1) at the centrosomes in prophase is essential for modulation of actin filaments and subsequent spindle formation. LIMK1 acts by inactivating the phosphorylation of the actin depolymerizing family protein cofilin, thus stabilizing the cortical actin network during spindle orientation (Ritchey et al, 2012). In mammary cell migration Aurora A promotes increased expression of the cofilin phosphatase SSH1, resulting in cofilin activation and actin reorganization and migration (Wang et al, 2010). However, our data show that Aurora A

inhibition affects neither actin accumulation during IS formation nor cell spreading. Indeed, we found that Aurora A-inhibited T cells form normal-shaped lamellae. During IS formation, Nck acts as a bridge between the TCR activation and actin cytoskeleton reorganization at the IS. When the TCR recognizes a specific antigen, a conformational change in the CD3ε chain unmasks a neoepitope to which Nck binds, leading to transmission of the activation signal through the actin cytoskeleton (Gil et al, 2002). CD3ε-NcK association is not affected by Aurora A inhibition, a finding in accordance with the absence of changes in actin accumulation at the IS in MLN8237-pretreated T cells. Moreover, this is consistent with the observed accumulation of the TCR/CD3 complex at the IS, by the tracking forces exerted by actin (Comrie & Burkhardt, 2016).

5.4 Early T cell activation

Our results show regulatory effects of Aurora A on early and late T cell signaling. Inhibition of Aurora A abrogates proper T cell activation determined by the phosphorylation profile of TCR-signaling proteins such as CD3 and the adapter proteins and kinases LAT, PLCγ1 and PKCθ. These effects on TCR pathway phosphorylation events were observed in response to the Aurora A inhibitor MLN8237 and Aurora A gene ablation in mouse T cells, indicating that this is a specific consequence of Aurora A inhibition. The initial activation of T cells occurs at the plasma membrane, but its continued progress requires the contribution of intracellular components such as the MTOC and the MT-dependent vesicular traffic and mitochondrial activity (Martin-Cofreces et al, 2014). Aurora A thus contributes to the propagation of TCR activation to the intracellular compartment, leading to activation of genes such as IL-2, CD69 and CD25. Moreover, the strength of T cell activation can determine the ability of T cells to divide asymmetrically, thereby promoting functional differentiation into subpopulations of T cells that regulate the immune response (King et al). Our data suggest that T lymphocytes defective in Aurora A do not become properly activated, possibly affecting the outcome of the adaptive immune response.

However, neither the defect on MT dynamics nor the impairment in CD3ζ vesicles transport can explain the blockade of the initial trigger of TCR signaling. These early defects of CD3ζ-dependent signaling in Aurora A-targeted cells are more likely explained by altered activity of Src- kinases. This family includes Lck and Fyn, the first kinases to phosphorylate the ITAMs in CD3, which are required for full activation and signal transmission (Palacios & Weiss, 2004; Schoenborn et al, 2011). Our data demonstrate that Lck location and phosphorylation are altered by chemical inhibition of Aurora A, demonstrating that Aurora A controls TCR pathways dependent on CD3-ITAM phosphorylation.

5.4.1 Direct Lck regulation by Aurora A

During IS formation, Lck localizes near the TCR/CD3 complexes, which is required for Lck-mediated phosphorylation of CD3 immunoreceptor tyrosine-based activation motifs (ITAMs) (Palacios & Weiss, 2004). Lck appears in specific membrane microdomains (rafts) containing MAL and Caveolin-1 (Cav-1). These proteins are required for Lck clustering to the membrane during the IS, and MAL or Cav-1 depletion decreases the efficiency of CD3 ITAM motifs phosphorylation (Anton et al, 2008; Schonle et al, 2016). MAL is present in vesicles containing Lck, enabling the association of Lck with the plasma membrane at the IS (Fig. D2) (Martin-Cofreces et al, 2014). Since Aurora-A gene depletion or pharmacological inhibition impedes the proper traffic of CD3ζ-bearing vesicles to the IS, we postulated that Lck bearing vesicles traffic may also be affected by the absence of Aurora-A activity. Interestingly, Aurora A inhibition prevented the rescue of CD3 phosphorylation in a cell line lacking Lck (JCAM.1) transfected with a construction of full-length Lck fused to the transmembrane domain of CD4. In these cells, Lck-CD4 is localized at the IS in a vesicle-independent manner, suggesting that Aurora A may control the enzymatic activation of Lck that is already bound to the plasma membrane, and not only its localization (Fig. D2).

Lck, and SFKs in general, are regulated reciprocally by phosphorylation and de-phosphorylation of two conserved tyrosine residues (Palacios & Weiss, 2004). Lck is phosphorylated in residue Tyr394, which is used as a fiduciary marker of its activation. One study has shown that TCR activation does not control the phosphorylation level of Y394, suggesting that Lck is activated prior to T cell activation (Nika et al, 2010). Another study showed Lck to be regulated through conformational changes, clustering and spatio-temporal proximity to other proteins, e.g. the Lck inhibitory kinase Csk and the transmembrane phosphatase CD45. Csk regulates the phosphorylation of residue Y505, which is inhibitory and CD45 dephosphorylates both Y505 and Y394 residues (Hui & Vale, 2014). However, other authors have reported an increase of nearly 20% in Lck phosphorylation upon TCR priming, as measured by Western blot after immunoprecipitation, or through FLIM-FRET analysis with a biosensor that detects conformational opening and closing (Stirnweiss et al, 2013). Aurora A inhibition decreases Y394 phosphorylation before TCR triggering. Since Aurora A is a serine/threonine kinase, Y394 is not expected to be its substrate. In fact, Y394 is an autophosphorylation site (Palacios & Weiss, 2004). Based on these observations, a model can be drawn in which Aurora A phosphorylates a yet unidentified residue in Lck, which may in turn influence Y394 autophosphorylation by affecting the conformation of Lck (Fig. D2).

Several Ser residues have been identified in Lck upon activation; mainly S59 at the unique N-terminal domain and S122, S158, S192 and S194 at the SH2 domain. S59 and S122 seem to

reduce Lck activity either in vivo or in vitro. In particular, S59 seems to act on the ability of the SH2 domain to interact with partners and it is phosphorylated during mitosis (Joung et al, 1995; Kesavan et al, 2002; Nguyen et al, 2016; Soula et al, 1993). However, the fact that Aurora A disruption decreases Lck activity points to other residues as substrates for this enzyme. Mass spectrometry analysis combined with the use of Aurora A conditional knock out mice could help us to identify other putative phosphorylatable sites on Lck. Moreover, FLIM-FRET and super-resolution analyses would be a proper experimental strategy to assess the conformational changes that may occur in Lck protein and/or the possible partners of Lck during the IS.

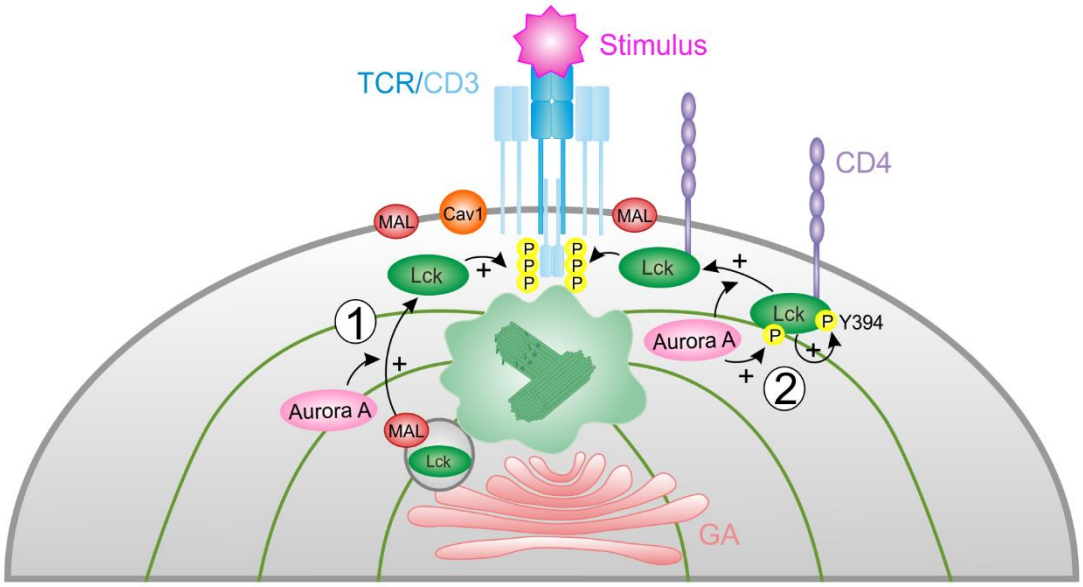

Figure D2. Lck direct regulation by Aurora A. (1) Aurora A regulates the vesicular traffic of Lck trough the microtubule network. (2) Possible phosphorylation of Lck by Aurora A in an unknown residue promotes autophosphorylation in Y394 and proper translocation to the IS region.

5.4.2 Lck indirect regulation by Aurora A

Although Aurora A may be directly regulating Lck phosphorylation, it is feasible that additional protein(s) may serve as "interaction bridges" between Aurora A and Lck. Csk and CD45 appears as suitable candidates. Phosphorylation of Lck at Y505 by Csk promotes the intramolecular interaction of the residue with the SH2 domain, favoring a closed conformation of Lck (Fig. D3) (Xu et al, 2015). Hence, phosphorylation of Y505 prior to Y394 maintains Lck in a closed, inactive form, whereas phosphorylation of Y394 promotes Lck activation, even though Y505 is phosphorylated afterwards (Palacios & Weiss, 2004). Moreover, CD45 dephosphorylates both residues in Lck and also CD3 ITAMs, although its effect is more noticeable in the ITAMs (Dustin, 2012; Hermiston et al, 2003; Hui & Vale, 2014). Aurora A could phosphorylate and

inactivate Csk, and thus Lck Y505 phosphorylation, which would maintain Lck in an active conformation (Fig. D3). The described phosphorylation of Csk on S364 increases its activity, and therefore would not fit in this model (Vang et al, 2001). Csk is regulated by the phosphoprotein associated with glycosphingolipid-enriched microdomains/Csk binding protein (PAG/Cbp) complex, which is phosphorylated in lipid rafts in resting T cells, thereby inducing Lck inhibition. Phospho-PAG/Cbp promotes the binding of Csk to Lck and the phosphorylation of Y505 (Fig. D3) (Brdicka et al, 2000; Kawabuchi et al, 2000). After TCR triggering, dephosphorylation of PAG/Cbp in tyrosines leads to the dissociation of Csk from lipid rafts and allows Lck activation (Davidson et al, 2003). However, a recent study based on proteomic approaches has shown that an increase in PAG phosphorylation can be detected upon TCR activation, accompanied by Csk and SHIP1 and PTPN22 phosphatases interaction (Reginald et al, 2015). Hence, the absence of Aurora A could reinforce the PAG/Cbp interaction with Csk, enhancing Lck inhibition due to the phosphorylation of the PAG/Cbp complex. Therefore, Aurora A might be regulating the kinase that acts on PAG. These studies, together with the observed mislocalization of Lck at the IS in Aurora A-inhibited cells and the fact that non-phosphorylatable Aurora A cannot be properly recruited to the IS, suggest that Aurora A may spatio-temporally regulate the localization of other proteins involved in TCR activation (Fig. D3).

The spatial localization of the phosphatase CD45 is essential for TCR activation. When the eye-shaped IS forms, CD45 is sterically excluded from the T cell-APC proximal contact area to prevent the dephosphorylation of CD3 and Lck (Varma et al, 2006). Interestingly, Aurora A inhibition decreased both Lck phosphorylation at Y394 and that of the CD3 ITAMs. However, although CD45 activity could explain the enhanced dephosphorylation of both residues in Aurora A depleted cells, the sterically exclusion model for CD45 makes unlikely for Aurora A to regulate its activity directly.

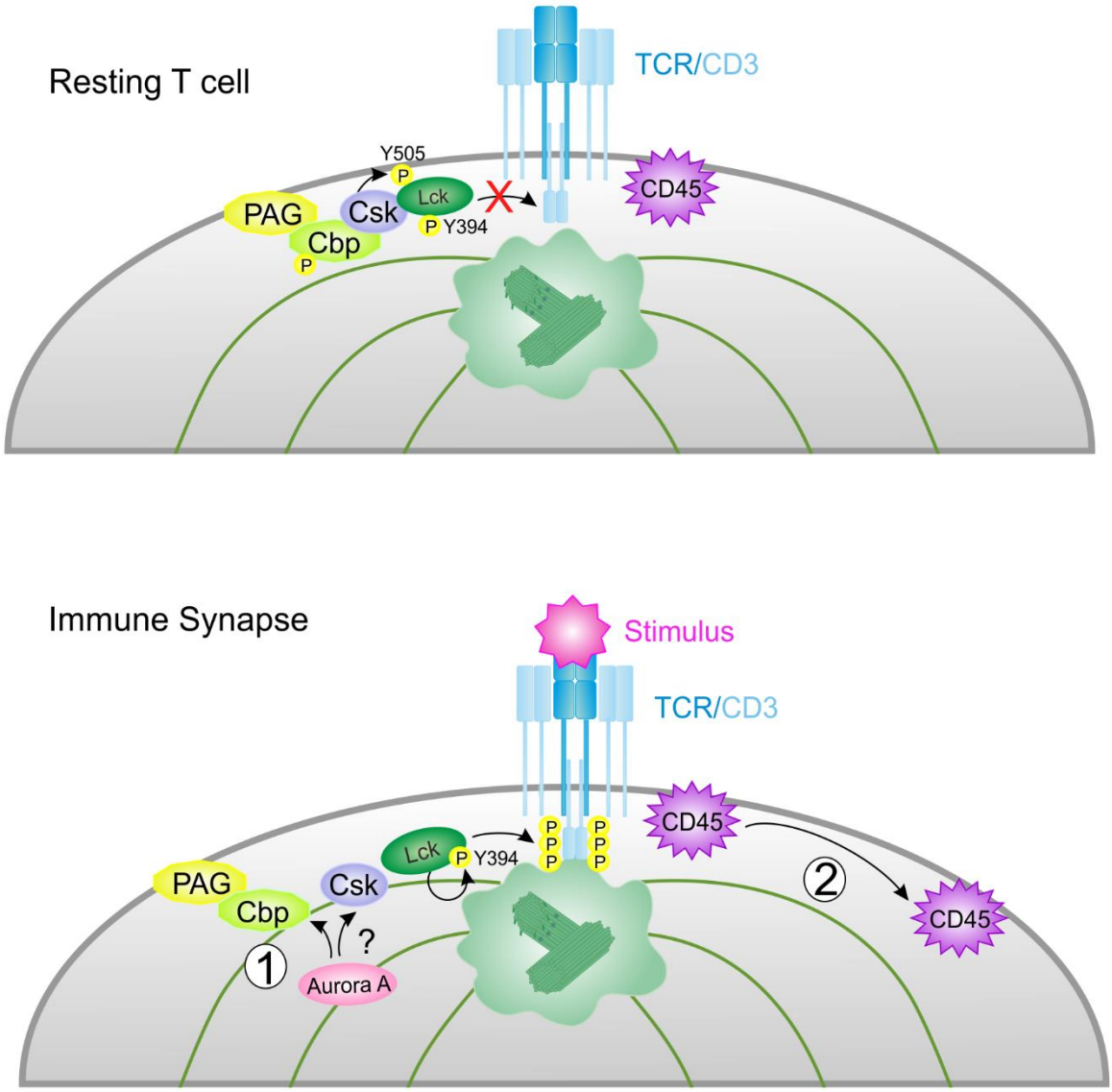

Figure D3. Lck indirect regulation by Aurora A. In resting T cells, the PAG/Cbp complex bound to Csk promotes the binding of Csk with Lck, inhibiting it by the phosphorylation of Y505 residue. The phosphatase CD45 is located at the IS region. During T cell activation (1) the PAG/Cbp complex promotes the release of Lck by Csk, activating it. Proper Aurora A localization at the IS could be regulating this mechanism through the phosphorylation of the PAG/Cbp complex or Csk directly. (2) After TCR triggering, the phosphatase CD45 is excluded from the IS. GA, Golgi apparatus; TCR, T cell receptor.

In summary, our results show that Aurora A plays an important role in the early events initiated upon TCR stimulation, and unravel a novel molecular mechanism that regulates early signaling and cytoskeletal and vesicle dynamics in T cells. The prevention of T cell activation by Aurora A inhibition has important clinical implications. Aurora A inhibitors are currently under evaluation for cancer therapy in Phase I-II clinical trials (Malumbres & Perez de Castro, 2014). In these trials, aggressive B-

cell and T-cell non-Hodgkin lymphomas have shown an overall positive response, promoting new Phase III studies. It will be important to define the extent to which the new function reported here participates in these responses and to determine whether the T cell activation pathway can provide new biomarkers, critical for understanding these therapeutic effects. Very recently, a transcriptomic analysis points Aurora A as a targetable molecule for GVHD (Graft Versus Host Disease) prevention in a primate model (Furlan et al, 2015). Hence, our data provide a mechanistic explanation by how Aurora A controls T cell activation. Given the importance of Aurora A inhibitors in cancer therapy, these results may provide new opportunities for treating lymphocyte diseases such as GVHD, T-cell lymphomas or leukemias.

Conclusions

6. Conclusions

The findings presented herein support the following conclusions:

1) Antigenic T cell stimulation promotes Aurora A activation and localization at the immune synapse.

2) Chemical inhibition or genetic ablation of Aurora A interrupt the microtubule growth and the dynamics of CD3-signaling vesicles at the immune synapse.

3) Actin polymerization during the immune synapse formation is not altered by Aurora A inhibition.

4) The pharmacological inhibition and the specific silencing of Aurora A impair early TCR signalling pathway.

5) Chemical inhibition of Aurora A decreases the expression of IL-2, CD69 and CD25.

6) The activity and the location of the tyrosine kinase Lck is controlled by Aurora A for proper T cell activation.

Conclusiones

7. Conclusiones

Los resultados presentados en esta tesis doctoral son compatibles con las siguientes conclusiones:

1) La estimulación antigénica de linfocitos T promueve la activación y la localización de Aurora A en la sinapsis inmune.

2) La inhibición farmacológica y la interrupción genética de Aurora A bloquean el crecimiento de microtúbulos y la dinámica de vesículas de señalización de CD3 en la sinapsis inmune.

3) La polimerización de actina durante la formación de la sinapsis inmune no se afecta por la inhibición de Aurora A.

4) La inhibición química de Aurora A y su silenciamiento específico bloquean la ruta de activación del TCR.

5) La inhibición de Aurora A disminuye la expresión de IL-2, CD69 y CD25.

6) Aurora A regula la actividad y la localización de la tirosina quinasa Lck, necesaria para una correcta activación del linfocito T.

References

8. References

Anton O, Batista A, Millan J, Andres-Delgado L, Puertollano R, Correas I, Alonso MA (2008) An essential role for the MAL protein in targeting Lck to the plasma membrane of human T lymphocytes. *The Journal of experimental medicine* **205:** 3201-3213

Baetz NW, Goldenring JR (2013) Rab11-family interacting proteins define spatially and temporally distinct regions within the dynamic Rab11a-dependent recycling system. *Molecular biology of the cell* **24:** 643-658

Baier G, Wagner J (2009) PKC inhibitors: potential in T cell-dependent immune diseases. *Current opinion in cell biology* **21:** 262-267

Balagopalan L, Coussens NP, Sherman E, Samelson LE, Sommers CL (2010) The LAT story: a tale of cooperativity, coordination, and choreography. *Cold Spring Harbor perspectives in biology* **2:** a005512

Barr AR, Gergely F (2007) Aurora-A: the maker and breaker of spindle poles. *Journal of cell science* **120:** 2987-2996

Barretta ML, Spano D, D'Ambrosio C, Cervigni RI, Scaloni A, Corda D, Colanzi A (2016) Aurora-A recruitment and centrosomal maturation are regulated by a Golgi-activated pool of Src during G2. *Nature communications* **7:** 11727

Bayliss R, Sardon T, Vernos I, Conti E (2003) Structural basis of Aurora-A activation by TPX2 at the mitotic spindle. *Molecular cell* **12:** 851-862

Beard C, Hochedlinger K, Plath K, Wutz A, Jaenisch R (2006) Efficient method to generate single-copy transgenic mice by site-specific integration in embryonic stem cells. *Genesis* **44:** 23-28

Beemiller P, Jacobelli J, Krummel MF (2012) Integration of the movement of signaling microclusters with cellular motility in immunological synapses. *Nature immunology* **13:** 787-795

Berdnik D, Knoblich JA (2002) Drosophila Aurora-A is required for centrosome maturation and actin-dependent asymmetric protein localization during mitosis. *Current biology : CB* **12:** 640-647

Bischoff JR, Anderson L, Zhu Y, Mossie K, Ng L, Souza B, Schryver B, Flanagan P, Clairvoyant F, Ginther C, Chan CS, Novotny M, Slamon DJ, Plowman GD (1998) A homologue of Drosophila aurora kinase is oncogenic and amplified in human colorectal cancers. *The EMBO journal* **17:** 3052-3065

Bonello G, Blanchard N, Montoya MC, Aguado E, Langlet C, He HT, Nunez-Cruz S, Malissen M, Sanchez-Madrid F, Olive D, Hivroz C, Collette Y (2004) Dynamic recruitment of the adaptor

protein LAT: LAT exists in two distinct intracellular pools and controls its own recruitment. *Journal of cell science* **117:** 1009-1016

Bonzon-Kulichenko E, Perez-Hernandez D, Nunez E, Martinez-Acedo P, Navarro P, Trevisan-Herraz M, Ramos Mdel C, Sierra S, Martinez-Martinez S, Ruiz-Meana M, Miro-Casas E, Garcia-Dorado D, Redondo JM, Burgos JS, Vazquez J (2011) A robust method for quantitative high-throughput analysis of proteomes by 18O labeling. *Molecular & cellular proteomics : MCP* **10:** M110 003335

Brdicka T, Pavlistova D, Leo A, Bruyns E, Korinek V, Angelisova P, Scherer J, Shevchenko A, Hilgert I, Cerny J, Drbal K, Kuramitsu Y, Kornacker B, Horejsi V, Schraven B (2000) Phosphoprotein associated with glycosphingolipid-enriched microdomains (PAG), a novel ubiquitously expressed transmembrane adaptor protein, binds the protein tyrosine kinase csk and is involved in regulation of T cell activation. *The Journal of experimental medicine* **191:** 1591-1604

Brown RE (1998) Sphingolipid organization in biomembranes: what physical studies of model membranes reveal. *Journal of cell science* **111 (Pt 1):** 1-9

Bustos-Moran E, Blas-Rus N, Martin-Cofreces NB, Sanchez-Madrid F (2016) Orchestrating Lymphocyte Polarity in Cognate Immune Cell-Cell Interactions. *International review of cell and molecular biology* **327:** 195-261

Calabia-Linares C, Robles-Valero J, de la Fuente H, Perez-Martinez M, Martin-Cofreces N, Alfonso-Perez M, Gutierrez-Vazquez C, Mittelbrunn M, Ibiza S, Urbano-Olmos FR, Aguado-Ballano C, Sanchez-Sorzano CO, Sanchez-Madrid F, Veiga E (2011) Endosomal clathrin drives actin accumulation at the immunological synapse. *Journal of cell science* **124:** 820-830

Carmena M, Earnshaw WC (2003) The cellular geography of aurora kinases. *Nature reviews Molecular cell biology* **4:** 842-854

Cazales M, Schmitt E, Montembault E, Dozier C, Prigent C, Ducommun B (2005) CDC25B phosphorylation by Aurora-A occurs at the G2/M transition and is inhibited by DNA damage. *Cell Cycle* **4:** 1233-1238

Cervigni RI, Barretta ML, Persico A, Corda D, Colanzi A (2011) The role of Aurora-A kinase in the Golgi-dependent control of mitotic entry. *Bioarchitecture* **1:** 61-65

Combs J, Kim SJ, Tan S, Ligon LA, Holzbaur EL, Kuhn J, Poenie M (2006) Recruitment of dynein to the Jurkat immunological synapse. *Proceedings of the National Academy of Sciences of the United States of America* **103:** 14883-14888

Comrie WA, Burkhardt JK (2016) Action and Traction: Cytoskeletal Control of Receptor Triggering at the Immunological Synapse. *Frontiers in immunology* **7:** 68

Crotzer VL, Mabardy AS, Weiss A, Brodsky FM (2004) T cell receptor engagement leads to phosphorylation of clathrin heavy chain during receptor internalization. *The Journal of experimental medicine* **199:** 981-991

Das V, Nal B, Roumier A, Meas-Yedid V, Zimmer C, Olivo-Marin JC, Roux P, Ferrier P, Dautry-Varsat A, Alcover A (2002) Membrane-cytoskeleton interactions during the formation of the immunological synapse and subsequent T-cell activation. *Immunological reviews* **189:** 123-135

Davidson D, Bakinowski M, Thomas ML, Horejsi V, Veillette A (2003) Phosphorylation-dependent regulation of T-cell activation by PAG/Cbp, a lipid raft-associated transmembrane adaptor. *Molecular and cellular biology* **23:** 2017-2028

Davis DM, Dustin ML (2004) What is the importance of the immunological synapse? *Trends in immunology* **25:** 323-327

Davis SJ, van der Merwe PA (2006) The kinetic-segregation model: TCR triggering and beyond. *Nature immunology* **7:** 803-809

de Anda FC, Pollarolo G, Da Silva JS, Camoletto PG, Feiguin F, Dotti CG (2005) Centrosome localization determines neuronal polarity. *Nature* **436:** 704-708

Dixit R, Ross JL (2010) Studying plus-end tracking at single molecule resolution using TIRF microscopy. *Methods in cell biology* **95:** 543-554

Dranoff G (2004) Cytokines in cancer pathogenesis and cancer therapy. *Nature reviews Cancer* **4:** 11-22

Dustin ML (2012) Signaling at neuro/immune synapses. *The Journal of clinical investigation* **122:** 1149-1155

Dustin ML, Chakraborty AK, Shaw AS (2010) Understanding the structure and function of the immunological synapse. *Cold Spring Harbor perspectives in biology* **2:** a002311

Dutertre S, Prigent C (2003) Aurora-A overexpression leads to override of the microtubule-kinetochore attachment checkpoint. *Molecular interventions* **3:** 127-130

Etienne-Manneville S (2010) From signaling pathways to microtubule dynamics: the key players. *Current opinion in cell biology* **22:** 104-111

Fernandez-Arenas E, Calleja E, Martinez-Martin N, Gharbi SI, Navajas R, Garcia-Medel N, Penela P, Alcami A, Mayor F, Jr., Albar JP, Alarcon B (2014) beta-Arrestin-1 mediates the TCR-triggered re-routing of distal receptors to the immunological synapse by a PKC-mediated mechanism. *The EMBO journal* **33:** 559-577

Filbert EL, Le Borgne M, Lin J, Heuser JE, Shaw AS (2012) Stathmin regulates microtubule dynamics and microtubule organizing center polarization in activated T cells. *Journal of immunology* **188:** 5421-5427

Finetti F, Patrussi L, Galgano D, Cassioli C, Perinetti G, Pazour GJ, Baldari CT (2015) The small GTPase Rab8 interacts with VAMP-3 to regulate the delivery of recycling T-cell receptors to the immune synapse. *Journal of cell science* **128:** 2541-2552

Friedl P, den Boer AT, Gunzer M (2005) Tuning immune responses: diversity and adaptation of the immunological synapse. *Nature reviews Immunology* **5:** 532-545

Fu MM, Holzbaur EL (2014) Integrated regulation of motor-driven organelle transport by scaffolding proteins. *Trends in cell biology* **24:** 564-574

Furlan SN, Watkins B, Tkachev V, Flynn R, Cooley S, Ramakrishnan S, Singh K, Giver C, Hamby K, Stempora L, Garrett A, Chen J, Betz KM, Ziegler CG, Tharp GK, Bosinger SE, Promislow DE, Miller JS, Waller EK, Blazar BR, Kean LS (2015) Transcriptome analysis of GVHD reveals aurora kinase A as a targetable pathway for disease prevention. *Science translational medicine* **7:** 315ra191

Gascoigne NR, Casas J, Brzostek J, Rybakin V (2011) Initiation of TCR phosphorylation and signal transduction. *Frontiers in immunology* **2:** 72

Gil D, Schamel WW, Montoya M, Sanchez-Madrid F, Alarcon B (2002) Recruitment of Nck by CD3 epsilon reveals a ligand-induced conformational change essential for T cell receptor signaling and synapse formation. *Cell* **109:** 901-912

Goldenson B, Crispino JD (2015) The aurora kinases in cell cycle and leukemia. *Oncogene* **34:** 537-545

Goldsmith MA, Weiss A (1987) Isolation and characterization of a T-lymphocyte somatic mutant with altered signal transduction by the antigen receptor. *Proceedings of the National Academy of Sciences of the United States of America* **84:** 6879-6883

Gomez TS, Billadeau DD (2008) T cell activation and the cytoskeleton: you can't have one without the other. *Advances in immunology* **97:** 1-64

Gomez TS, Kumar K, Medeiros RB, Shimizu Y, Leibson PJ, Billadeau DD (2007) Formins regulate the actin-related protein 2/3 complex-independent polarization of the centrosome to the immunological synapse. *Immunity* **26:** 177-190

Gopalan G, Chan CS, Donovan PJ (1997) A novel mammalian, mitotic spindle-associated kinase is related to yeast and fly chromosome segregation regulators. *The Journal of cell biology* **138:** 643-656

Grigoriev I, Akhmanova A (2010) Microtubule dynamics at the cell cortex probed by TIRF microscopy. *Methods in cell biology* **97:** 91-109

Gruss OJ, Carazo-Salas RE, Schatz CA, Guarguaglini G, Kast J, Wilm M, Le Bot N, Vernos I, Karsenti E, Mattaj IW (2001) Ran induces spindle assembly by reversing the inhibitory effect of importin alpha on TPX2 activity. *Cell* **104:** 83-93

Gruss OJ, Vernos I (2004) The mechanism of spindle assembly: functions of Ran and its target TPX2. *The Journal of cell biology* **166:** 949-955

Hannak E, Kirkham M, Hyman AA, Oegema K (2001) Aurora-A kinase is required for centrosome maturation in Caenorhabditis elegans. *The Journal of cell biology* **155:** 1109-1116

Hartzell CA, Jankowska KI, Burkhardt JK, Lewis RS (2016) Calcium influx through CRAC channels controls actin organization and dynamics at the immune synapse. *eLife* **5**

Hashimoto-Tane A, Yokosuka T, Sakata-Sogawa K, Sakuma M, Ishihara C, Tokunaga M, Saito T (2011) Dynein-driven transport of T cell receptor microclusters regulates immune synapse formation and T cell activation. *Immunity* **34:** 919-931

He HT, Marguet D (2008) T-cell antigen receptor triggering and lipid rafts: a matter of space and time scales. Talking Point on the involvement of lipid rafts in T-cell activation. *EMBO reports* **9:** 525-530

Hermiston ML, Xu Z, Weiss A (2003) CD45: a critical regulator of signaling thresholds in immune cells. *Annual review of immunology* **21:** 107-137

Hochegger H, Hegarat N, Pereira-Leal JB (2013) Aurora at the pole and equator: overlapping functions of Aurora kinases in the mitotic spindle. *Open biology* **3:** 120185

Hui E, Vale RD (2014) In vitro membrane reconstitution of the T-cell receptor proximal signaling network. *Nature structural & molecular biology* **21:** 133-142

Huse M (2012) Microtubule-organizing center polarity and the immunological synapse: protein kinase C and beyond. *Frontiers in immunology* **3:** 235

Huse M, Le Floc'h A, Liu X (2013) From lipid second messengers to molecular motors: microtubule-organizing center reorientation in T cells. *Immunological reviews* **256:** 95-106

Huse M, Quann EJ, Davis MM (2008) Shouts, whispers and the kiss of death: directional secretion in T cells. *Nature immunology* **9:** 1105-1111

Ilani T, Vasiliver-Shamis G, Vardhana S, Bretscher A, Dustin ML (2009) T cell antigen receptor signaling and immunological synapse stability require myosin IIA. *Nature immunology* **10:** 531-539

Joung I, Kim T, Stolz LA, Payne G, Winkler DG, Walsh CT, Strominger JL, Shin J (1995) Modification of Ser59 in the unique N-terminal region of tyrosine kinase p56lck regulates specificity of its Src homology 2 domain. *Proceedings of the National Academy of Sciences of the United States of America* **92:** 5778-5782

Kawabuchi M, Satomi Y, Takao T, Shimonishi Y, Nada S, Nagai K, Tarakhovsky A, Okada M (2000) Transmembrane phosphoprotein Cbp regulates the activities of Src-family tyrosine kinases. *Nature* **404:** 999-1003

Kesavan KP, Isaacson CC, Ashendel CL, Geahlen RL, Harrison ML (2002) Characterization of the in vivo sites of serine phosphorylation on Lck identifying serine 59 as a site of mitotic phosphorylation. *The Journal of biological chemistry* **277:** 14666-14673

Kienzle C, von Blume J (2014) Secretory cargo sorting at the trans-Golgi network. *Trends in cell biology* **24:** 584-593

Kikkawa M (2013) Big steps toward understanding dynein. *The Journal of cell biology* **202:** 15-23

King CG, Koehli S, Hausmann B, Schmaler M, Zehn D, Palmer E T cell affinity regulates asymmetric division, effector cell differentiation, and tissue pathology. *Immunity* **37:** 709-720

Krummel MF, Sjaastad MD, Wulfing C, Davis MM (2000) Differential clustering of CD4 and CD3zeta during T cell recognition. *Science* **289:** 1349-1352

Kufer TA, Sillje HH, Korner R, Gruss OJ, Meraldi P, Nigg EA (2002) Human TPX2 is required for targeting Aurora-A kinase to the spindle. *The Journal of cell biology* **158:** 617-623

Larghi P, Williamson DJ, Carpier JM, Dogniaux S, Chemin K, Bohineust A, Danglot L, Gaus K, Galli T, Hivroz C (2013) VAMP7 controls T cell activation by regulating the recruitment and phosphorylation of vesicular Lat at TCR-activation sites. *Nature immunology* **14:** 723-731

Lee YC, Que J, Chen YC, Lin JT, Liou YC, Liao PC, Liu YP, Lee KH, Lin LC, Hsiao M, Hung LY, Huang CY, Lu PJ (2013) Pin1 acts as a negative regulator of the G2/M transition by interacting with the Aurora-A-Bora complex. *Journal of cell science* **126:** 4862-4872

Li QJ, Dinner AR, Qi S, Irvine DJ, Huppa JB, Davis MM, Chakraborty AK (2004) CD4 enhances T cell sensitivity to antigen by coordinating Lck accumulation at the immunological synapse. *Nature immunology* **5:** 791-799

Lillemeier BF, Mortelmaier MA, Forstner MB, Huppa JB, Groves JT, Davis MM (2010) TCR and Lat are expressed on separate protein islands on T cell membranes and concatenate during activation. *Nature immunology* **11:** 90-96

Liu X, Kapoor TM, Chen JK, Huse M (2013) Diacylglycerol promotes centrosome polarization in T cells via reciprocal localization of dynein and myosin II. *Proceedings of the National Academy of Sciences of the United States of America* **110:** 11976-11981

Lowin-Kropf B, Shapiro VS, Weiss A (1998) Cytoskeletal polarization of T cells is regulated by an immunoreceptor tyrosine-based activation motif-dependent mechanism. *The Journal of cell biology* **140:** 861-871

Lukasiewicz KB, Lingle WL (2009) Aurora A, centrosome structure, and the centrosome cycle. *Environmental and molecular mutagenesis* **50:** 602-619

Malumbres M, Perez de Castro I (2014) Aurora kinase A inhibitors: promising agents in antitumoral therapy. *Expert opinion on therapeutic targets* **18:** 1377-1393

Manfredi MG, Ecsedy JA, Chakravarty A, Silverman L, Zhang M, Hoar KM, Stroud SG, Chen W, Shinde V, Huck JJ, Wysong DR, Janowick DA, Hyer ML, Leroy PJ, Gershman RE, Silva MD, Germanos MS, Bolen JB, Claiborne CF, Sells TB (2011) Characterization of Alisertib (MLN8237), an investigational small-molecule inhibitor of aurora A kinase using novel in vivo pharmacodynamic assays. *Clinical cancer research : an official journal of the American Association for Cancer Research* **17:** 7614-7624

Manneville JB (2006) Use of TIRF microscopy to visualize actin and microtubules in migrating cells. *Methods in enzymology* **406:** 520-532

Martin-Cofreces NB, Alarcon B, Sanchez-Madrid F (2011) Tubulin and actin interplay at the T cell and antigen-presenting cell interface. *Frontiers in immunology* **2:** 24

Martin-Cofreces NB, Baixauli F, Lopez MJ, Gil D, Monjas A, Alarcon B, Sanchez-Madrid F (2012) End-binding protein 1 controls signal propagation from the T cell receptor. *The EMBO journal* **31:** 4140-4152

Martin-Cofreces NB, Baixauli F, Sanchez-Madrid F (2014) Immune synapse: conductor of orchestrated organelle movement. *Trends in cell biology* **24:** 61-72

Martin-Cofreces NB, Robles-Valero J, Cabrero JR, Mittelbrunn M, Gordon-Alonso M, Sung CH, Alarcon B, Vazquez J, Sanchez-Madrid F (2008) MTOC translocation modulates IS formation and controls sustained T cell signaling. *The Journal of cell biology* **182:** 951-962

Martin-Cofreces NB, Sancho D, Fernandez E, Vicente-Manzanares M, Gordon-Alonso M, Montoya MC, Michel F, Acuto O, Alarcon B, Sanchez-Madrid F (2006) Role of Fyn in the

rearrangement of tubulin cytoskeleton induced through TCR. *Journal of immunology* **176:** 4201-4207

Mittelbrunn M, Gutierrez-Vazquez C, Villarroya-Beltri C, Gonzalez S, Sanchez-Cabo F, Gonzalez MA, Bernad A, Sanchez-Madrid F (2011) Unidirectional transfer of microRNA-loaded exosomes from T cells to antigen-presenting cells. *Nature communications* **2:** 282

Monjas A, Alcover A, Alarcon B (2004) Engaged and bystander T cell receptors are down-modulated by different endocytotic pathways. *The Journal of biological chemistry* **279:** 55376-55384

Monks CR, Freiberg BA, Kupfer H, Sciaky N, Kupfer A (1998) Three-dimensional segregation of supramolecular activation clusters in T cells. *Nature* **395:** 82-86

Mori D, Yano Y, Toyo-oka K, Yoshida N, Yamada M, Muramatsu M, Zhang D, Saya H, Toyoshima YY, Kinoshita K, Wynshaw-Boris A, Hirotsune S (2007) NDEL1 phosphorylation by Aurora-A kinase is essential for centrosomal maturation, separation, and TACC3 recruitment. *Molecular and cellular biology* **27:** 352-367

Navarro MN, Cantrell DA (2014) Serine-threonine kinases in TCR signaling. *Nature immunology* **15:** 808-814

Navarro MN, Sinclair LV, Feijoo-Carnero C, Clarke R, Matthews SA, Cantrell DA (2012) Protein kinase D2 has a restricted but critical role in T-cell antigen receptor signalling in mature T-cells. *The Biochemical journal* **442:** 649-659

Nguyen TD, Carrascal M, Vidal-Cortes O, Gallardo O, Casas V, Gay M, Phan VC, Abian J (2016) The phosphoproteome of human Jurkat T cell clones upon costimulation with anti-CD3/anti-CD28 antibodies. *Journal of proteomics* **131:** 190-198

Nika K, Soldani C, Salek M, Paster W, Gray A, Etzensperger R, Fugger L, Polzella P, Cerundolo V, Dushek O, Hofer T, Viola A, Acuto O (2010) Constitutively active Lck kinase in T cells drives antigen receptor signal transduction. *Immunity* **32:** 766-777

Obino D, Farina F, Malbec O, Saez PJ, Maurin M, Gaillard J, Dingli F, Loew D, Gautreau A, Yuseff MI, Blanchoin L, Thery M, Lennon-Dumenil AM (2016) Actin nucleation at the centrosome controls lymphocyte polarity. *Nature communications* **7:** 10969

Palacios EH, Weiss A (2004) Function of the Src-family kinases, Lck and Fyn, in T-cell development and activation. *Oncogene* **23:** 7990-8000

Pauker MH, Hassan N, Noy E, Reicher B, Barda-Saad M (2012) Studying the dynamics of SLP-76, Nck, and Vav1 multimolecular complex formation in live human cells with triple-color FRET. *Science signaling* **5:** rs3

Perez de Castro I, Aguirre-Portoles C, Fernandez-Miranda G, Canamero M, Cowley DO, Van Dyke T, Malumbres M (2013) Requirements for Aurora-A in tissue regeneration and tumor development in adult mammals. *Cancer research* **73:** 6804-6815

Perez de Castro I, Aguirre-Portoles C, Martin B, Fernandez-Miranda G, Klotzbucher A, Kubbutat MH, Megias D, Arlot-Bonnemains Y, Malumbres M (2011) A SUMOylation Motif in Aurora-A: Implications for Spindle Dynamics and Oncogenesis. *Frontiers in oncology* **1:** 50

Peset I, Seiler J, Sardon T, Bejarano LA, Rybina S, Vernos I (2005) Function and regulation of Maskin, a TACC family protein, in microtubule growth during mitosis. *The Journal of cell biology* **170:** 1057-1066

Petretti C, Savoian M, Montembault E, Glover DM, Prigent C, Giet R (2006) The PITSLRE/CDK11p58 protein kinase promotes centrosome maturation and bipolar spindle formation. *EMBO reports* **7:** 418-424

Piazzolla D, Palla AR, Pantoja C, Canamero M, de Castro IP, Ortega S, Gomez-Lopez G, Dominguez O, Megias D, Roncador G, Luque-Garcia JL, Fernandez-Tresguerres B, Fernandez AF, Fraga MF, Rodriguez-Justo M, Manzanares M, Sanchez-Carbayo M, Garcia-Pedrero JM, Rodrigo JP, Malumbres M, Serrano M (2014) Lineage-restricted function of the pluripotency factor NANOG in stratified epithelia. *Nature communications* **5:** 4226

Plotnikova OV, Nikonova AS, Loskutov YV, Kozyulina PY, Pugacheva EN, Golemis EA (2012) Calmodulin activation of Aurora-A kinase (AURKA) is required during ciliary disassembly and in mitosis. *Molecular biology of the cell* **23:** 2658-2670

Quann EJ, Liu X, Altan-Bonnet G, Huse M (2011) A cascade of protein kinase C isozymes promotes cytoskeletal polarization in T cells. *Nature immunology* **12:** 647-654

Quann EJ, Merino E, Furuta T, Huse M (2009) Localized diacylglycerol drives the polarization of the microtubule-organizing center in T cells. *Nature immunology* **10:** 627-635

Reginald K, Chaoui K, Roncagalli R, Beau M, Goncalves Menoita M, Monsarrat B, Burlet-Schiltz O, Malissen M, Gonzalez de Peredo A, Malissen B (2015) Revisiting the Timing of Action of the PAG Adaptor Using Quantitative Proteomics Analysis of Primary T Cells. *Journal of immunology* **195:** 5472-5481

Ritchey L, Ottman R, Roumanos M, Chakrabarti R (2012) A functional cooperativity between Aurora A kinase and LIM kinase1: implication in the mitotic process. *Cell Cycle* **11:** 296-309

Rivero S, Cardenas J, Bornens M, Rios RM (2009) Microtubule nucleation at the cis-side of the Golgi apparatus requires AKAP450 and GM130. *The EMBO journal* **28:** 1016-1028

Robles-Valero J, Martin-Cofreces NB, Lamana A, Macdonald S, Volkov Y, Sanchez-Madrid F (2010) Integrin and CD3/TCR activation are regulated by the scaffold protein AKAP450. *Blood* **115:** 4174-4184

Romeo Y, Zhang X, Roux PP (2012) Regulation and function of the RSK family of protein kinases. *The Biochemical journal* **441:** 553-569

Sander EE, van Delft S, ten Klooster JP, Reid T, van der Kammen RA, Michiels F, Collard JG (1998) Matrix-dependent Tiam1/Rac signaling in epithelial cells promotes either cell-cell adhesion or cell migration and is regulated by phosphatidylinositol 3-kinase. *The Journal of cell biology* **143:** 1385-1398

Sardon T, Peset I, Petrova B, Vernos I (2008) Dissecting the role of Aurora A during spindle assembly. *The EMBO journal* **27:** 2567-2579

Schoenborn JR, Tan YX, Zhang C, Shokat KM, Weiss A (2011) Feedback circuits monitor and adjust basal Lck-dependent events in T cell receptor signaling. *Science signaling* **4:** ra59

Schonle A, Hartl FA, Mentzel J, Noltner T, Rauch KS, Prestipino A, Wohlfeil SA, Apostolova P, Hechinger AK, Melchinger W, Fehrenbach K, Guadamillas MC, Follo M, Prinz G, Ruess AK, Pfeifer D, Angel Del Pozo M, Schmitt-Graeff A, Duyster J, Hippen KI, Blazar BR, Schachtrup K, Minguet S, Zeiser R (2016) Caveolin-1 regulates TCR signal strength and regulatory T-cell differentiation into alloreactive T cells. *Blood* **127:** 1930-1939

Seki A, Coppinger JA, Jang CY, Yates JR, Fang G (2008) Bora and the kinase Aurora a cooperatively activate the kinase Plk1 and control mitotic entry. *Science* **320:** 1655-1658

Serrador JM, Cabrero JR, Sancho D, Mittelbrunn M, Urzainqui A, Sanchez-Madrid F (2004) HDAC6 deacetylase activity links the tubulin cytoskeleton with immune synapse organization. *Immunity* **20:** 417-428

Simons K, Ikonen E (1997) Functional rafts in cell membranes. *Nature* **387:** 569-572

Soares H, Henriques R, Sachse M, Ventimiglia L, Alonso MA, Zimmer C, Thoulouze MI, Alcover A (2013a) Regulated vesicle fusion generates signaling nanoterritories that control T cell activation at the immunological synapse. *The Journal of experimental medicine* **210:** 2415-2433

Soares H, Lasserre R, Alcover A (2013b) Orchestrating cytoskeleton and intracellular vesicle traffic to build functional immunological synapses. *Immunological reviews* **256:** 118-132

Soula M, Rothhut B, Camoin L, Guillaume JL, Strosberg D, Vorherr T, Burn P, Meggio F, Fischer S, Fagard R (1993) Anti-CD3 and phorbol ester induce distinct phosphorylated sites in the SH2 domain of p56lck. *The Journal of biological chemistry* **268:** 27420-27427

Stinchcombe JC, Griffiths GM (2007) Secretory mechanisms in cell-mediated cytotoxicity. *Annual review of cell and developmental biology* **23:** 495-517

Stirnweiss A, Hartig R, Gieseler S, Lindquist JA, Reichardt P, Philipsen L, Simeoni L, Poltorak M, Merten C, Zuschratter W, Prokazov Y, Paster W, Stockinger H, Harder T, Gunzer M, Schraven B (2013) T cell activation results in conformational changes in the Src family kinase Lck to induce its activation. *Science signaling* **6:** ra13

Straus DB, Weiss A (1992) Genetic evidence for the involvement of the lck tyrosine kinase in signal transduction through the T cell antigen receptor. *Cell* **70:** 585-593

Swamy M, Beck-Garcia K, Beck-Garcia E, Hartl FA, Morath A, Yousefi OS, Dopfer EP, Molnar E, Schulze AK, Blanco R, Borroto A, Martin-Blanco N, Alarcon B, Hofer T, Minguet S, Schamel WW (2016) A Cholesterol-Based Allostery Model of T Cell Receptor Phosphorylation. *Immunity* **44:** 1091-1101

Takahashi M, Yamagiwa A, Nishimura T, Mukai H, Ono Y (2002) Centrosomal proteins CG-NAP and kendrin provide microtubule nucleation sites by anchoring gamma-tubulin ring complex. *Molecular biology of the cell* **13:** 3235-3245

Tsun A, Qureshi I, Stinchcombe JC, Jenkins MR, de la Roche M, Kleczkowska J, Zamoyska R, Griffiths GM (2011) Centrosome docking at the immunological synapse is controlled by Lck signaling. *The Journal of cell biology* **192:** 663-674

Vang T, Torgersen KM, Sundvold V, Saxena M, Levy FO, Skalhegg BS, Hansson V, Mustelin T, Tasken K (2001) Activation of the COOH-terminal Src kinase (Csk) by cAMP-dependent protein kinase inhibits signaling through the T cell receptor. *The Journal of experimental medicine* **193:** 497-507

Varma R, Campi G, Yokosuka T, Saito T, Dustin ML (2006) T cell receptor-proximal signals are sustained in peripheral microclusters and terminated in the central supramolecular activation cluster. *Immunity* **25:** 117-127

Wang LH, Xiang J, Yan M, Zhang Y, Zhao Y, Yue CF, Xu J, Zheng FM, Chen JN, Kang Z, Chen TS, Xing D, Liu Q (2010) The mitotic kinase Aurora-A induces mammary cell migration and breast cancer metastasis by activating the Cofilin-F-actin pathway. *Cancer research* **70:** 9118-9128

Wei JH, Zhang ZC, Wynn RM, Seemann J (2015) GM130 Regulates Golgi-Derived Spindle Assembly by Activating TPX2 and Capturing Microtubules. *Cell* **162:** 287-299

Wiese C, Zheng Y (2006) Microtubule nucleation: gamma-tubulin and beyond. *Journal of cell science* **119:** 4143-4153

Xu H, Littman DR (1993) A kinase-independent function of Lck in potentiating antigen-specific T cell activation. *Cell* **74:** 633-643

Xu Q, Malecka KL, Fink L, Jordan EJ, Duffy E, Kolander S, Peterson JR, Dunbrack RL, Jr. (2015) Identifying three-dimensional structures of autophosphorylation complexes in crystals of protein kinases. *Science signaling* **8:** rs13

Yang J, Ikezoe T, Nishioka C, Tasaka T, Taniguchi A, Kuwayama Y, Komatsu N, Bandobashi K, Togitani K, Koeffler HP, Taguchi H, Yokoyama A (2007) AZD1152, a novel and selective aurora B kinase inhibitor, induces growth arrest, apoptosis, and sensitization for tubulin depolymerizing agent or topoisomerase II inhibitor in human acute leukemia cells in vitro and in vivo. *Blood* **110:** 2034-2040

Yang KT, Tang CJ, Tang TK (2015) Possible Role of Aurora-C in Meiosis. *Frontiers in oncology* **5:** 178

Yu Y, Smoligovets AA, Groves JT (2013) Modulation of T cell signaling by the actin cytoskeleton. *Journal of cell science* **126:** 1049-1058

Yudushkin IA, Vale RD (2010) Imaging T-cell receptor activation reveals accumulation of tyrosine-phosphorylated CD3zeta in the endosomal compartment. *Proceedings of the National Academy of Sciences of the United States of America* **107:** 22128-22133

Zhu X, Kaverina I (2013) Golgi as an MTOC: making microtubules for its own good. *Histochemistry and cell biology* **140:** 361-367

Annexes

9. Annexes

9.1 Supplementary information

- **Supplementary Movie 1. 4D imaging of Microtubule growing in control and Aurora A-inhibited Jurkat cells.** Control Jurkat T cells transfected with EB3-GFP were pre-treated with MLN8237 or vehicle, allowed to settle on stimulatory anti-CD3/CD28-coated surfaces and recorded under a confocal microscope. Fluorescence and bright field images for XYZ-stacks were taken every 1.2 s. MLN8237 or vehicle was present in the imaging medium. Movie was mounted at 10 fps.

- **Supplementary Movie 2. 4D imaging of Microtubule growing in control and Aurora A-inhibited WT and KO cells.** WT and KO cells were transfected with EB3-GFP, pre-treated with MLN8237 or vehicle and allowed to settle on stimulatory anti-CD3/CD28-coated surfaces and recorded under a confocal microscope. Fluorescence and bright field images for XYZ-stacks were taken every 1.2 s. MLN8237 or vehicle was present in the imaging medium. Movie was mounted at 10 fps.

- **Supplementary Movie 3. Tracking of EB3-GFP-decorated, growing TIPs at the IS in control Jurkat cells.** Control Jurkat T cells stably expressing EB3-GFP were allowed to settle on stimulatory anti-CD3/CD28-coated surfaces and recorded under a TIRFm, at a 150 nm of penetrance upon excitation with a 488 nm laser. Images were taken every 300 ms. MLN8237 or vehicle was present in the imaging medium. Imaris Software was used to recognize fluorescence corresponding to the decorated tips and to calculate the trajectories and growing speed of the tips. Movie was mounted at 30 fps.

- **Supplementary Movie 4. Tracking of EB3-GFP-decorated, growing TIPs at the IS in Aurora A-inhibited Jurkat cells.** MLN8237-treated Jurkat T cells stably expressing EB3-GFP were allowed to settle on stimulatory anti-CD3/CD28-coated surfaces and recorded under a TIRFm, at a 150 nm of penetrance upon excitation with a 488 nm laser. Images were taken every 300 ms. MLN8237 or vehicle was present in the imaging medium. Imaris Software was used to recognize fluorescence corresponding to the decorated tips and to calculate the trajectories and growing speed of the tips. Movie was mounted at 30 fps.

- **Supplementary Movie 5. Tracking of EB3-GFP-decorated, growing TIPs at the IS in control $CD4^+$ T cells.** $CD4^+$ T cells isolated from Aurka(lox/lox); RERT(ert/ert) and

transfected with EB3-GFP were allowed to settle on stimulatory anti-CD3/CD28-coated surfaces and recorded under a TIRFm, at a 150 nm of penetrance upon excitation with a 488 nm laser. Images were taken every 300 ms. MLN8237 or vehicle was present in the imaging medium. Imaris Software was used to recognize fluorescence corresponding to the decorated tips and to calculate the trajectories and growing speed of the tips. Movie was mounted at 30 fps.

- **Supplementary Movie 6. Tracking of EB3-GFP-decorated, growing TIPs at the IS in Aurora A-deficient CD4$^+$ T cells**. CD4$^+$ T cells isolated from Aurka(lox/lox); RERT(ert/ert) treated with tamoxifen and transfected with EB3-GFP were allowed to settle on stimulatory anti-CD3/CD28-coated surfaces and recorded under a TIRFm, at a 150 nm of penetrance upon excitation with a 488 nm laser. Images were taken every 300 ms. MLN8237 or vehicle was present in the imaging medium. Imaris Software was used to recognize fluorescence corresponding to the decorated tips and to calculate the trajectories and growing speed of the tips. Movie was mounted at 30 fps.

- **Supplementary Movie 7. Tracking of CD3ξ-bearing vesicles at the IS in control Jurkat cells.** Control Jurkat T cells transfected with CD3ξ-mCherry were allowed to settle on stimulatory anti-CD3/CD28-coated surfaces and recorded under a TIRFm, at a 200 nm of penetrance upon excitation with a 561 nm laser. Images were taken every 100 ms. MLN8237 or vehicle was present in the imaging medium. Imaris Software was used to recognize fluorescence corresponding to the vesicles and to calculate the trajectories, their duration and the speed of the vesicles. Movie was mounted at 20 fps.

- **Supplementary Movie 8. Tracking of CD3ξ-bearing vesicles at the IS in Aurora A-inhibited Jurkat cells.** MLN8237-treated Jurkat T cells transfected with CD3ξ-mCherry were allowed to settle on stimulatory anti-CD3/CD28-coated surfaces and recorded under a TIRFm, at a 200 nm of penetrance upon excitation with a 561 nm laser. Images were taken every 100 ms. MLN8237 or vehicle was present in the imaging medium. Imaris Software was used to recognize fluorescence corresponding to the vesicles and to calculate the trajectories, their duration and the speed of the vesicles. Movie was mounted at 20 fps.

- **Supplementary Movie 9. Tracking of CD3ξ-bearing vesicles at the IS in control or Aurora A inhibited CD4$^+$ T cells.** CD4$^+$ T cells isolated from Aurka(lox/lox); RERT(ert/ert), transfected with EB3-GFP and CD3ξ-mCherry, treated with MLN8237 or vehicle and allowed to settle on stimulatory anti-CD3/CD28-coated surfaces.

Recording was performed under a TIRFm, at a 200 nm of penetrance upon excitation with a 561 nm laser. Images were taken every 110 ms. MLN8237 or vehicle was present in the imaging medium. Movie was mounted at 20 fps.

- **Supplementary Movie 10. 4D imaging of Actin ring formation in conjugates of in control and Aurora A-inhibited Jurkat cells.** Control Jurkat T cells transfected with mCherry-β-actin were pre-treated with MLN8237 or vehicle, allowed to settle on stimulatory anti-CD3/CD28-coated surfaces and recorded under a confocal microscope. Fluorescence and bright field images for XYZ-stacks were taken every 25 s. MLN8237 or vehicle was present in the imaging medium. Bar, 10 µm. Movie was mounted at 10 fps.

9.2 Publications related to this Thesis work

I. Blas-Rus N, Bustos-Moran E, Perez de Castro I, de Carcer G, Borroto A, Camafeita E, Jorge I, Vazquez J, Alarcon B, Malumbres M, Martin-Cofreces NB, Sanchez-Madrid F (2016) Aurora A drives early signalling and vesicle dynamics during T-cell activation. *Nature communications* 7: 11389

II. Bustos-Moran E, Blas-Rus N, Martin-Cofreces NB, Sanchez-Madrid F (2016) Orchestrating Lymphocyte Polarity in Cognate Immune Cell-Cell Interactions. *International review of cell and molecular biology* **327:** 195-261

III. Blas-Rus N, Bustos-Moran E, Sanchez-Madrid F, Martin-Cofreces NB (2016) Analysis of microtubules and microtubule-organizing centre at the immune synapse. *Methods in molecular biology*. *In press.*

IV. Blas-Rus N, Bustos-Moran E, Martin-Cofreces NB, Sanchez-Madrid F (2016) Aurora A shines on T cell activation through the regulation of Lck. *BioEssays*. *In press*.

9.3 Other publications

I. Bustos-Moran E, Blas-Rus N, Martin-Cofreces NB, Sanchez-Madrid F. Microtubule associated protein-4 (MAP4) controls nanovesicles dynamics and T cell activation. *Submitted*.

Annexe I

nature COMMUNICATIONS

ARTICLE

Received 12 Aug 2015 | Accepted 21 Mar 2016 | Published 19 Apr 2016

DOI: 10.1038/ncomms11389 OPEN

Aurora A drives early signalling and vesicle dynamics during T-cell activation

Noelia Blas-Rus[1], Eugenio Bustos-Morán[2], Ignacio Pérez de Castro[3], Guillermo de Cárcer[3], Aldo Borroto[4], Emilio Camafeita[5], Inmaculada Jorge[5], Jesús Vázquez[5], Balbino Alarcón[4], Marcos Malumbres[3], Noa B. Martín-Cófreces[1,2,*] & Francisco Sánchez-Madrid[1,2,*]

Aurora A is a serine/threonine kinase that contributes to the progression of mitosis by inducing microtubule nucleation. Here we have identified an unexpected role for Aurora A kinase in antigen-driven T-cell activation. We find that Aurora A is phosphorylated at the immunological synapse (IS) during TCR-driven cell contact. Inhibition of Aurora A with pharmacological agents or genetic deletion in human or mouse T cells severely disrupts the dynamics of microtubules and CD3ζ-bearing vesicles at the IS. The absence of Aurora A activity also impairs the activation of early signalling molecules downstream of the TCR and the expression of IL-2, CD25 and CD69. Aurora A inhibition causes delocalized clustering of Lck at the IS and decreases phosphorylation levels of tyrosine kinase Lck, thus indicating Aurora A is required for maintaining Lck active. These findings implicate Aurora A in the propagation of the TCR activation signal.

[1] Servicio de Inmunología, Hospital Universitario de la Princesa, Instituto Investigación Sanitaria Princesa (IIS-IP), Universidad Autónoma de Madrid, C/ Diego de León 62, Madrid 28006, Spain. [2] Cell-cell Communication Laboratory, Vascular Pathophysiology Area, Centro Nacional Investigaciones Cardiovasculares (CNIC), C/ Melchor Fdz Almagro 3, Madrid 28029, Spain. [3] Cell Division and Cancer Group, Centro Nacional de Investigaciones Oncológicas (CNIO), C/ Melchor Fdz Almagro 3, Madrid 28029, Spain. [4] Centro de Biología Molecular Severo Ochoa, Consejo Superior de Investigaciones Científicas, Universidad Autónoma de Madrid, C/ Nicolás cabrera 1, Madrid 28049, Spain. [5] Laboratory of Cardiovascular Proteomics, Centro Nacional Investigaciones Cardiovasculares (CNIC), C/ Melchor Fdz Almagro 3, Madrid 28029, Spain. * These authors contributed equally to this work. Correspondence and requests for materials should be addressed to F.S.-M. (email: fsmadrid@salud.madrid.org).

T-cell activation depends on the ability of the T-cell receptor (TCR) to recognize specific antigen peptides presented in the context of the major histocompatibility complex (MHCp) on the antigen-presenting cell (APC)[1]. The binding of the TCR to MHCp promotes the formation of the immune synapse (IS). In this process, the TCR and its associated molecules localize to a central area of the T cell–APC contact, the central supramolecular activating complex (cSMAC). Adhesion molecules relocate to the peripheral SMAC[2–4]. Essential proteins in this process are the Src family kinase members (Lck and Fyn). Lck phosphorylates the immunoreceptor tyrosine-based activation (ITAM) motifs of the TCR/CD3 complex[5], leading to the recruitment of crucial molecules for the downstream signalling pathways and the IS formation[3]. The formation of the IS also triggers changes in the tubulin cytoskeleton, including the translocation of the centrosome, or microtubule (MT)-organizing centre (MTOC), to the IS, accompanied by the Golgi apparatus, multivesicular bodies and mitochondria[6–8]. These changes facilitate the polarized secretion of cytokines and exosomes towards the APC[9–11]. MTOC polarization orchestrates active MT growth and forms the core of a dense MT network that regulates vesicular traffic at the IS[12].

The Aurora family of serine/threonine kinases comprises three members in humans—Auroras A, B and C—which are encoded by three different genes[13] and are key regulators of different mitotic processes[14]. Aurora A plays a critical role in centrosome and spindle dynamics during mitosis, whereas Aurora B regulates the attachment of the kinetochore to MTs and cytokinesis[15]. Aurora A expression and activity peak in late G2 and the protein is concentrated at centrosomes[13,16]. During centrosome maturation, Aurora A promotes MT assembly by recruiting nucleation and stabilization factors[17]. Aurora A is self-activated by autophosphorylation at T288 in its T loop, helped by cofactors including Bora, Tpx2, Ajuba and PAK1 (refs 14,18,19).

Owing to its role in controlling MT dynamics, we hypothesize that Aurora A may play a role in the activation of T lymphocytes during IS formation. Consistent with our hypothesis, we report here that Aurora A is activated on TCR stimulation and controls the dynamics of MT and CD3ζ vesicles at the IS. We have also found an unexpected contribution of Aurora A to the early and late signalling events in T cells. Specific targeting of Aurora A impairs activation of the TCR/CD3 complex, by deregulating Lck phosphorylation and location, preventing early T-cell activation and downstream expression of CD69, CD25 and interleukin (IL)-2. Our data reveal a novel role for Aurora A as a major regulator of early signalling and the tubulin cytoskeleton during T-cell activation.

Results

Active Aurora A localizes to the IS. To assess the specific location of activated Aurora A, we conjugated human CD4$^+$ T cells from peripheral blood from healthy donors with beads coated with stimulatory anti-CD3 and anti-CD28 antibodies, and stained with anti-phospho-specific antibody against the Aurora-T288 residue, which detects active Aurora A. In these experiments, T288-phosphorylated endogenous Aurora A was found in two different pools: one in the centrosome and the other at the T-cell-bead contact region (examples of conjugates at different stages of the process are shown; Fig. 1a); the low signal of activated Aurora A in non-stimulated control conjugates was not detected at the IS (Fig. 1a). Pretreatment of peripheral-blood-derived human CD4$^+$ T cells with the specific Aurora A inhibitor MLN8237 blocked the phosphorylation of Aurora A (Fig. 1a). Quantitative analyses showed that phosphorylated Aurora A is accumulated at the IS in stimulated CD4$^+$ T cells, and that this is prevented by MLN8237 treatment (Fig. 1b). Staining of phosphorylated endogenous Aurora A on TCR stimulation was also abolished in T cells silenced with specific small interfering RNAs (siRNAs) for Aurora A, confirming the specific binding of the antibody (Supplementary Fig. 1a). Active Aurora A also localized at the IS in conjugates of naive mouse OTII T lymphocytes with primary dendritic cells pulsed with OVA peptide (Fig. 1c). These results clearly show that TCR triggering promotes the activation of Aurora A and its recruitment to the IS. However, pretreatment of J77 cells with the specific Aurora A inhibitor MLN8237 did not alter the number of conjugates formed with staphylococcal enterotoxin E (SEE)-pulsed Raji cells (Supplementary Fig. 1b), indicating that inhibition of Aurora A does not result in a global defect in cytoskeleton dynamics.

To parse the localization of activated Aurora A with respect to total Aurora A, we transfected primary CD4$^+$ T cells with Aurora A-GFP wild type (WT) or Aurora A-GFP KD (kinase dead mutant) and then conjugated the transfected cells with stimulatory anti-CD3/CD28-coated beads (Fig. 1d,e). Quantitative analysis of Aurora A-GFP or active Aurora A (Aurora A T288) accumulation demonstrated that it is mainly found at the IS. However, Aurora A KD accumulation at the IS is significantly decreased, compared with WT. Moreover, overexpression of the Aurora A-GFP KD mutant, disperses the remaining active protein. Thus, the phosphorylated active form of Aurora A is specifically recruited to the IS.

Aurora A controls MT dynamics at the IS. Aurora A plays an important role in the dynamics of the centrosome during mitosis[20,21]. To ascertain its possible function in MT dynamics and centrosomal polarity during T-cell activation, we analysed the dynamics of the microtubular network in CH7C17 T cells transiently transfected or stably expressing an EB3-GFP fusion protein (EB3 cells; Fig. 2a–d and Supplementary Movie 1). EB3 and EB1 (end-binding proteins) are plus-tip-tracking proteins that are also found in the pericentrosomal matrix and promote MT growth[22]. Cells were settled on anti-CD3/CD28-coated chambers and time-lapse confocal three-dimensional (3D) imaging was performed by *XYZ* stack acquisition. The stimulating surface allows IS-like formation, associated centrosome polarization and MT polymerization[12]. EB3 cells were pretreated or not (vehicle) with MLN8237 for 30 min before imaging. Maximal projection of the *XYZ* stack (Fig. 2a and Supplementary Movie 1) revealed that the relative amount of EB3-GFP incorporated into MT plus ends (+tips) was clearly decreased in Aurora A-inhibited cells. This effect was measured in 3D as the ratio of EB3-GFP fluorescence incorporated in +tips with respect to the whole-cell fluorescence using Imaris software, confirming that Aurora A-inhibited cells polymerize MTs less efficiently (Fig. 2b and Supplementary Movie 1). The amount of polymerized MT observed along the time course was clearly decreased in MLN8237-treated cells (Fig. 2a). We also analysed the localization of the MTOC and the EB3-GFP fluorescence by 3D and orthogonal projections of the *XYZ* stacks. Fluorescence was mainly detected close to the stimulating surface (Fig. 2c,d). This can be also observed by comparing bottom and top slices of the *XYZ* stacks (Supplementary Fig. 2a). Despite the effect of Aurora A inhibition on MT dynamics, no significant change on MTOC translocation in cell conjugates was observed either at 10 or at 30 min of activation (Fig. 2e).

To further assess the function of Aurora A in primary naive T cells, we used a mouse model of conditional Aurora deficiency. CD4$^+$ cells were isolated from lymph nodes and spleens of experimental [Aurka(lox/lox); RERT(ert/ert)] (knockout (KO)

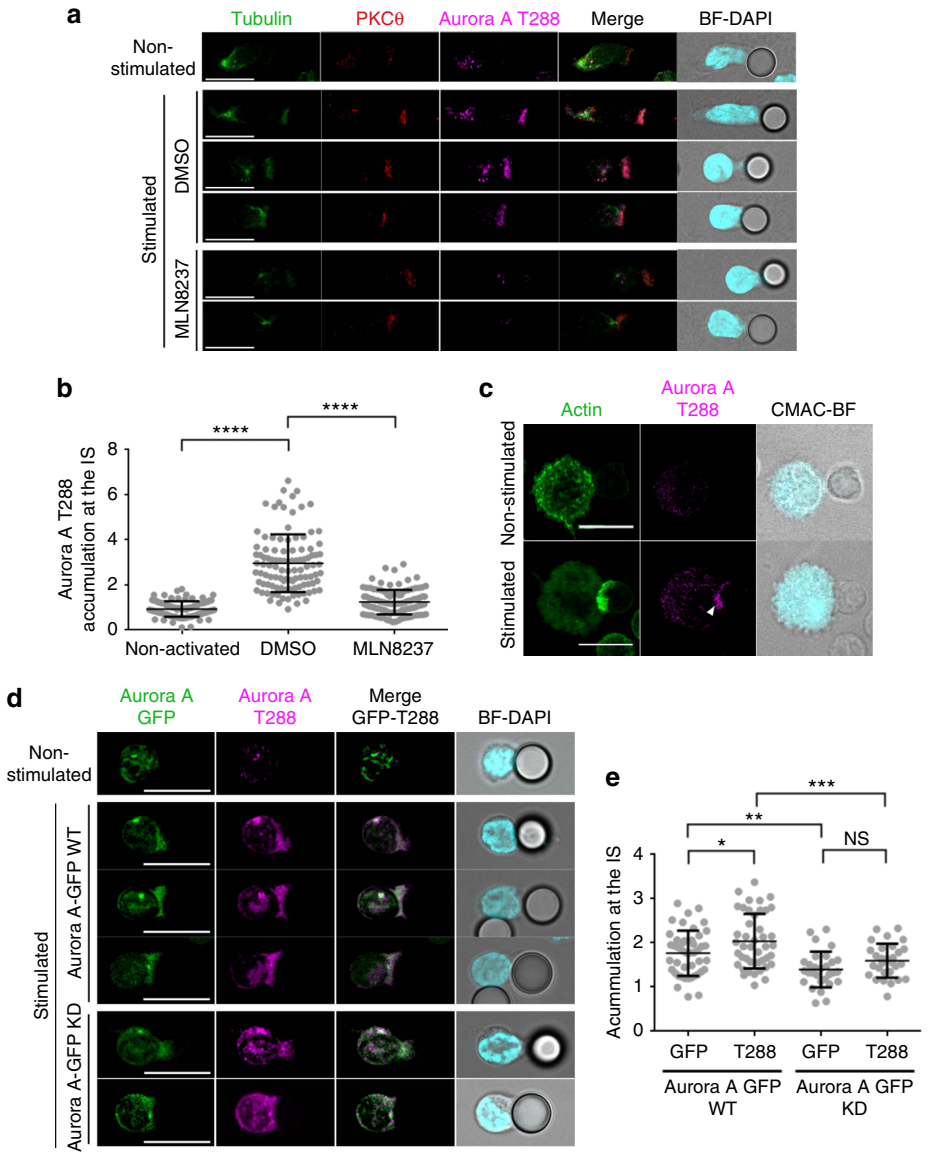

Figure 1 | Aurora A is located at the IS contact area and is activated on TCR triggering. (**a**) Maximum *Z* projection of a confocal stack of human primary CD4$^+$ T cells pretreated with vehicle (DMSO) or Aurora A inhibitor (MLN8237, 10 μM) and conjugated with anti CD3/CD28-coated beads. Images show three representative conjugates in DMSO and two in MLN8237-treated cells at different stages of cell conjugation. Cells were fixed and stained for PKCθ (red), T288-phosphorylated Aurora A (magenta) and α-tubulin–fluorescein isothiocyanate (FITC) (green). Bright field with DAPI frames are included. Scale bar, 10 μm. (**b**) Quantification of T288-phosphorylated Aurora A accumulation at the IS contact area in conjugates as in **a** from three independent experiments ($n=93$ in non-activated, $n=105$ in DMSO, $n=109$ in MLN8237). Data represent means ± s.d. Means were compared with a *t*-test. (**c**) Maximum *Z* projections of confocal stacks of transgenic OTII CD4$^+$ cells conjugated with OVA peptide-pulsed bone-marrow-derived dendritic cells (DCs). Cells were incubated for 30 min, fixed and immunostained for T288-phosphorylated Aurora A (magenta) and actin (green). The right-hand image shows CMAC cell tracker labelling of DCs (cyan) and bright field. Scale bar, 10 μm. (**d**) Maximum *Z* projection of a confocal stack of human primary CD4$^+$ T cells transfected with Aurora A-GFP WT or Aurora A-GFP KD (green) and conjugated with anti CD3/CD28-coated beads. Cells were incubated for 30 min, fixed and stained for T288-phosphorylated Aurora A (magenta). Bright field with DAPI frames are included. Scale bar, 10 μm. (**e**) Quantification of T288-phosphorylated Aurora A and transfected Aurora A accumulation at the IS contact area in conjugates as in **d** ($n=45$ in Aurora A-GFP WT, $n=29$ in Aurora A-GFP KD). Data represent means ± s.d. Means were compared with a *t*-test. n.s., nonsignificant. $^*P<0.05$, $^{**}P<0.01$, $^{***}P<0.001$, $^{****}P<0.0001$.

mice) and control [Aurka(+/+); RERT(ert/ert)] (WT mice), treated with tamoxifen and IL-7 for 96 h, to suppress Aurora A expression (Fig. 3a). These cells were transfected with a plasmid encoding EB3-GFP and then activated with anti-CD3/CD28 stimulating monoclonal antibodies (Fig. 3b,c and Supplementary Movie 2). We found that Aurora A-deficient T cells had significantly less EB3 incorporation in MT +tips than their WT counterparts (Fig. 3b,c and Supplementary Movie 2). Furthermore, the effect of Aurora A deficiency was similar to the effect of the MLN8237 inhibitor on WT cells, whereas the inhibitor did not have additional effects on Aurora A KO cells, suggesting that these and previously recorded effects of the inhibitor were Aurora A specific. MTOC and EB3-GFP tracking of MTs was also observed at the bottom of the cells (Supplementary Fig. 2b,c).

We next tracked the dynamics of MT growth using EB3-GFP imaging and total internal reflection fluorescence (TIRF) microscopy in cells settled on anti-CD3/CD28-coated surfaces,

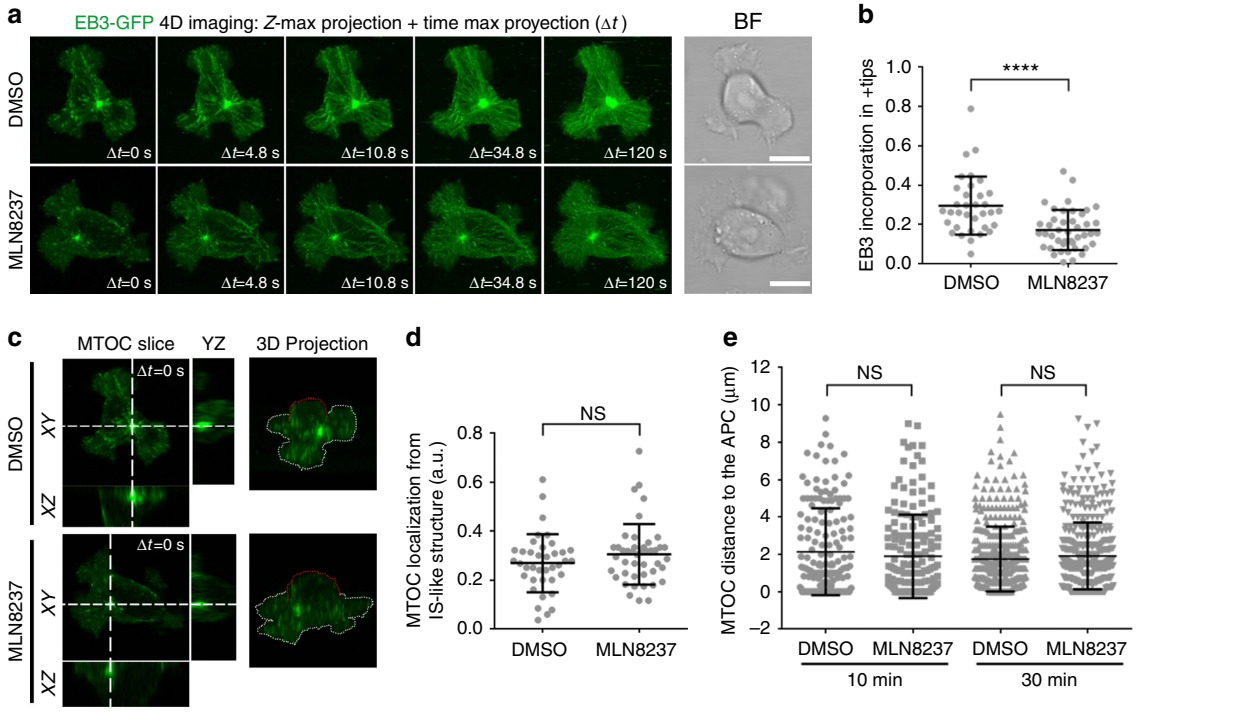

Figure 2 | MT dynamics at the IS is impaired by Aurora A chemical inhibition. (**a**–**d**) Imaging of EB3-GFP-expressing CH7C17 T cells (pretreated with DMSO or MLN8237 and settled on corresponding anti-CD3/CD28-coated glass-bottom chambers). Maximal projection of *XYZ* stacks for fluorescence and single bright-field (BF) images are shown. Scale bar, 10 μm. (**b**) Ratio of EB3-GFP fluorescence incorporated in + tips from *XYZ* stacks (0 s; $n=34$ in DMSO and $n=43$ in MLN8237). Data represent means ± s.d. Means were compared with a Mann–Whitney test. (**c**) Orthogonal and 3D projections from *XYZ* stacks. Dotted white or red lines indicate contact with substrate or media, respectively. (**d**) Ratio of the MTOC location from the IS-like structure ($n=38$ in DMSO, $n=44$ in MLN8237). (**e**) Distance from the T-cell MTOC to the APC contact area in conjugates of T cells with SEE-pulsed APCs (10 min, $n=166$ in DMSO, $n=168$ in MLN8237; 30 min, $n=412$ in DMSO, $n=394$ in MLN8237). Data represent means ± s.d. from three independent experiments. Means were compared with a *t*-test.

to improve the *XY* spatial and time resolution[23–25]. EB3 cells were treated with MLN8237 or dimethyl sulfoxide (DMSO; vehicle) for 30 min before imaging and images were taken every 300 ms. MLN8237-treated EB3-GFP cells had fewer EB3-decorated tips emerging from the centrosome, indicating impaired MT growth (Fig. 3d,e and Supplementary Movies 3 and 4). MT growth was similarly impaired in Aurora-KO primary $CD4^+$ T cells, displaying fewer and slower growing MTs than control cells (0.140 ± 0.037 and $0.190 \pm 0.023\ \mu m\ s^{-1}$, respectively; mean ± s.d.) (Fig. 3f,g and Supplementary Movies 5 and 6). Thus, these results show that the MT network at the IS is disrupted in T cells with defective Aurora A activation.

Aurora A regulates CD3ζ-bearing vesicles traffic at the IS. The impaired MT growth observed in Aurora A-targeted T cells did not affect the localization of the surface TCR/CD3 complexes at the IS, as TCR/CD3ε was comparably clustered at the IS of untreated and MLN8237-treated T-cell conjugates with APC (Fig. 4a,b). We next assessed the dynamics of CD3ζ-bearing vesicles at the IS. CD3ζ traffics through endosomal compartments towards the IS[26]. These vesicles move associated to MTs and support the sustained activation of the T cell at the IS[12,27]. The vesicles enter and leave the TIRF plane, some of them moving towards the position of the centrosome at the centre of the IS-like structure, probably along the MTs. Jurkat T cells expressing CD3ζ-mCherry were treated with DMSO or MLN8237, settled onto anti-CD3/CD28 and analysed by TIRF microscopy. Images were taken every 100 ms (200 nm penetrance) and the trajectories of detected vesicles were tracked. Treatment with MLN8237 decreased the number of vesicles at the IS-like structure and disrupted the movement of those that were present (Fig. 4c,d and Supplementary Movies 7 and 8). Therefore, the effect of Aurora A inhibition on MT dynamics impedes the movement of vesicles towards the IS structure, a finding confirmed by the reduced speed of vesicles in Aurora A-inhibited cells (Fig. 4d). A similar phenotype was observed in Aurora KO cells, with few or no vesicles moving towards the centre of the IS-like structure. Treatment of WT cells with the Aurora A inhibitor caused a similar effect to Aurora A-deficiency (Fig. 4e,f and Supplementary Movie 9).

Aurora A blockade does not affect TCR-driven actin dynamics. To further analyse the role of Aurora A in the control of cytoskeletal dynamics at the IS, we assessed the effect of Aurora A inhibition on the activation-dependent interaction of TCR/CD3 with the actin–cytoskeleton-associated protein Nck. This interaction is enabled by the conformational change in the TCR/CD3ε complex on antigenic triggering[28]. Aurora A inhibition had no effect on CD3ζ–Nck association in pull-down assays (Fig. 5a). This is in agreement with a surface recruitment and accumulation of TCR/CD3ε to the IS in Aurora A-inhibited cells (Fig. 4a,b). Using a similar approach, we assessed whether Aurora A impairment affects the activation of the small GTPase Rac1, a hallmark for TCR-dependent actin polymerization[29]. Likewise, no effect was detected in Rac1 pull-down assays with the GST-PAK-CD (p21-activated kinase CRIB Domain[30]) in stimulated $CD4^+$ T cells when using MLN8327 inhibitor (Fig. 5b). Furthermore, the Aurora A inhibitor did not affect

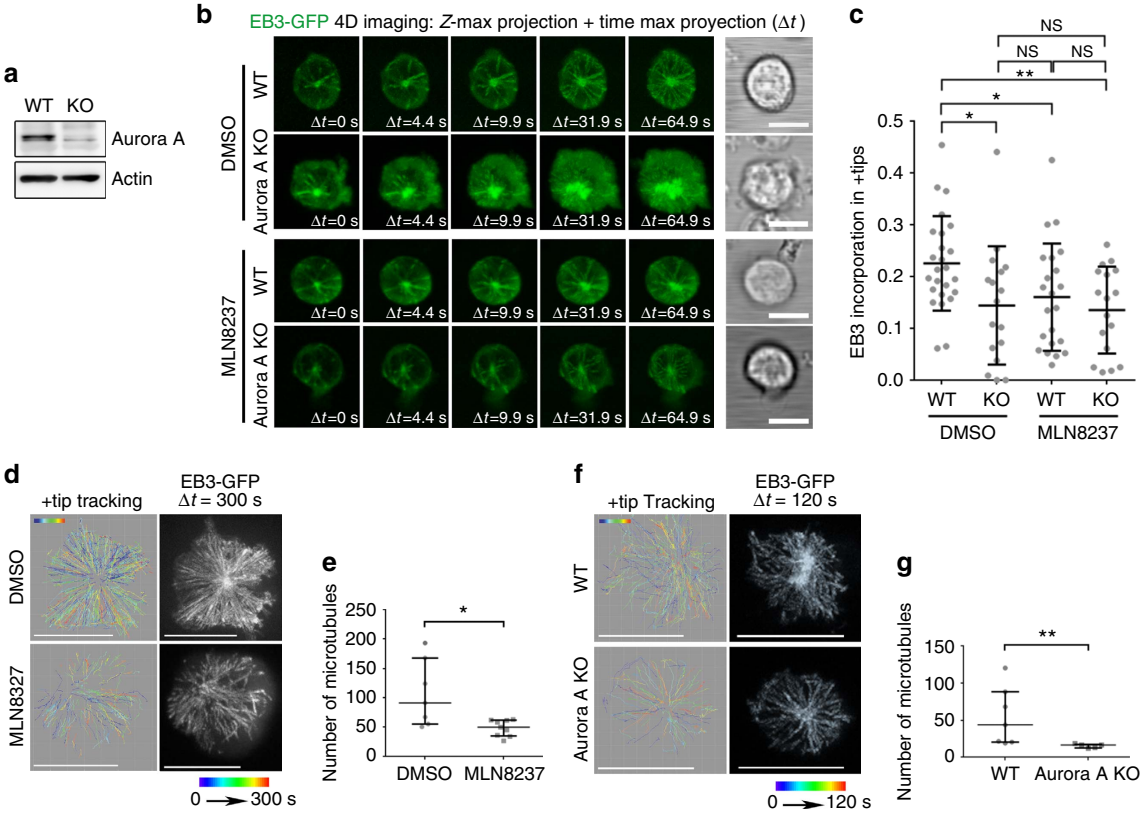

Figure 3 | Aurora A gene ablation impairs MT dynamics at the IS. (**a**) Immunoblot analysis of Aurora A protein expression in CD4$^+$ T cells WT and KO. (**b**,**c**) Imaging of EB3-GFP-expressing Aurora-A-deficient and control CD4$^+$ T cells, pretreated with DMSO or MLN8237 and settled on corresponding anti-CD3/CD28-coated glass-bottom chambers. Maximal projection of *XYZ* stacks for fluorescence and single bright-field (BF) images are shown. Scale bar, 5 μm. (**c**) Ratio of EB3-GFP fluorescence incorporated in +tips from *XYZ* stack (0 s, $n=25$ in WT, $n=17$ in KO, $n=22$ in WT MLN8237 and $n=17$ in KO MLN823). Data represent means ± s.d. Means were compared with a Mann–Whitney test. Map of the trajectories of EB3-GFP-decorated MT plus tips in human CH7C17 T cells pretreated with DMSO or MLN8237 (**d**,**e**), or in Aurora-A-deficient and control CD4$^+$ T cells (**f**,**g**) and settled on anti-CD3/CD28-coated glass-bottom chambers. Images were taken every 300 ms under a TIRF microscope at a penetrance of 150 nm. MT +tips were tracked with Imaris software over 5 (**d**) or 2 min (**f**). Maximal projections of the time lapse from representative cells are shown. Scale bar, 10 μm. (**e**,**g**) Quantification of the number of MT plus tip tracks presented in **d** (**e**; $n=7$ in DMSO, $n=9$ in MLN8237) and **g** (**f**; $n=6$). Error bars represent interquartile rage. Medians were compared with a Mann–Whitney test. n.s., nonsignificant. *$P<0.05$, **$P<0.01$, ***$P<0.001$, ****$P<0.0001$.

the spreading of mCherry–β-actin-expressing T cells on anti-CD3/CD28-coated coverslips, measured either as the total occupied surface or as the rate of membrane extension on the coverslip (Fig. 5c,d). This finding correlated with a similar distribution of mCherry–β-actin at the peripheral SMAC and cSMAC in control and Aurora A-inhibited cells. Aurora A inhibition also had no effect on the total area occupied by adhered cells or their lamellae (Fig. 5d). Similarly, actin accumulation at the IS in T cell–APC conjugates was not significantly affected by inhibition of Aurora A (Fig. 5e,f). We therefore analysed the formation of the actin ring in cell conjugates using time-lapse 3D confocal imaging. Actin accumulation and ring formation was similar in control and MLN8237-treated cells (Fig, 5g,h and Supplementary Movie 10). Therefore, Aurora A appears to specifically affect the tubulin cytoskeleton at the IS, without affecting actin-based dynamics.

Aurora A inhibition impairs early TCR signalling. To assess the possible role of Aurora A in TCR signalling, we analysed the phosphorylation of several canonical downstream molecules that are phosphorylated in response to cognate interactions in SEE-stimulated Jurkat T cells (Fig. 6a,b) and anti-CD3/CD28-stimulated human primary CD4$^+$ T cells (Fig. 6c,d). The phosphorylation of specific residues in CD3ζ (Y83), LAT (Linker for Activation of T cell; Y132), PLCγ1 (Phospholipase C; Y783), PKCθ (T538) and ERK1/2 (T202/Y204) was greatly diminished on Aurora A inhibition with MLN8237. The role of Aurora A in TCR signalling was also confirmed in an MHC/peptide-specific system, in which MLN8237-treated CH7C17 Jurkat T cells were stimulated with Hom2 lymphoblastoid B cells preloaded with haemagglutinin (HA) peptide (Fig. 7a,b). The effect of Aurora A inhibition on TCR downstream signalling was dose dependent (Supplementary Fig. 3a,b). As a control of MLN8237 specificity, we added the inhibitor just before the activation of T cells and the same effect was observed (Supplementary Fig. 3c). By extensively washing the inhibitor before activation, the phosphorylation levels of these specific residues were restored, indicating that the effects of the inhibitor were reversible (Supplementary Fig. 3d). MLN8237 shows a 200-fold higher selectivity for Aurora A over Aurora B[31]; nonetheless, to rule out a possible role of Aurora B, we treated J77 T cells with AZD1152 (100 nM), which is 3,700 times more selective for Aurora B[32]. AZD1152 had no effect on the phosphorylation of T-cell proteins (Supplementary Fig. 4), confirming that proper T-cell activation critically depends of the isoform A, but not B, of Aurora kinase. This was further confirmed in conjugates of Aurora-A-silenced Jurkat T cells and Staphylococcal enterotoxin B (SEB)-preloaded Hom2 B cells as

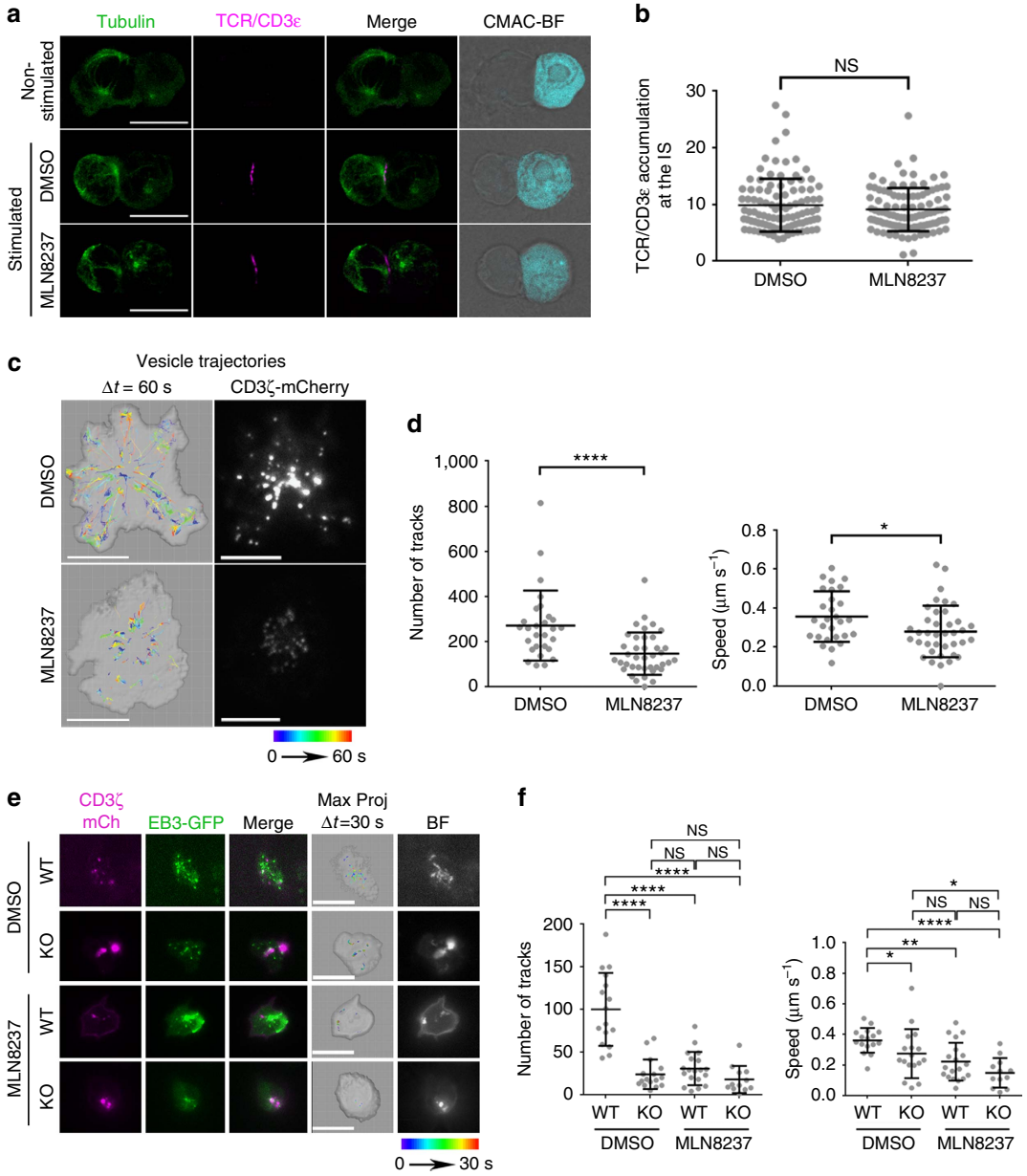

Figure 4 | Trafficking of CD3-bearing vesicles at the IS is impaired by Aurora A chemical inhibition or gene ablation. (**a**) Maximum *Z* projections of confocal stacks of Jurkat T cells pretreated with vehicle (DMSO) or Aurora A inhibitor (MLN8237) and conjugated with SEE-pulsed Raji B cells. Cells were incubated for 30 min, fixed and stained for α-tubulin (green) and TRC/CD3ε (magenta). The right-hand image shows CMAC cell tracker labelling of Raji B cells (cyan) and bright field. Scale bar, 10 μm. (**b**) Graph shows quantification of TRC/CD3ε clustering at the IS from as in **a**. Means ± s.d. is shown; *t*-test was used to compare means ($n=101$ in DMSO and in MLN8237). Map of the trajectories of CD3ζ-cherry-bearing vesicles in human CH7C17 T cells (**c**) or Aurora-A-deficient and control CD4$^+$ T cells (**e**) pretreated with vehicle (DMSO) or MLN8237 inhibitor and settled on corresponding anti-human or anti-mouse stimulating anti-CD3/CD28-coated glass-bottom chambers. Images were taken every 100 (**c**) or 110 ms (**e**) under a TIRF microscope at a penetrance of 200 nm with 561 nm laser; vesicles were tracked with Imaris software over 60 (**c**) or 30 s (**e**) and maximal projections of the time lapse are shown for tracks. A representative cell is shown for each case. Fluorescence images from CD3ζ-mCherry (**c**,**e**) and EB3-GFP are also shown (**e**). (**d**,**f**) Quantification of the number of vesicle tracks and the speed of vesicles from cells analysed in **c** and **e** from three independent experiments (**d**, $n=28$ in DMSO, $n=39$ in MLN8237; **f**, $n=16$ in WT, $n=17$ in KO, $n=19$ in WT MLN8237, $n=12$ in KO MLN8237). Data represent means ± s.d. Means were compared with a Mann–Whitney test. n.s., nonsignificant. *$P<0.05$, **$P<0.01$, ***$P<0.001$, ****$P<0.0001$.

APCs. The activation of CD3ζ-dependent molecules was defective in Aurora-A-silenced cells, with below-normal LAT phosphorylation on residue Y132, probably responsible for the concomitant decreases in PLCγ1 (Y783) and PKCθ (T538) phosphorylation (Supplementary Fig. 5a).

To determine the role of Aurora A in late events of T-cell activation, we examined the messenger RNA expression of IL-2, CD25 and CD69. Human CD4$^+$ T lymphocytes were treated with MLN8237 and AZD1152 or vehicle for 30 min, and stimulated with anti-CD3/CD28 antibodies for 3 h. Inhibition of Aurora A impaired the upregulation of IL-2, CD25 and CD69 mRNA determined by reverse transcriptase–PCR (Fig. 7c), indicating a defect in late T-cell activation. In contrast, Aurora B inhibition had no effect on the mRNA production of these

genes, supporting a specific role for Aurora A and its regulated pathways in T-cell activation.

TCR signalling is impaired in Aurora-A-deficient mice. Pharmacologic inhibition of Aurora A also impaired early T-cell activation in mouse naive CD4$^+$ T cells polyclonally stimulated with anti-CD3/CD28 (Fig. 8a). To further assess the function of Aurora A in primary naive T cells, we deleted Aurora A expression in CD4$^+$ cells from the conditional Aurora KO mice and activated them with anti-CD3/CD28 antibodies. Tamoxifen-induced suppression of Aurora A expression in Aurka(lox/lox); RERT(ert/ert) cells (Fig. 3a) correlated with clear decreases in the phosphorylation of CD3ζ (Y83), LAT (Y132), PLCγ1 (Y783), PKCθ (T538) and ERK1/2 (T202/Y204) (Fig. 8b,c). CD4$^+$ T cells from the conditional Aurora KO mice were also treated with MLN8237, obtaining a slight decrease in the phosphorylation of PLCγ1 (Y783) when compared with vehicle-treated CD4$^+$ T cells from the conditional Aurora KO mice (Supplementary Fig. 5b). In complementary experiments, we examined a transgenic mouse model of Aurora A overexpression[33]. Naive CD4$^+$ T cells isolated from lymph nodes and spleens of *Col1a1tetO-Aurka/+; Rosa26rtTA/rtTA* mice (Aurora KI) and controls were treated with doxycycline and IL-7 for 24 h, followed by activation with anti-CD3/CD28 antibodies. Doxycycline treatment increased Aurora A expression in the conditionally transgenic cells (Fig. 8d), correlating with increased levels of TCR-dependent signalling (Fig. 8e,f).

Aurora A controls Lck kinase location and phosphorylation. To study the mechanism underlying the earliest T-cell activation defects in the absence of Aurora A, we assessed the possible regulation of the Src kinase Lck by Aurora A. Lck phosphorylates CD3 ITAMs at tyrosine residues on TCR triggering and shows autophosphorylation activity towards its Y394 residue, an activatory residue[34]. By quantitative analysis of Lck accumulation at the IS we have detected a significant reduction in Lck relocation to the IS contact area, as a result of Aurora A inhibition in Jurkat T cells (Fig. 9a,b). In accordance with a perturbed Lck localization, pharmacologic inhibition of Aurora A in human primary CD4$^+$ T cells impaired Lck autophosphorylation at Y394, a hallmark of its catalytic activity (Fig. 9c,d). Notably, these experiments showed that Lck-Y394 phosphorylation was impaired before TCR stimulation, suggesting a role of Aurora A in the maintenance of the preactivated pool of Lck[34].

To analyse whether the effect of Aurora A on Lck activation is dependent on the intracellular traffic of Lck[27] and taking into account that Lck recruitment at the IS is also driven by its association with CD4 (ref. 35), we decided to assess T-cell activation in a Lck-deficient cell line (J.CAM1 (refs 36,37)) reconstituted with full-length Lck-GFP or murine CD4-Lck chimeric proteins. CD4-Lck is mainly localized at the plasma membrane[38,39]. A murine CD4 lacking its cytosolic tail and fused to GFP was used as a negative control[40] (Fig. 9e; CD4-ΔCyt-GFP). We found that Lck-GFP expression rescued CD3 phosphorylation and thus T-cell activation in J.CAM1, whereas MLN8237 treatment prevented such an effect. Rescue of J.CAM1 signalling with CD4-Lck chimera was also prevented with the Aurora A inhibitor. Therefore, Aurora A activity is needed for Lck activity independently of its intracellular trafficking during IS formation.

Immunoprecipitation (IP) of Lck followed by mass spectrometry (MS) analysis revealed that Aurora A inhibition resulted in a decrease of Lck phosphorylation at the activation residue Y394 in resting and stimulatory conditions (Fig. 9f). This was further corroborated by *in vitro* kinase assays of purified recombinant Lck protein by immunoprecipitated Aurora A proteins. Although WT Aurora A protein keeps Lck phosphorylated at residue Y394, a KD form of Aurora is unable to maintain Lck phosphorylation at Y394 (Fig. 9g). Treatment with the Aurora A inhibitor corroborated the KD results (Fig. 9g). Together, these results highlight the relationship of Aurora A-mediated signal spreading at the IS with Lck location, phosphorylation and, therefore, regulation.

Discussion

In this study we have analysed the influence of a well-known cell cycle regulator, Aurora A kinase, in T-cell activation. Our results provide novel evidence that Aurora A is a key regulator of early TCR-dependent signalling pathways and controls signalling vesicle and microtubular dynamics. However, the direct interaction of TCR/CD3 with Nck and actin polymerization at IS are not affected by Aurora A inhibition. Aurora A localizes at the IS and appears activated on antigen- and superantigen-driven T-cell activation. Early activation of Aurora A seems to be essential for TCR downstream signalling, leading to LAT and PLC activation. In addition, our data provide mechanistic insight into how Aurora A acts as master regulator of T-cell activation by controlling Lck phosphorylation and clustering at the IS.

Aurora A localization to centrosomes and along spindle MTs at the beginning of mitosis is well characterized[13,17]. The location of Aurora A in interphase is not well established, although the human protein atlas indicates that nuclear and cytoplasmic pools co-exist (http://www.proteinatlas.org/). Our data reveal that a fraction of active Aurora A (T288) appears at the IS contact area and a second pool is concentrated at the pericentrosomal area. The active form at the IS was observed on TCR stimulation, whereas the centrosome fraction seemed to be basally active in primary CD4$^+$ T cells. The active pool and the total protein showed a similar pattern, indicating that there is an active redistribution of the protein on stimulation. This highlights the possibility that Aurora A autophosphorylation might have a role on its own localization at the IS, which is also supported by the fact that the expression of an Aurora A KD mutant provokes the delocalization of the active protein at the IS. However, further studies should be conducted to prove this view. The presence of two detectable pools suggest that Aurora A may play a possible dual role in controlling MT dynamics and T-cell activation. Although Aurora A can autophosphorylate, it is conceivable that other kinases are also involved in its activation. The MT-associated protein Tpx2 can activate Aurora A through its stabilization during cell division and prevents PP1 phosphatase from inactivating Aurora A[41]. Therefore, the distribution of activated Aurora A at the IS, a zone where a complex microtubular network is rapidly organized, may be responsible for its stabilization and activation, establishing a positive feedback for tubulin dynamics.

Aurora A contributes to centrosome maturation through the recruitment of MT nucleation factors. However, its absence does not prevent the formation of the centrosomal MT aster but instead affects the density of the aster formed in other systems[17]. Our TIRF microscopy analysis demonstrates that Aurora A controls growing MT arising from the MTOC on TCR activation, while having no apparent effect on MTOC translocation at the IS. In addition, during the M phase Aurora A is required for the recruitment of adaptor proteins such as NEDD1 for the correct formation of the mitotic spindle[42]. Previous work on proteins implicated in MT regulation such as EB1 or HDAC6 (refs 12,43) showed a defect in late T-cell activation. The role of these proteins in MT cytoskeleton dynamics and T-cell activation seemed to be mainly related to the maintenance of the TCR signal rather than

its initial activation. Aurora A might regulate late T-cell activation through a similar mechanism. Our data indicate that the decrease in the number of MTs nucleated near the contact area may affect polarized secretion from this area and vesicular trafficking at the IS and throughout the T cell. Hence, Aurora A inhibition prevents movement of CD3ζ vesicles around the MTOC almost completely, possibly reflecting a global effect on vesicle trafficking. In addition, as CD3 is tightly regulated by its cycle of degradation and recycling[44], the absence of this pool of CD3ζ vesicles at the cSMAC may explain why the TCR signal cascade is not properly propagated. It has been proved that there is a pool of phosphorylated CD3ζ that, instead of going to a degradation pathway, keeps accumulated at the endosomal compartment, ready to maintain CD3ζ phosphorylation signalling[26]. Although Aurora A inhibition has no effect in TCR/CD3ε subunit surface clustering at the IS, the transport of vesicles of the CD3ζ subunit is clearly impaired. Taking into account the presence of this phosphorylated CD3ζ pool at the endosomal compartment, Aurora A might have an effect mainly over this recycling of the active CD3ζ and, therefore, over TCR signal propagation.

Although Aurora A contributes to actin cytoskeleton dynamics in mitosis and during mammary cell migration, no such effect was observed during IS formation by spreading T cells. Aurora-A-mediated phosphorylation of LIM kinase 1 at the centrosomes in prophase is essential for modulation of actin filaments and subsequent spindle formation. LIM kinase 1 acts by inactivating the phosphorylation of the actin depolymerizing family protein cofilin, thus stabilizing the cortical actin network during spindle orientation[45]. In mammary cell migration, Aurora A promotes increased expression of the cofilin phosphatase SSH1, resulting in cofilin activation and actin reorganization and migration[46]. However, our data show that Aurora A inhibition affects neither actin accumulation during IS formation nor cell spreading. Indeed, we found that Aurora-A-inhibited T cells form normal-shaped lamellae. During IS formation, Nck acts as a bridge between the TCR activation and actin cytoskeleton reorganization at the IS. When the TCR recognizes a specific antigen, a conformational change in the CD3ε chain unmasks a neoepitope to which Nck binds, leading to transmission of the activation signal through the actin cytoskeleton[28]. CD3ε-NcK association is not affected by Aurora A inhibition, a finding in accordance with the absence of changes in actin accumulation at the IS in MLN8237-pretreated T cells.

Our results show regulatory effects of Aurora A on early and late T-cell signalling. Inhibition of Aurora A abrogates proper T-cell activation determined by the phosphorylation profile of TCR signalling proteins such as CD3, and the adapter proteins and kinases LAT, PLCγ1 and PKCθ. These effects on TCR pathway phosphorylation events were observed in response to the Aurora A inhibitor MLN8237 and Aurora A gene ablation in mouse T cells, indicating that this is a specific consequence of Aurora A inhibition. The initial activation of T cells occurs at the plasma membrane; however, its continued progress requires the contribution of intracellular components such as the MTOC and the MT-dependent vesicular traffic and mitochondrial activity[3]. Thus, Aurora A contributes to the propagation of TCR activation to the intracellular compartment, leading to activation of genes such as *IL-2*, *CD69* and *CD25*. Moreover, the strength of T-cell activation can determine the ability of T cells to divide asymmetrically, thereby promoting functional differentiation into subpopulations of T cells that regulate the immune response[47]. Our data suggest that T lymphocytes defective in Aurora A do not become properly activated, possibly affecting the outcome of the adaptive immune response.

However, neither the defect on MT dynamics nor the impairment in CD3ζ vesicle transport can explain the blockade of the initial trigger of TCR signalling. These early defects of CD3ζ-dependent signalling in Aurora A-targeted cells are more likely to be explained by altered activity of Src kinases. This family includes Lck and Fyn, the first kinases to phosphorylate the ITAMs in CD3, which are required for full activation and signal transmission[5,48]. Our data demonstrate that Lck location and phosphorylation are altered by chemical inhibition of Aurora A, demonstrating that Aurora A controls TCR pathways dependent on CD3-ITAM phosphorylation. Nevertheless, the interaction of the kinase with the HSP90 and HSP70 chaperones is maintained in the presence of MLN8237, indicating that the inhibitor does not seem to affect its life time (Blas-Rus *et al.*, unpublished data).

Previous work on Lck regulation has described the initial steps on the activation of this protein. A 'standby' model has been proposed, where there is a pool of preactivated Lck whose phosphorylation does not change on TCR activation[34]. In this context, Lck function could be regulated through conformational changes, clustering and the spatio-temporal proximity to CD45 phosphatase, as well as with the exposition of the phosphorylatable ITAMs on TCR engagement[34,49,50]. However, other recent works detected a pool of Lck that became activated on TCR triggering assessed either by FRET-FLIM techniques[51] or other different methods[52]. On the other hand, other studies addressed the importance of Lck spatial distribution in specific lipid rafts that rearrange on MHC–TCR binding[49,53,54]. In this regard, our results by complementary experimental strategies including western blot (WB) analysis of protein activation and MS analysis of endogenous Lck, and of *in vitro* kinase assays with

Figure 5 | Aurora A inhibition does not affect actin cytoskeleton dynamics. (**a**) Immunoblot of a pull-down assay of GST-Nck fusion protein from cell lysates of control (DMSO; vehicle) or Aurora A inhibitor (MLN8237)-pretreated human T lymphoblasts. Activation was performed with soluble anti-CD3ε antibodies for indicated times. CD3ζ and GST are shown. CD3ζ content in whole-cell lysates is indicated in the bottom row. (**b**) Immunoblotting of Rac1 pull-down assay of GST and GST-PAK-CD from cell lysates of DMSO- or MLN8237-pretreated Jurkat T cells activated with SEE-pulsed Raji B cells (APCs) for the indicated times. Loading control for Rac1 in whole-cell lysates is shown. (**c**) Images from TIRFm time-lapse analysis of mCherry–β-actin-expressing Jurkat T cells spreading over anti-CD3/CD28-coated glass-bottom chambers. Cells were pretreated with DMSO or MLN8237. Images were taken every 100 ms for 5 min at 90 nm penetrance. A corresponding bright-field image is shown. Scale bar, 10 μm. (**d**) Quantification of the area occupied by the whole cell (lamella), the actin-rich area (peripheral SMAC (pSMAC)), the central area (cSMAC) and the distribution of mean fluorescence intensity per area (ratios cSMAC:cell; pSMAC:cell and cSMAC/pSMAC) from cells in **c** ($n=48$ and $n=36$, three independent experiments). Cells were fixed after spreading (4 min) and fluorescence images were taken. Data represent means ± s.d.; *t*-test. n.s., nonsignificant. (**e**) Maximum *Z* projections of confocal stacks from DMSO- or MLN8237-pretreated Jurkat T cells conjugated with SEE-APCs. Cells were incubated for 30 min, fixed and stained for α-tubulin (green) or actin (magenta). The right-hand image shows CMAC cell tracker labelling of APCs (cyan) and bright field. Scale bar, 10 μm. (**f**) Quantification of actin accumulation at the IS contact area in conjugates as in **e** from three independent experiments ($n=100$). Data represent means ± s.d.; *t*-test. (**g**) Image sequence for IS formation between mCherry–β-actin-expressing T cells and SEB-APCs (DMSO- or MLN8237-treated). *XYZ* stacks were acquired every 25 s (maximal projections of *XYZ* stacks and 3D reconstructions with Imaris Software are shown from representative conjugates). (**h**) Ratio of T cells forming lamella on contact with an APC from **g**. Data represent median ± interquartile range. Mann–Whitney test (DMSO: 28 cells ($n=4$); MLN8237: 25 cells ($n=3$)).

purified recombinant Lck protein indicate that the activating Lck residue Y394 is phosphorylated in T cells before TCR stimulation. Remarkably, the targeting of Aurora A decreases Y394 phosphorylation and shows a delocalized Lck clustering at the IS. Reconstitution experiments in the Lck-deficient cell line J.CAM1 by either Lck-GFP or CD4-Lck, which retains Lck at the plasma membrane, revealed that Aurora A is required for TCR signalling in both situations. Taking into account the importance of Lck spatial distribution and proper phosphorylation for its activity, the dephosphorylation and mislocalization of Lck in the absence of Aurora A activity may explain the observed defects in TCR signalling pathways. A detailed analysis of other phosphorylated residues, including Ser/Thr, is needed to understand the complex regulation of Lck by Aurora A and this deserves future

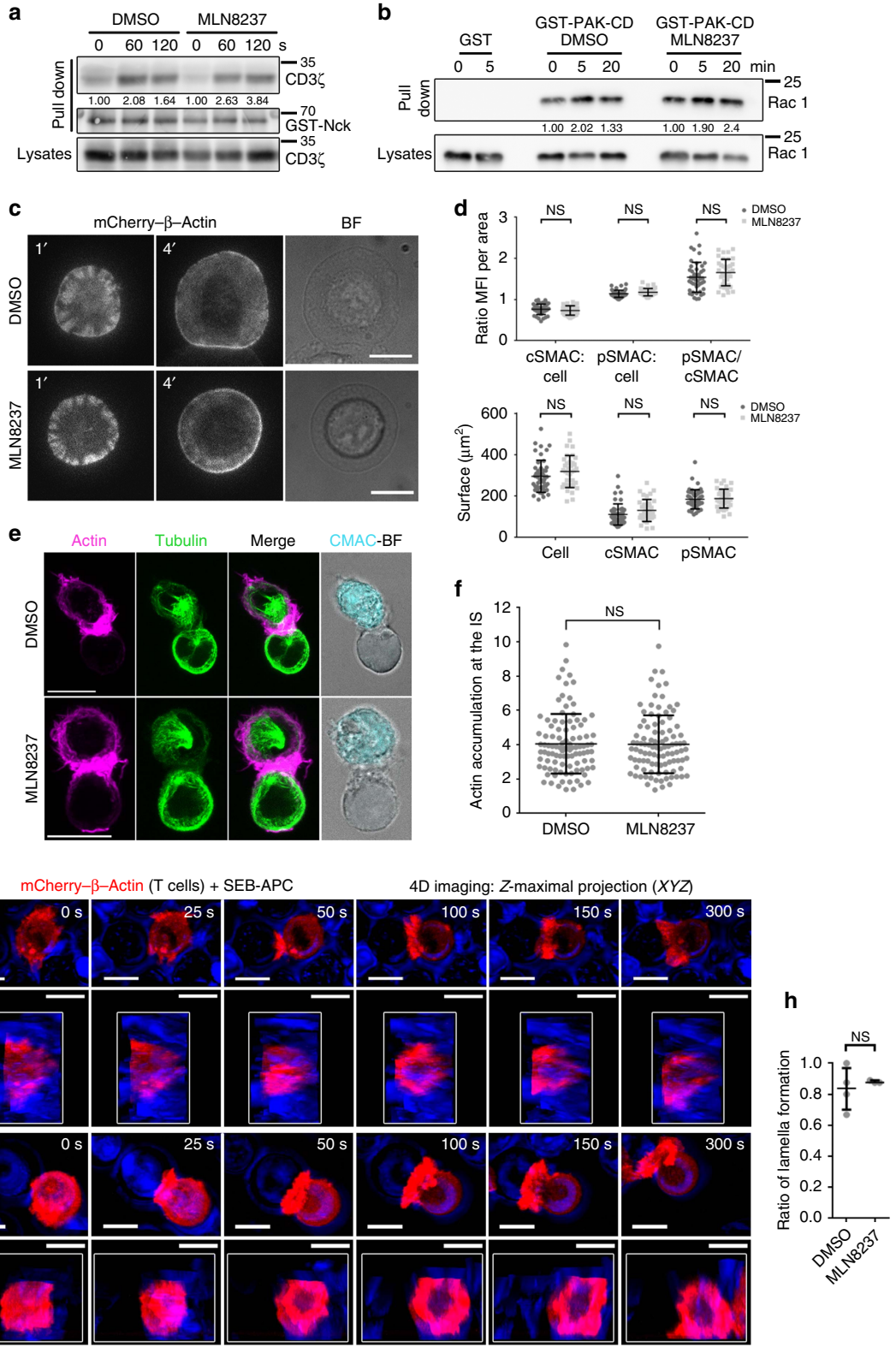

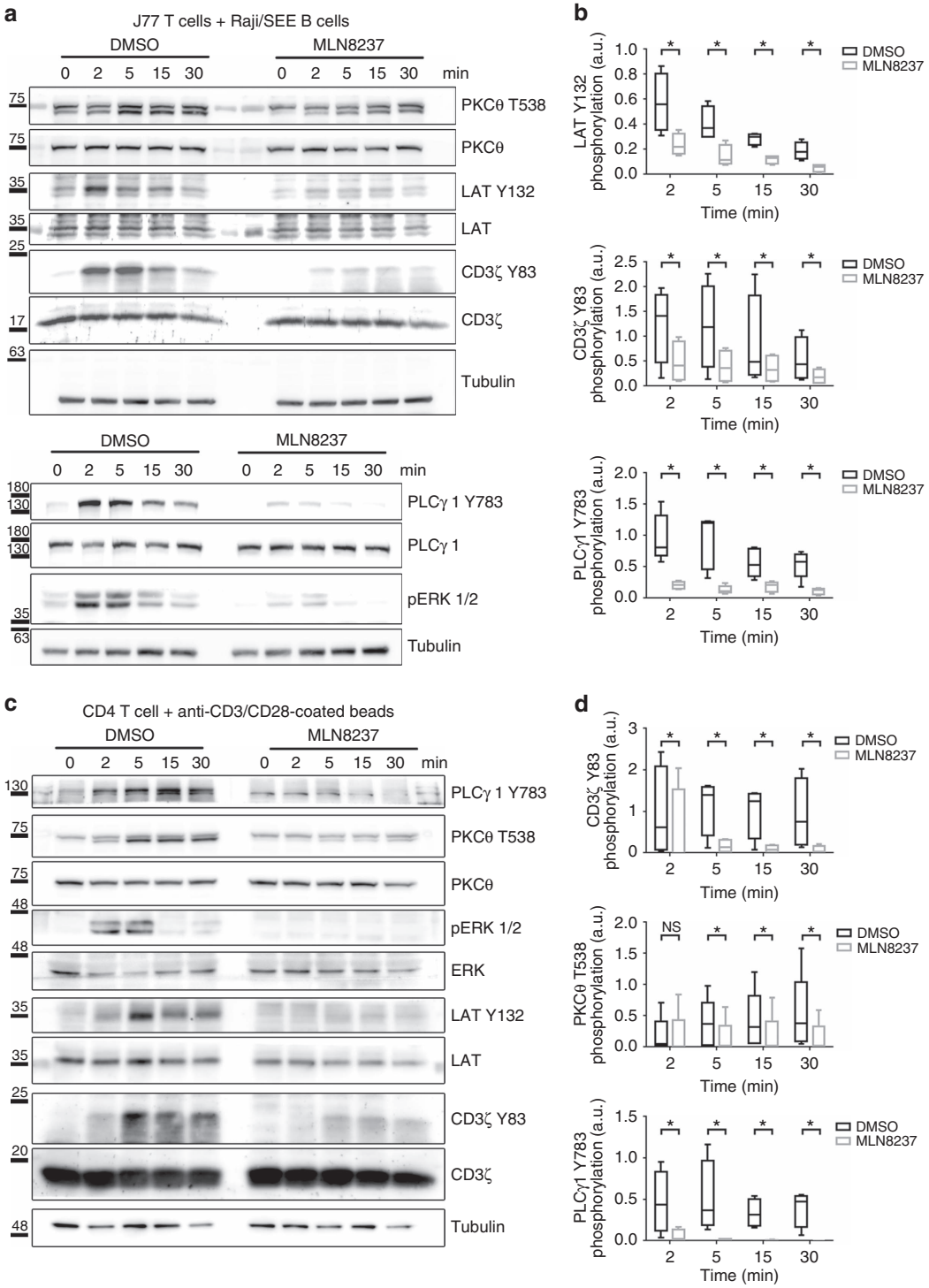

Figure 6 | Aurora A inhibition impairs TCR signalling pathways. (**a**) Immunoblottings showing phosphorylation of the indicated molecules in lysates of J77 Jurkat T cells pretreated with vehicle (DMSO) or Aurora A inhibitor (MLN8237) and conjugated for the indicated times with SEE-pulsed Raji B cells. (**b**) Quantification of blots as in **a** from four to six independent experiments. Error bars represent interquartile range. Medians were compared with a Friedman test (*$P<0.05$). n.s., nonsignificant. (**c**) Immunoblottings showing phosphorylation of the indicated molecules in lysates of DMSO- or MLN8237-pretreated primary human CD4$^+$ T cells conjugated for the indicated times with anti-CD3/CD28-coated beads. (**d**) Quantification of blottings as in **c** from four to six independent experiments. Error bars represent interquartile range. Medians were compared with a Friedman test (*$P<0.05$). n.s., nonsignificant.

investigation. Furthermore, the assessment of how Aurora A controls Lck activity, either directly or indirectly through associated kinases, is an issue that remains to be explored.

In summary, our results show that Aurora A plays an important role in the early events initiated on TCR stimulation and unravel a novel molecular mechanism that regulates early signalling and cytoskeletal and vesicle dynamics in T cells. The prevention of T-cell activation by Aurora A inhibition has important clinical implications. Aurora A inhibitors are currently under evaluation for cancer therapy in Phase I–II clinical trials[55].

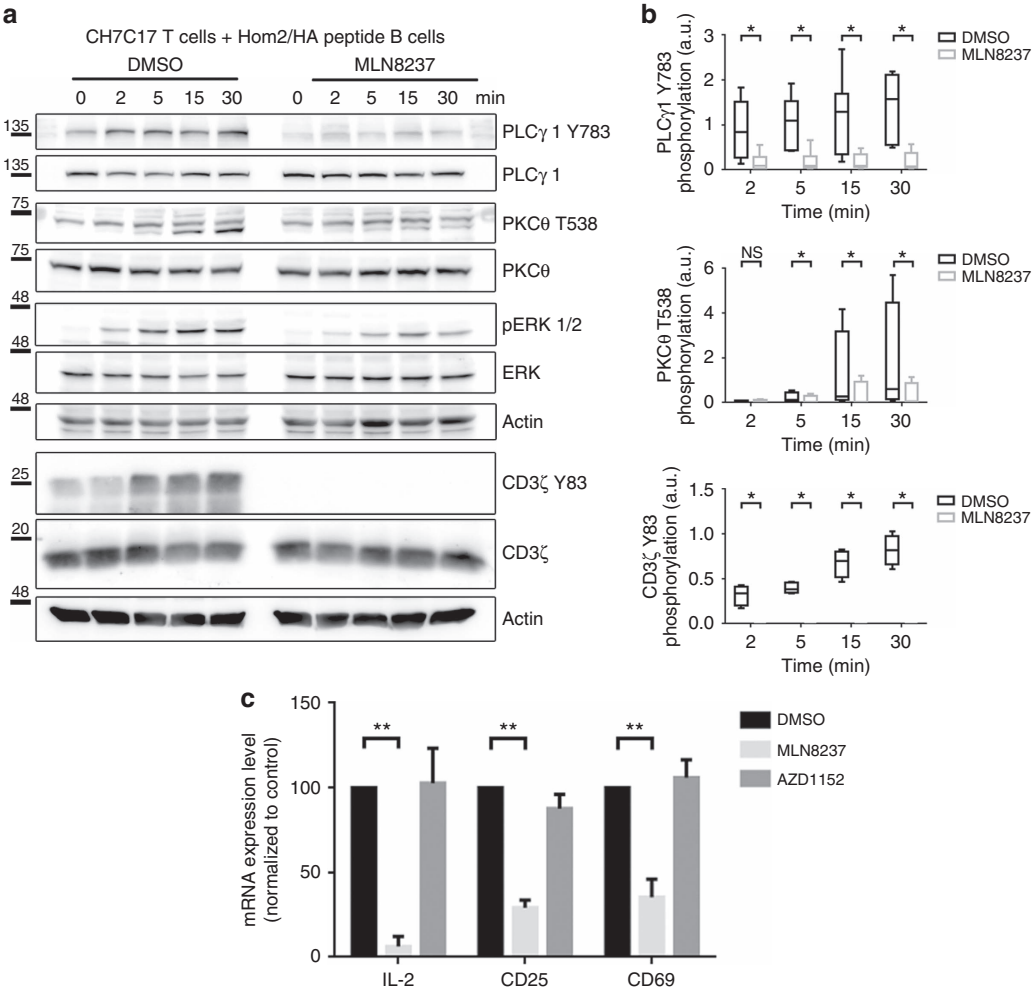

Figure 7 | Aurora A inhibition impairs TCR signalling and gene expression. (**a**) Immunoblottings showing phosphorylation of the molecules indicated in lysates of CH7C17 Jurkat T cells pretreated with DMSO or MLN8237 and conjugated for the indicated times with HA-peptide-pulsed Hom2 B cells. (**b**) Quantification of blots as in **a**–**c** from four to six independent experiments. Error bars represent interquartile range. Medians were compared with a Friedman test (*$P<0.05$). n.s., nonsignificant. (**c**) *IL2*, *CD69* and *CD25* mRNA levels in primary human CD4$^+$ T cells pretreated with DMSO, MLN8237 (10 μM) or the Aurora B inhibitor AZD1152 (100 nM) and activated by settling on anti-CD3/CD28-coated plates for 4 h. mRNA levels were normalized to the housekeeping gene *GAPDH* and the levels of the target mRNA in non-stimulated cell levels. Error bars represent interquartile rage. Medians were compared with a Mann–Whitney test. **$P<0.01$.

In these trials, aggressive B-cell and T-cell non-Hodgkin lymphomas have shown an overall positive response, promoting new Phase III studies. It will be important to define the extent to which the new function reported here participates in these responses and to determine whether the T-cell activation pathway can provide new biomarkers, critical for understanding these therapeutic effects. Very recently, a transcriptomic analysis points Aurora A as a targetable molecule for graft versus host disease prevention in a primate model[56]. Hence, our data provide a mechanistic explanation by how Aurora A controls T-cell activation. Given the importance of Aurora A inhibitors in cancer therapy, these results may provide new opportunities for treating lymphocyte diseases such as graft versus host disease, T-cell lymphomas or leukaemias.

Methods

Cells. The human Jurkat-derived T-cell lines J77 (Vα1.2 Vβ8+ TCR) and J.CAM1 (refs 36,37), the lymphoblastoid B-cell lines Raji (Burkitt lymphoma; acquired from the DSMZ Organization; ACC-319) and Hom2 (HLA-DR1 EBV-transformed) were cultured in RPMI 1640 + GlutaMAX–I + 25 mM HEPES (Gibco–Invitrogen) supplemented with 10% fetal bovine serum (Hyclone, Thermofisher). The human Jurkat-derived CH7C17 cells (Vβ3+ transgenic TCR, specific for HA peptide) were grown in the same medium supplemented with 400 μg ml^{-1} hygromycin B (Roche Diagnostics) and 4 μg ml^{-1} puromycin (Invitrogen, Eugene, OR, USA). CH7C17 (ref. 57) clones expressing EB3-GFP were generated by CH7C17 transfection and post selection with G418 (1 mg ml^{-1}). All lymphoid cell lines were tested for specific expression of CD (clusters of differentiation) with specific antibodies by flow cytometry. HEK293T cells were cultured in DMEM medium (Invitrogen) supplemented with 10% fetal bovine serum, 50 IU ml^{-1} penicillin and 50 μg ml^{-1} streptomycin, and exclusively used to produce and purify recombinant proteins. All cell lines were routinely tested for mycoplasm. Human peripheral blood mononuclear cells (PBMCs) were isolated from buffy coats obtained from healthy donors by separation on a Biocoll gradient (Biochrom) according to standard procedures. Monocytes were separated from PBMCs by a 30-min adherence step at 37 °C in RPMI supplemented with 10% FCS. Non-adherent cells were washed off and CD4$^+$ T cells were purified from PBMCs using magnetic-activated cell sorting (MACS; Miltenyi Biotech). Non-adherent cells were obtained after 30 min of the adhesion step at 37 °C. To generate SEE-responsive human T lymphoblasts, PBMCs were cultured for 5 days in the presence of SEE (0.1 μg ml^{-1}) and then phytohaemagglutinin (5 μg ml^{-1}) was added for 2 days. To favour its proliferation, IL-2 (50 U ml^{-1}) was added later to the medium every 2 days for a time period of 8 days. These studies were performed according to the principles of the Declaration of Helsinki and approved by the local Ethics Committee for Basic Research at the Hospital La Princesa (Madrid); informed consent was obtained from all human volunteers. These studies were performed according to the principles of the Declaration of Helsinki and approved by the local

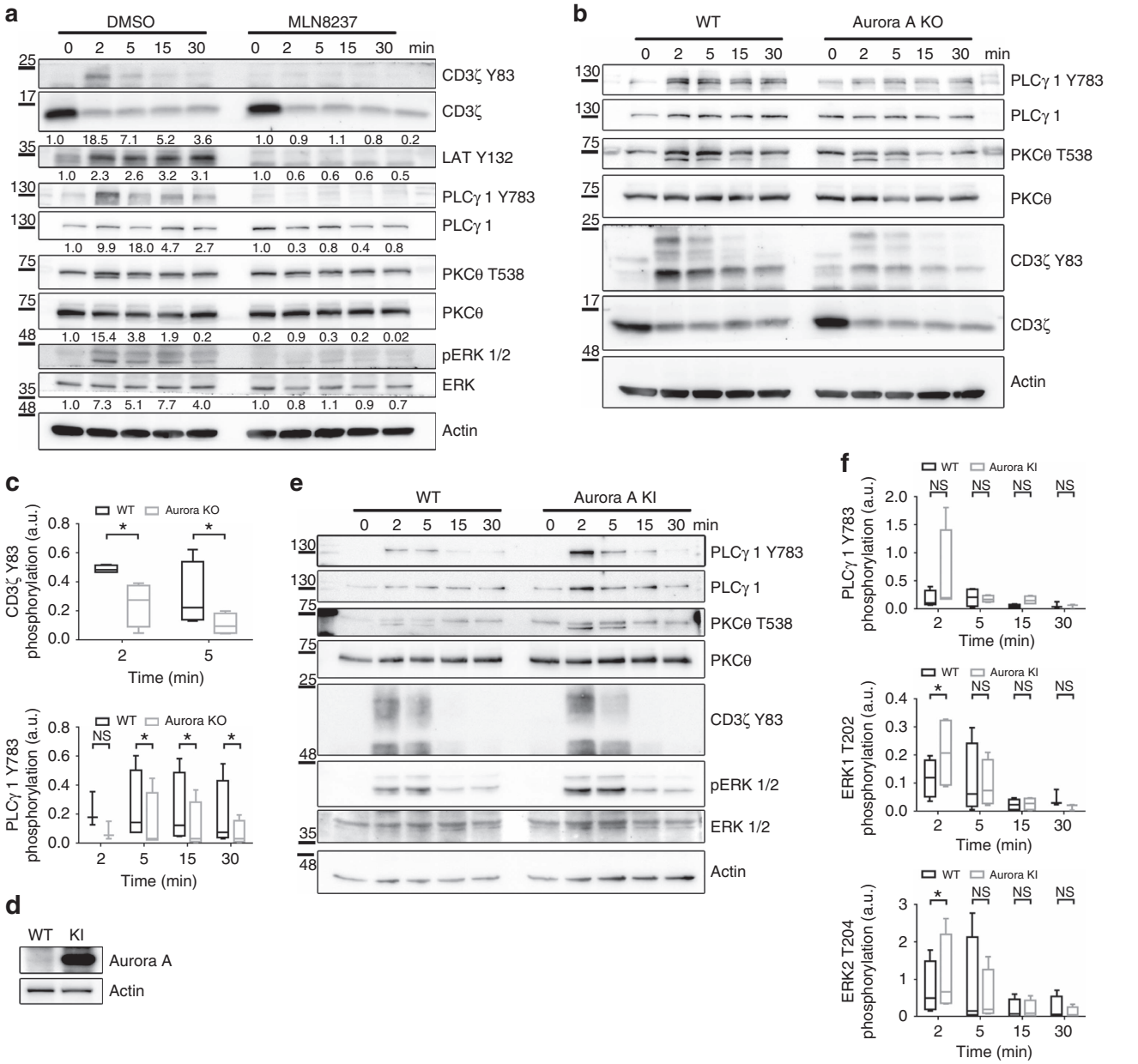

Figure 8 | Aurora A gene ablation blocks TCR signalling pathways. (**a**) Immunoblottings showing phosphorylation of the indicated molecules in cell lysates of WT mouse CD4$^+$ T cells pretreated with vehicle (DMSO) or Aurora A inhibitor (MLN8237) and activated for the indicated times with anti-CD3/CD28 antibodies. (**b**) Immunoblottings showing phosphorylation of the indicated molecules in cell lysates of Aurora KO and control CD4$^+$ T cells conjugated for the indicated times with anti-CD3/CD28 antibodies. (**c**) Quantification of data from four independent experiments as in **b**. Error bars represent interquartile range. Medians were compared with a Friedman test (*$P<0.05$). n.s., nonsignificant. (**d**) Immunoblot analysis of Aurora A protein expression in CD4$^+$ T cells isolated from *Col1a1tetO-Aurka/+*; *Rosa26rtTA/rtTA* mice and treated with doxycycline for 20 h to induce Aurora A expression (KI). Control cells (WT) were maintained without doxycycline. Actin is shown as a loading control. (**e**) Immunoblottings showing phosphorylation of the indicated molecules in cell lysates of Aurora KI CD4$^+$ T cells conjugated for the indicated times with anti-CD3/CD28 antibodies. (**f**) Quantification of data from four independent experiments as in **e**. Error bars represent interquartile rage. Medians were compared with a Friedman test (*P-value<0.05). n.s., nonsignificant.

Ethics Committee for Basic Research at the Hospital La Princesa (Madrid); informed consent was obtained from all human volunteers.

Mice. The Aurora A conditional model has been described[58]. These mice carry an *Aurka(lox)* conditional allele and the RERTert allele expressing an inducible Cre recombinase. After the appropriate crosses, we obtained the experimental *Aurka(lox/lox); RERT(ert/ert)* and control *Aurka(+/+); RERT(ert/ert)* mice used in this study. Cre activation on tamoxifen treatment induces conversion of the *Aurka(lox)* allele to the Aurka(Δ) allele. The Aurora kinase A (AurkA)-inducible mouse model has been reported recently[33]. This model was generated using the tetracycline-inducible single-copy transgenic system[59] and carries the *M2-rtTA* gene inserted within the *Rosa26* allele and a cassette containing the Aurora-A complementary DNA under the control of the doxycycine-responsive promoter (tetO) inserted downstream of the *Col1a1* locus. The final mouse model, *Col1a1tetO-Aurka/+; Rosa26rtTA/rtTA*, overexpresses exogenous Aurora-A on doxycycline treatment in a wide range of proliferative and non-proliferative tissues and cells.

Both Aurora A mouse models were maintained in a mixed background (*129/Sv, CD1, C57BL/6J* and *FVB/N*). Mice were housed in the pathogen-free animal facility of the Centro Nacional de Investigaciones Oncológicas (Madrid) in accordance with the animal care standards of the institution. For experimentation, genotyped littermates, male or female mice of 7–9 weeks were used. These animals were

observed on a daily basis and sick mice were killed humanely in accordance with the Guidelines for Humane Endpoints for Animals used in biomedical research. All animal protocols were approved by the Instituto de Salud Carlos III Committee for Animal Care and Research.

Mouse CD4$^+$ T cells were obtained from single-cell suspensions of the spleen and mesenteric lymph node. The cell suspensions were incubated with biotinylated antibodies against CD8, CD16, CD19, CD24, CD117, MHC class II (I-Ab), CD11b, CD11c and DX5, and were subsequently incubated with streptavidin microbeads (MACS; Miltenyi Biotec). CD4$^+$ T cells were negatively selected in an auto-MACS Pro Separator (Miltenyi Biotec). Cells were then labelled with antibodies to CD4 and CD25, and analysed by flow cytometry to confirm their purity and resting status. For conditional KO and knockin studies, mouse CD4$^+$ T cells were cultured with tamoxifen for 96 h (Aurora A gene deletion model) or doxycycline for 20 h (Aurora A overexpression model) in RPMI 1640 + GlutaMAX–I + 25 mM HEPES (Gibco–Invitrogen) supplemented with 10% fetal bovine serum (Hyclone, Thermofisher), 50 IU ml^{-1} per ml penicillin, 50 μg ml^{-1} per ml streptomycin and 5 ng ml^{-1} per ml murine IL-7.

Antibodies and reagents. The antibodies used in this study were anti-CD3ζ Y83 (ab68236; 1:1,000 for WB), anti-LAT Y132 (ab4476; 1:1,000 for WB), anti-Aurora A T288 (ab83968; 1:200 for immunofluorescence (IF)) and anti-Aurora A (a13824; [35C1]; 1:500 for WB) from Abcam; anti-α-Tubulin (T6199; clon DM1A; 1:2,000 for WB) and fluorescein isothiocyanate-conjugated anti-α-Tubulin (F2168; clon DM1A; 1:100 for IF) from Sigma; anti-ERK1/2 (SKU 13-6200; 1:500 for WB), anti-V5 (R960-25; 1:1,000 for WB and 0.5 μg per point for IP) and anti-Src pY418 (44-660G; that recognizes
Lck Y394 (ref. 34), 1:1,000 for WB) from Invitrogen; anti-ERK1/2 T202/Y204 (44285; 1:1,000 for WB) from Calbiochem; anti-Aurora A (04-1037; 1:1,000 for WB) and anti-Lck (05-435; 1 μg per point for IP) from Millipore; anti-PKCθ (610090; 1:1,000 for WB), anti-Rac1 (610651; 1:1,000 for WB), anti-mouse CD3ε (553057; clon 2C11; 10 μg ml^{-1}) and CD28 (553294; 5 μg ml^{-1}) and anti-human CD28 (555725; 2 μg ml^{-1}) from BD Pharmingen; anti-human CD3ε (317302; clon OKT3; 1:200 for IF) from BioLegend; anti-PKCθ T538 (9377S; 1:1,000 for WB), anti-PLCγ1 (2822S; 1:1,000 for WB), anti-PLCγ1 Y783 (#2821L; 1:1,000) and anti-Lck (2752; 1:1,000 for WB and 1:200 for IF) from Cell Signaling Tech; anti-PKCθ (sc-1875; 1:200 for IF) and anti-LAT (sc-7948; 1:500 for WB) from Santa Cruz. The anti-human CD3ε (300314; HIT3a; 5 μg ml^{-1}) was from eBioscience. The anti-human-CD3ζ and anti-GST antibodies were produced in Dr B. Alarcón's laboratory (Centro de Biología Molecular Severo Ochoa, Madrid). Goat anti-Armenian hamster IgG was from Jackson ImmunoResearch (127-005-160; 10 μg ml^{-1}). Cell tracker CMAC (7-amino-4-chloromethylcoumarin; C2110, 0.1 μM) was from Molecular Probes–Invitrogen. Enterotoxins E (SEE; 0.3 μg ml^{-1}) and B (SEB; 5 μg ml^{-1}) from *Staphylococcus aureus* were purchased from Toxin Technologies; the HA peptide (200 μg ml^{-1}) was synthesized by Lifetein LLC. Recombinant human Lck, histidine tagged was from MBL (RB-P3043). The Aurora A inhibitor MLN8237 and Aurora B inhibitor AZD1152 were from Selleckchem. Prolong Gold anti-fade mounting medium (P-36934), phalloidin conjugated to Alexa Flour 647 (A-22287; 1:100 for IF), goat anti-rabbit and goat anti-mouse highly cross-adsorbed secondary antibodies conjugated to Alexa Fluor 488 (A-11034 and A-11029, respectively; 1:500 for IF), 568 (A11036 and A-11031, respectively; 1:500 for IF) or 647 (A-21443 and A-21236, respectively; 1:500 for IF), donkey anti-goat highly cross-adsorbed secondary antibody conjugated to Alexa Fluor 647 (A-21447; 1:500 for IF) and donkey anti-rabbit secondary antibody conjugated to Alexa Flour 555 (A-31572; 1:500 for IF) were from Thermofisher Scientific. Fibronectin and Poly-L-Lys were from Sigma. Horseradish peroxidase-conjugated secondary antibodies for WB (anti-rabbit 31460, mouse 31430 or goat IgG + IgM 31460) were from Pierce–Thermofisher Scientific. Murine IL-7 was from PreproTech (217-17).

Plasmids and siRNAs and transfection. The plasmid encoding GFP-EB3 was generously provided by Dr A. Akhmanova (Utrecht University, Utrecht, The Netherlands)[24]. The plasmids encoding WT or KD Aurora A-GFP and WT or KD V5-Aurora A were reported previously[60]. CD4-Lck[38] in pRC3.1 plasmid was sub-cloned in the laboratory of Dr M Alonso; Dr M Alonso also provided the Lck-GFP[39] and CD4ΔCyt-GFP[40] constructs (CBM, Madrid, Spain), and Actin–mCherry-expressing CH7C17 T-cell clones were generated in the laboratory of Dr JM Serrador (CBM). The GST-PAK-CD (p21-activated kinase-CRIB-Domain)[30] was generously provided by Dr Collard (NKI, Amsterdam, The Netherlands). The plasmid pGEX2TK (Pharmacia) was used as control. T-cell lines were transfected with specific double-stranded siRNA against human Aurora Kinase A 3′-untranslated region (5′-CCCUCAAUCUAGAACGCUA-3′)[61] or a scramble negative control (5′-CUAGGGUGCCGAGUGUGUU-3′). For transfection, T-cell lines were centrifuged at 1,200 r.p.m. for 5 min and washed with Hank's balance salt solution(HBSS); Lonza) and resuspended in Opti-Mem I (Gibco–Invitrogen) (15×10^6 cells in 400 μl). Corresponding plasmids (10 μg) were added to cell lines and transfection was performed with the gene-pulser III system from Bio-Rad Laboratories (240 V, 975 mΩ, ~27 ms). After electroporation, cells were cultured in 9 ml RPMI 1640 + GlutaMAXTM–I + 25 mM HEPES medium. After 4 h, 500 μl fetal bovine serum was added to the cell medium. Experiments were performed 24 h after transfection. For mouse and human primary CD4$^+$ T cells, corresponding plasmids (10 μg) were added to cells and transfection was performed with the Nucleofector I from Amaxa Biosystems (X-01). The plasmids encoding Aurora A-V5 WT or KD (24 μg) were tranfected with Lipofectamine (Invitrogen) in HEK293T cells. Experiments were performed 24 h after transfection.

T cell activation and lysis for pull-down and immunoblotting. For human TCR stimulation, T cells were incubated for the indicated times with latex microbeads (6.4 μm diameter) conjugated to anti-CD3 antibody (10 μg ml^{-1}) and anti-CD28 antibody (5 μg ml^{-1}). For mouse TCR stimulation, T cells were incubated with anti-CD3 antibody (10 μg ml^{-1}) and anti-CD28 antibody (5 μg ml^{-1}) for 15 (4 °C) followed by incubation with goat anti-Armenian hamster IgG for 15 min (4 °C). For antigen stimulation, Raji cells were pulsed with 0.3 μg ml^{-1} SEE (30 min) and mixed with J77 or J.CAM1 cells (1:5); alternatively, Hom2 cells pulsed with 200 μg ml^{-1} HA peptide (2 h) or with 5 μg ml^{-1} SEB (30 min) and were mixed with CH7C17 cells (1:5) in HBSS. Where indicated, cells were pretreated with MLN8237 (10 μM) or AZD1152 (100 nM), or vehicle for 45 min at 37 °C in HBSS before stimulation with the corresponding APC or anti-CD3 and anti-CD28 antibodies. Cells were centrifuged at low speed for the indicated times at 37 °C to favour the formation of conjugates. Cells were lysed in 5 mM Tris-HCl pH 7.5 containing 1% NP40, 0.2% Triton X-100, 150 mM NaCl, 2 mM EDTA, 1.5 mM $MgCl_2$, and phosphatase and protease inhibitors. Lysates were spin at 14,000 r.p.m. (4 °C, 10 min) to remove debris and nuclei. For GST-Nck or GST-PAK-CD, pull-down assay experiments were performed as described previously[28,30]. Proteins were resolved by SDS–PAGE and transferred to nitrocellulose membranes. After blocking with TBS containing 0.2% TWEEN and 5% BSA, membranes were blotted with primary antibodies (o/n at 4 °C) and peroxidase-labelled secondary antibodies (30 min), and detected with the ImageQuant LAS-4000 chemiluminiscence and fluorescence imaging system (Fujifilm). Source images from relevant WB are available in the Supplementary Figs 6–9.

Cell conjugate and IF and IS analysis. Raji B cells or Hom2 B cells were washed once with HBSS and loaded with the CMAC cell tracker (10 μM) and with SEE or SEB for 30 min or HA peptide for 2 h at 37 °C. T cells (1×10^5 cells) were mixed with the corresponding APC (1:1) and plated onto Poly-L-Lys-coated slides (50 μg ml^{-1}; 1 h at 37 °C). Cells were allowed to settle for 20 min at 37 °C, fixed with 4% paraformaldehyde and 0.12 mM sucrose in PHEM (60 mM PIPES, 25 mM

Figure 9 | Aurora controls localization and phosphorylation of the tyrosine kinase Lck. (**a**) Maximum *Z* projection of *XYZ* stack of human Jurkat T cells pretreated with vehicle (DMSO) or Aurora A inhibitor (MLN8237) and conjugated with SEE-preloaded Raji B cells (APCs; 30 min). Cells were fixed and stained for α-tubulin–fluorescein isothiocyanate (FITC) (green), PKCθ (magenta) and Lck (red). Bright-field images are included. Scale bar, 10 μm. (**b**) Quantification of Lck accumulation at the IS in conjugates as in **a** from three independent experiments (DMSO, $n = 96$. MLN8237, $n = 94$). Data represent means ± s.d. Means were compared with a *t*-test; $^{****}P < 0.0001$. (**c**) Immunoblotting of Lck phosphorylation at Y394 in primary human CD4$^+$ T cells. Cells were pretreated with DMSO or MLN8237 and conjugated for the indicated times with anti-CD3/CD28-coated beads. Total Lck and actin are included as loading controls. Arrows point Lck band. (**d**) Quantification of data from four independent experiments as in **c**. Error bars represent s.d. Medians were compared with a Friedman test ($^*P < 0.05$). (**e**) Immunoblots of CD3ζ phosphorylation in lysates of J.CAM1 T cells transfected with Lck-GFP, CD4-Lck or CD4-ΔCyt-GFP, pretreated with DMSO or MLN8237 and conjugated for 5 min with SEE-pulsed APCs. (**f**) T-cell lymphoblasts pretreated with DMSO or MLN8237 were activated or not with SEE-pulsed APCs (2 min) and subjected to IP using an anti-Lck antibody. The immunoprecipitates were subjected to MS analysis. Upper panel, MS/MS extracted ion chromatograms of the Y394-phosphorylated and non-modified forms of Lck peptide LIEDNEYTAR. Lower panel, phosphorylated:non-modified peak ratios. (**g**) Recombinant Lck was incubated with Aurora A WT (in the absence or presence of MLN8237) or Aurora A KD immunoprecipitated from nocodazole-treated (16 h), transfected HEK293 cells. Lck and Aurora were incubated for 30 min in the presence of ATP and the mixture analysed by MS. Upper panel, MS/MS extracted ion chromatograms of the Y394-phosphorylated and non-modified forms of Lck peptide LIEDNEYTAR. Lower panel, phosphorylated:non-modified peak ratios. See Supplementary Table 1 for representative MS/MS spectra of the phosphorylated and non-phosphoryated forms of the peptide at the peaks.

Hepes, 5 mM EGTA and 2 mM $MgCl_2$), and permeabilized for 5 min at room temperature with 0.2% Triton X-100 in immunofluorescence solution (PHEM containing 3% BSA, 100 µg ml^{-1} γ-globulin and 0.2% azide). Cells were blocked for 30 min with immunofluorescence solution and stained with the indicated primary antibodies (5 µg ml^{-1}) followed by Alexa Fluor 488-, 568- or 647-labelled secondary antibodies, Alexa-conjugated phalloidin (5 µg ml^{-1}) or fluorescein isothiocyanate-conjugated anti-α-tubulin (0.1 µg ml^{-1}). Cells were mounted on Prolong Gold and analysed with a Leica SP5 confocal microscope (Leica) fitted with a HCX PL APO ×63/1.40–0.6 oil objective and images were processed and assembled using Image J software (http://rsbweb.nih.gov/ij/) and Photoshop software. For quantification in individual ISs, we used a home-made plugin for Image J software (http://rsbweb.nih.gov/ij/) called '*Synapse Measures*'. By comparing fluorescence signals from multiple regions of the T cell, APC, IS and background fluorescence, the programme yields accurate measurements of localized immunofluorescence. A detailed description of *Synapse Measures* including the algorithms used is described[62].

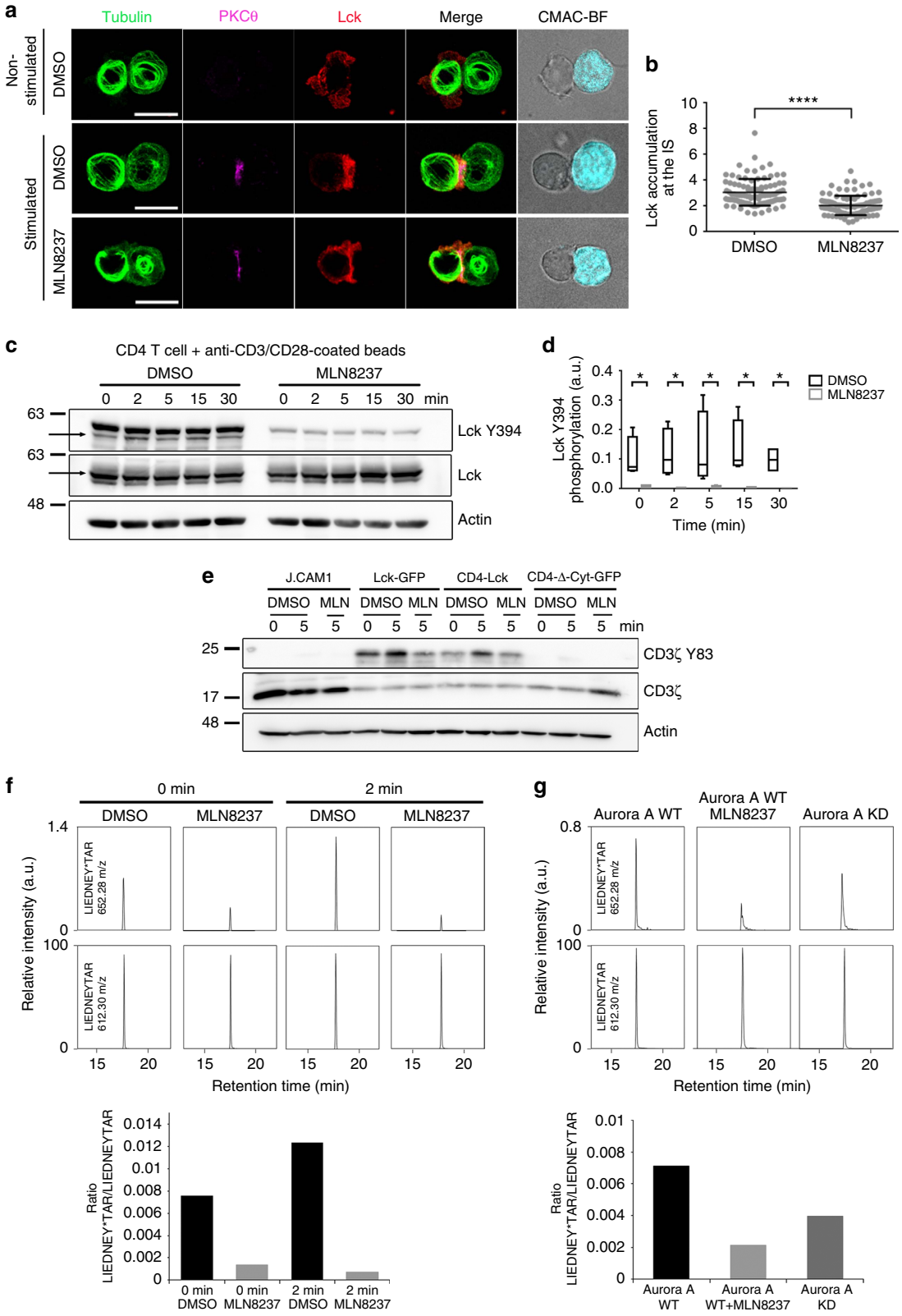

IP and MS and phosphorylation. For Lck IP assay, human lymphoblast pretreated with MLN8237 (10 μM) or vehicle (DMSO) for 30 min were activated with Raji preloaded with SEE for 2 min at 37 °C. Next, cells were lysated for 40 min at 4 °C in extraction buffer with 5 mM Tris-HCl pH 7.5 containing 0.5% NP40, 150 mM NaCl, 2 mM EDTA, 1.5 mM MgCl2, and phosphatase and protease inhibitors. Lysates were spun at 14,000 r.p.m. (4 °C, 10 min) to remove debris and nuclei. The anti-Lck antibody was allowed to bind with Protein G-conjugated sepharose beads (GE Healthcare) overnight at 4 °C and then mixed with the extracts. The mixture was left in agitation at 4 °C for 2 h and then beads were washed ten times with the same buffer used for lysate without detergents. As a control, we used beads preincubated with the extracts. For Aurora A IP, V5-Aurora A WT- or KD-transfected HEK293T cells were lysated with RIPA buffer, with 1% Triton X-100, 0.5% deoxycholate (Sigma-Aldrich), 0.1% SDS in Tris buffer saline and sonicated (3 × 30 s pulses). The anti-V5 antibody was mixed with the extracts and left in agitation at 4 °C for 2 h, and then Protein G-conjugated sepharose (GE Healtcare) was added for 1 h in agitation at 4 °C. Beads were washed three times with the buffer kinase with 20 mM Hepes pH 7.4 containing 150 mM KCl, 10 mM $MgCl_2$, 1 mM EGTA, 0.5 mM dithiothreitol, and phosphatase and protease inhibitors, and once with buffer kinase plus NaCl 0.5 mM. Beads were incubated with 0.5 μg of recombinant Lck in buffer kinase plus 10 mM ATP during 30 min at 30 °C. For proteomic analysis, the samples were trypsin-digested using the whole proteome in-gel digestion protocol[63]. The peptides produced by digestion were vacuum dried and redissolved in 1% trifluoroacetic acid for desalting in reversed-phase C-18 extraction cartridges (Oasis, Waters Corporation, Milford, MA, USA). High-resolution parallel reaction monitoring of phosphorylated peptides was carried out on an Easy nLC 1000 nano-HPLC apparatus (Thermo Scientific, San Jose, CA, USA) coupled to a hybrid linear ion trap-orbitrap (Orbitrap Elite, Thermo Scientific). Peptides were suspended in 0.1% formic acid and then loaded onto a C-18 reversed-phase nano-column (75 μm I.D., 50 cm) and separated in a continuous gradient consisting of 8–30% B for 15 min and 30–90% B for 2 min (B = 90% acetonitrile, 0.1% formic acid) at 200 nl min^{-1}. Peptides were ionized using a Picotip emitter nanospray needle (New Objective, Woburn, MA, USA). Each MS run consisted of enhanced FT-resolution spectra (30,000 resolution) in the 390–1,600 m/z range followed by data-independent MS/MS spectra of 11 parent ions acquired along the chromatographic run. The AGC target value in the Orbitrap for the survey scan was set to 1,000,000. Fragmentation in the linear ion trap was performed at 35% normalized collision energy with a target value of 10,000 ions and the dynamic exclusion was set to 0.5 min. Data analysis was performed with Xcalibur 2.2 (Thermo Scientific).

Time-lapse confocal and TIRF movie microscopy. For cell conjugates, 3D imaging was performed with CMAC-loaded Raji APCs (5×10^5; SEE-pulsed (Jurkat cells), SEB-pulsed (CH7C17 cells) or unpulsed) and were allowed to adhere to fibronectin-coated coverslips in Attofluor open chambers (Molecular Probes–Invitrogen) at 37 °C in a 5% CO_2 atmosphere or in glass-bottom dishes (No. 1.5 Mattek; Ashland, MA, USA). The cells were maintained in 1 ml HBSS (1% fetal bovine serum and 25 mM HEPES). Cells were pretreated with the MLN8237 inhibitor and maintained in its presence during imaging when needed. T cells were added (1:1 ratio) and a series of fluorescence and differential interference contrast or bright-field frames were captured using a TCS SP5 confocal laser scanning unit attached to an inverted epifluorescence microscope (DMI6000) fitted with an HCX PL APO × 63/1.40–0.6 oil objective. Images were acquired and processed with the accompanying confocal software (LCS; Leica) and Image J software (http://rsbweb.nih.gov/ij/). For 3D imaging of MT growing, cells were allowed to settle onto glass-bottom dishes coated with anti-CD3 (10 μg ml^{-1}) and anti-CD28 (3 μg ml^{-1}) monoclonal antibodies specific for human or mouse T cells and XYZ series were captured with the resonant scanner of the TCS SP5 confocal (8,000 Hz) each 1.2 s or 1.1 s. Cells were pretreated with the MLN8237 inhibitor and maintained in its presence during imaging. For TIRF microscopy, T cells stably expressing EB3-GFP or transfected with EB3-GFP and CD3ξ-mCherry were allowed to settle onto glass-bottom dishes coated with anti-CD3 (10 μg ml^{-1}) and anti-CD28 (3 μg ml^{-1}). Cells were pretreated with the MLN8237 inhibitor and it was maintained in the imaging medium during acquisition. Recording was initiated 3 min after cells were plated and cells were visualized with a Leica AM TIRF MC M system mounted on a Leica DMI 6000B microscope coupled to an Andor-DU8285_VP-4094 camera fitted with a HCX PL APO × 100.0, 1.46 oil objective. For mCherry–β-actin-expressing T cells, recording was initiated on addition of cells to the glass-bottom dishes. Images were processed with the accompanying confocal software (LCS; Leica). The laser penetrance used was 150 or 200 nm for both laser channels (488 and 561 nm), using the same objective angle. Time-lapse settings were optimized for each type of experiment and are specified throughout the text. Synchronization was performed with the accompanying Leica software and images were processed with Leica software, Matlab and Image J software (http://rsbweb.nih.gov/ij/).

Quantitative real-time PCR. Reverse transcriptase–PCR was performed with 1 μg of RNA isolated with Trizol RNA reagent (Invitrogen) from $CD4^+$ T cells obtained from healthy donors. mRNA levels of IL-2, CD25 and CD69 were determined in triplicate using the Power SYBR Green PCR master mix obtained from Applied Biosystems (Warrington, UK). Expression levels were normalized to the expression of glyceraldehyde-3-phosphate dehydrogenase. Primer sequences are listed in Supplementary Table 2.

References

1. Chakraborty, A. K. & Weiss, A. Insights into the initiation of TCR signaling. *Nat. Immunol.* **15,** 798–807 (2014).
2. Vicente-Manzanares, M. & Sanchez-Madrid, F. Role of the cytoskeleton during leukocyte responses. *Nat. Rev. Immunol.* **4,** 110–122 (2004).
3. Martin-Cofreces, N. B., Baixauli, F. & Sanchez-Madrid, F. Immune synapse: conductor of orchestrated organelle movement. *Trends Cell Biol.* **24,** 61–72 (2014).
4. Dustin, M. L. & Groves, J. T. Receptor signaling clusters in the immune synapse. *Annu. Rev. Biophys.* **41,** 543–556 (2012).
5. Palacios, E. H. & Weiss, A. Function of the Src-family kinases, Lck and Fyn, in T-cell development and activation. *Oncogene* **23,** 7990–8000 (2004).
6. Quintana, A. *et al.* T cell activation requires mitochondrial translocation to the immunological synapse. *Proc. Natl Acad. Sci. USA* **104,** 14418–14423 (2007).
7. Dustin, M. L. What counts in the immunological synapse? *Mol. Cell* **54,** 255–262 (2014).
8. Baixauli, F. *et al.* The mitochondrial fission factor dynamin-related protein 1 modulates T-cell receptor signalling at the immune synapse. *EMBO J.* **30,** 1238–1250 (2011).
9. Huse, M., Quann, E. J. & Davis, M. M. Shouts, whispers and the kiss of death: directional secretion in T cells. *Nat. Immunol.* **9,** 1105–1111 (2008).
10. Mittelbrunn, M. *et al.* Unidirectional transfer of microRNA-loaded exosomes from T cells to antigen-presenting cells. *Nat. Commun.* **2,** 282 (2011).
11. Choudhuri, K. *et al.* Polarized release of T-cell-receptor-enriched microvesicles at the immunological synapse. *Nature* **507,** 118–123 (2014).
12. Martin-Cofreces, N. B. *et al.* End-binding protein 1 controls signal propagation from the T cell receptor. *EMBO J.* **31,** 4140–4152 (2012).
13. Carmena, M. & Earnshaw, W. C. The cellular geography of aurora kinases. *Nat. Rev. Mol. Cell Biol.* **4,** 842–854 (2003).
14. Barr, A. R. & Gergely, F. Aurora-A: the maker and breaker of spindle poles. *J. Cell Sci.* **120,** 2987–2996 (2007).
15. Hochegger, H., Hegarat, N. & Pereira-Leal, J. B. Aurora at the pole and equator: overlapping functions of Aurora kinases in the mitotic spindle. *Open Biol.* **3,** 120185 (2013).
16. Lukasiewicz, K. B. & Lingle, W. L. Aurora A, centrosome structure, and the centrosome cycle. *Environ. Mol. Mutagen* **50,** 602–619 (2009).
17. Sardon, T., Peset, I., Petrova, B. & Vernos, I. Dissecting the role of Aurora A during spindle assembly. *EMBO J.* **27,** 2567–2579 (2008).
18. Bischoff, J. R. *et al.* A homologue of Drosophila aurora kinase is oncogenic and amplified in human colorectal cancers. *EMBO J.* **17,** 3052–3065 (1998).
19. Gopalan, G., Chan, C. S. & Donovan, P. J. A novel mammalian, mitotic spindle-associated kinase is related to yeast and fly chromosome segregation regulators. *J. Cell Biol.* **138,** 643–656 (1997).
20. Berdnik, D. & Knoblich, J. A. *Drosophila* Aurora-A is required for centrosome maturation and actin-dependent asymmetric protein localization during mitosis. *Curr. Biol.* **12,** 640–647 (2002).
21. Hannak, E., Kirkham, M., Hyman, A. A. & Oegema, K. Aurora-A kinase is required for centrosome maturation in Caenorhabditis elegans. *J. Cell Biol.* **155,** 1109–1116 (2001).
22. Etienne-Manneville, S. From signaling pathways to microtubule dynamics: the key players. *Curr. Opin. Cell Biol.* **22,** 104–111 (2010).
23. Dixit, R. & Ross, J. L. Studying plus-end tracking at single molecule resolution using TIRF microscopy. *Methods Cell Biol.* **95,** 543–554 (2010).
24. Grigoriev, I. & Akhmanova, A. Microtubule dynamics at the cell cortex probed by TIRF microscopy. *Methods Cell Biol.* **97,** 91–109 (2010).
25. Manneville, J. B. Use of TIRF microscopy to visualize actin and microtubules in migrating cells. *Methods Enzymol.* **406,** 520–532 (2006).
26. Yudushkin, I. A. & Vale, R. D. Imaging T-cell receptor activation reveals accumulation of tyrosine-phosphorylated CD3zeta in the endosomal compartment. *Proc. Natl Acad. Sci. USA* **107,** 22128–22133 (2010).
27. Soares, H. *et al.* Regulated vesicle fusion generates signaling nanoterritories that control T cell activation at the immunological synapse. *J. Exp. Med.* **210,** 2415–2433 (2013).
28. Gil, D., Schamel, W. W., Montoya, M., Sanchez-Madrid, F. & Alarcon, B. Recruitment of Nck by CD3 epsilon reveals a ligand-induced conformational change essential for T cell receptor signaling and synapse formation. *Cell* **109,** 901–912 (2002).
29. Gomez, T. S. & Billadeau, D. D. T cell activation and the cytoskeleton: you can't have one without the other. *Adv. Immunol.* **97,** 1–64 (2008).
30. Sander, E. E. *et al.* Matrix-dependent Tiam1/Rac signaling in epithelial cells promotes either cell-cell adhesion or cell migration and is regulated by phosphatidylinositol 3-kinase. *J. Cell Biol.* **143,** 1385–1398 (1998).

31. Manfredi, M. G. *et al.* Characterization of Alisertib (MLN8237), an investigational small-molecule inhibitor of aurora A kinase using novel in vivo pharmacodynamic assays. *Clin. Cancer Res.* **17,** 7614–7624 (2011).
32. Yang, J. *et al.* AZD1152, a novel and selective aurora B kinase inhibitor, induces growth arrest, apoptosis, and sensitization for tubulin depolymerizing agent or topoisomerase II inhibitor in human acute leukemia cells *in vitro* and *in vivo*. *Blood* **110,** 2034–2040 (2007).
33. Piazzolla, D. *et al.* Lineage-restricted function of the pluripotency factor NANOG in stratified epithelia. *Nat. Commun.* **5,** 4226 (2014).
34. Nika, K. *et al.* Constitutively active Lck kinase in T cells drives antigen receptor signal transduction. *Immunity* **32,** 766–777 (2010).
35. Li, Q. J. *et al.* CD4 enhances T cell sensitivity to antigen by coordinating Lck accumulation at the immunological synapse. *Nat. Immunol.* **5,** 791–799 (2004).
36. Goldsmith, M. A. & Weiss, A. Isolation and characterization of a T-lymphocyte somatic mutant with altered signal transduction by the antigen receptor. *Proc. Natl Acad. Sci. USA* **84,** 6879–6883 (1987).
37. Straus, D. B. & Weiss, A. Genetic evidence for the involvement of the lck tyrosine kinase in signal transduction through the T cell antigen receptor. *Cell* **70,** 585–593 (1992).
38. Xu, H. & Littman, D. R. A kinase-independent function of Lck in potentiating antigen-specific T cell activation. *Cell* **74,** 633–643 (1993).
39. Anton, O. *et al.* An essential role for the MAL protein in targeting Lck to the plasma membrane of human T lymphocytes. *J. Exp. Med.* **205,** 3201–3213 (2008).
40. Krummel, M. F., Sjaastad, M. D., Wulfing, C. & Davis, M. M. Differential clustering of CD4 and CD3zeta during T cell recognition. *Science* **289,** 1349–1352 (2000).
41. Tsai, M. Y. *et al.* A Ran signalling pathway mediated by the mitotic kinase Aurora A in spindle assembly. *Nat. Cell Biol.* **5,** 242–248 (2003).
42. Pinyol, R., Scrofani, J. & Vernos, I. The role of NEDD1 phosphorylation by Aurora A in chromosomal microtubule nucleation and spindle function. *Curr. Biol.* **23,** 143–149 (2013).
43. Serrador, J. M. *et al.* HDAC6 deacetylase activity links the tubulin cytoskeleton with immune synapse organization. *Immunity* **20,** 417–428 (2004).
44. Monjas, A., Alcover, A. & Alarcon, B. Engaged and bystander T cell receptors are down-modulated by different endocytotic pathways. *J. Biol. Chem.* **279,** 55376–55384 (2004).
45. Ritchey, L., Ottman, R., Roumanos, M. & Chakrabarti, R. A functional cooperativity between Aurora A kinase and LIM kinase1: implication in the mitotic process. *Cell Cycle* **11,** 296–309 (2012).
46. Wang, L. H. *et al.* The mitotic kinase Aurora-A induces mammary cell migration and breast cancer metastasis by activating the Cofilin-F-actin pathway. *Cancer Res.* **70,** 9118–9128 (2010).
47. King, C. G. *et al.* T cell affinity regulates asymmetric division, effector cell differentiation, and tissue pathology. *Immunity* **37,** 709–720 (2012).
48. Schoenborn, J. R., Tan, Y. X., Zhang, C., Shokat, K. M. & Weiss, A. Feedback circuits monitor and adjust basal Lck-dependent events in T cell receptor signaling. *Sci. Signal.* **4,** ra59 (2011).
49. Rossy, J., Owen, D. M., Williamson, D. J., Yang, Z. & Gaus, K. Conformational states of the kinase Lck regulate clustering in early T cell signaling. *Nat. Immunol.* **14,** 82–89 (2013).
50. Roh, K. H., Lillemeier, B. F., Wang, F. & Davis, M. M. The coreceptor CD4 is expressed in distinct nanoclusters and does not colocalize with T-cell receptor and active protein tyrosine kinase p56lck. *Proc. Natl Acad. Sci. USA* **112,** E1604–E1613 (2015).
51. Stirnweiss, A. *et al.* T cell activation results in conformational changes in the Src family kinase Lck to induce its activation. *Sci. Signal.* **6,** ra13 (2013).
52. Ballek, O., Valecka, J., Manning, J. & Filipp, D. The pool of preactivated Lck in the initiation of T-cell signaling: a critical re-evaluation of the Lck standby model. *Immunol. Cell Biol.* **93,** 384–395 (2015).
53. James, J. R. & Vale, R. D. Biophysical mechanism of T-cell receptor triggering in a reconstituted system. *Nature* **487,** 64–69 (2012).
54. Ventimiglia, L. N. & Alonso, M. A. The role of membrane rafts in Lck transport, regulation and signalling in T-cells. *Biochem. J.* **454,** 169–179 (2013).
55. Malumbres, M. & Perez de Castro, I. Aurora kinase A inhibitors: promising agents in antitumoral therapy. *Expert. Opin. Ther. Targets* **18,** 1377–1393 (2014).
56. Furlan, S. N. *et al.* Transcriptome analysis of GVHD reveals aurora kinase A as a targetable pathway for disease prevention. *Sci. Transl. Med.* **7,** 315ra191 (2015).
57. Geyeregger, R., Zeyda, M., Zlabinger, G. J., Waldhausl, W. & Stulnig, T. M. Polyunsaturated fatty acids interfere with formation of the immunological synapse. *J. Leukoc. Biol.* **77,** 680–688 (2005).
58. Perez de Castro, I. *et al.* Requirements for Aurora-A in tissue regeneration and tumor development in adult mammals. *Cancer Res.* **73,** 6804–6815 (2013).
59. Beard, C., Hochedlinger, K., Plath, K., Wutz, A. & Jaenisch, R. Efficient method to generate single-copy transgenic mice by site-specific integration in embryonic stem cells. *Genesis* **44,** 23–28 (2006).
60. Perez de Castro, I. *et al.* A SUMOylation motif in Aurora-A: implications for spindle dynamics and oncogenesis. *Front. Oncol.* **1,** 50 (2011).
61. Plotnikova, O. V. *et al.* Calmodulin activation of Aurora-A kinase (AURKA) is required during ciliary disassembly and in mitosis. *Mol. Biol. Cell* **23,** 2658–2670 (2012).
62. Calabia-Linares, C. *et al.* Endosomal clathrin drives actin accumulation at the immunological synapse. *J. Cell Sci.* **124,** 820–830 (2011).
63. Bonzon-Kulichenko, E. *et al.* A robust method for quantitative high-throughput analysis of proteomes by 18O labeling. *Mol. Cell. Proteomics* **10,** 003335 (2011).

Acknowledgements

We thank S. Bartlett for English editing and critical reading of the manuscript, Dr A. Akhmanova for providing reagents, Maria Navarro for the her critical reading of the manuscript and scientific recommendations, Miguel Vicente-Manzanares for his critical reading of the manuscript, and Aitana Sanguino and María José López for the technical support. We also thank the Confocal Microscopy & Dynamic Imaging Unit (CNIC), Madrid, Spain. This study was supported by grants SAF2011-25834, SAF2014-55579-R and BIO2012-37926 from the Spanish Ministry of Economy and Competitiveness, INDISNET-S2011/BMD-2332 from the Comunidad de Madrid ERC-2011-AdG 294340-GENTRIS and ERC-2013-AdG 334763-NOVARIPP. Red Cardiovascular RD 12-0042-0056 from Instituto Salud Carlos III (ISCIII). The Centro Nacional de Investigaciones Cardiovasculares (CNIC, Spain) is supported by the Spanish Ministry of Science and Innovation, and the Pro-CNIC Foundation.

Author contributions

N.B.-R., E.B.-M., N.B.M.C. and F.S.-M. designed experimentation and analysed results. N.B.-R., E.B.-M. and N.B.M.C. collected and analysed the data. I.P.C., G.C. and M.M. provided Aurora KO and KI mice, and contributed with discussion and correction of the manuscript. A.B. and B.A. provided reagents and contributed with discussion and correction of the manuscript. E.C., I.J. and J.V. performed the MS analysis. N.B.-R. prepared the figures and wrote the manuscript with input from E.B.-M., N.B.M.C. and F.S.-M.

Additional information

Supplementary Information accompanies this paper at http://www.nature.com/naturecommunications

Competing financial interests: The authors declare no competing financial interests.

Reprints and permission information is available online at http://npg.nature.com/reprintsandpermissions/

How to cite this article: Blas-Rus, N. *et al.* Aurora A drives early signalling and vesicle dynamics during T-cell activation. *Nat. Commun.* 7:11389 doi: 10.1038/ncomms11389 (2016).